Stable Hydrogen Isotope Ratios:
New Insights into the Formation of Soil Organic Matter

Dissertation

der Mathematisch-Naturwissenschaftlichen Fakultät
der Eberhard Karls Universität Tübingen
zur Erlangung des Grades eines
Doktors der Naturwissenschaften
(Dr. rer. nat.)

vorgelegt von
M.Sc. Arnim Kessler
aus Bad Säckingen

Tübingen
2023

Gedruckt mit Genehmigung der Mathematisch-Naturwissenschaftlichen Fakultät der Eberhard Karls Universität Tübingen.

Tag der mündlichen Qualifikation:	20.03.2023
Dekan:	Prof. Dr. Thilo Stehle
1. Berichterstatterin:	Prof. Dr. Yvonne Oelmann
2. Berichterstatterin:	Prof. Dr. Eva Lehndorff

Zusammenfassung

Stabile Wasserstoff (H)-Isotopenverhältnisse (δ^2H-Werte) können zur Aufklärung biogeochemischer Prozesse, zur Untersuchung des Paläoklimas oder zur Identifizierung von Transformationsprozessen der organischen Bodensubstanz (SOM) verwendet werden. Allerdings ist nur wenig über die Quellen der SOM und die H-Austauschprozesse während des Abbaus der organischen Substanz (OM) bekannt. Das übergeordnete Vorhaben dieser Arbeit war es, die Mechanismen zu untersuchen, welche für die enge Korrelation zwischen den H-Isotopenverhältnissen des langfristigen regionalen Niederschlages und der Isotopensignatur des Kohlenstoff (C)-gebundenen H (δ^2H_n-Werte) der SOM verantwortlich sind. Hierbei wird vermutet, dass während des Abbaus von OM ein Einbau von Umgebungswasser-H in die C-gebundene H Fraktion der OM stattfindet, sodass es zu einer Verschiebung der δ^2H_n-Werte der oberirdischen Pflanzenstreu in Richtung der δ^2H_n-Werte der SOM kommt.

Ziel dieser Arbeit war es, den Einbau in die C-gebundene H-Fraktion von Bakterien, Laubstreu und in die ausgewaschenen OM (TOM) zu untersuchen und dessen Einfluss im Hinblick auf die Quellen der SOM zu bewerten. Hierzu wurde (i) der Einbau von Umgebungswasser-H in die C-gebundene Fraktion der Laubstreu und der gesamten ausgewaschenen OM (TOM) während eines vierwöchigen Streuinkubationsexperimentes mit *Fagus sylvatica* L. und *Acer pseudoplatanus* L. unter Laborbedingungen untersucht und die damit einhergehende H-Isotopenfraktionierung bestimmt, (ii) der Einbau von Umgebungswasser-H in die bakterielle Biomasse während des substanzspezifischen Metabolismus unter der Verwendung zweier Modellorganismen (*Bacillus atrophaeus* und *Escherichia coli*) und die damit verbundene H-Isotopenfraktionierung ermittelt und (iii) der Einbau von Umgebungswasser-H in die C-gebundene H-Fraktion von Laubstreu und der ausgewaschenen TOM während eines 20-wöchigen Streuabbauexperimentes (*F. sylvatica* und *Tilia platyphyllos* SCOPOLI) unter Freilandbedingungen untersucht.

Im Labor wurde der H-Einbau (i) in die Laubstreu, in die ausgewaschene TOM sowie (ii) in die bakterielle Biomasse mit Hilfe von Isotopen-Markierungsexperimenten untersucht. Dabei wurde Umgebungswasser mit unterschiedlichen δ^2H-Werten verwendet, welches ein H-Isotopenverhältnis außerhalb des Bereiches der natürlichen Abundanz aufweist. Für das Feldexperiment (iii) wurde im Gewächshaus ^{2}H-angereicherte Laubstreu erzeugt. Anschließend wurde die Laubstreu in Netzbeutel verpackt, um den Einbau von Umgebungswasser-H über den Austausch von ^{2}H mit dem isotopisch leichteren Umgebungswasser-H in die Laubstreu und in die ausgewaschene TOM während des Abbaus zu ermitteln. Als zentrale Methode dieser Arbeit wurde die Dampf-Äquilibrierung mit anschließender TC/EA-IRMS-Analyse genutzt, um den austauschbaren H-Anteil (H_{ex}) der OM zu ermitteln. Nachfolgend wurden die entsprechenden δ^2H_n-Werte mittels einer Massenbilanz bestimmt. (i) Innerhalb der vierwöchentlichen Inkubation betrug der Austausch des C-gebundenen H mit dem Umgebungswasser-H in der Laubstreu 3-5 % und 8-9 % in der ausgewaschene TOM. (ii) Der

H-Einbau die C-gebundenen H-Fraktion der Bakterien von bis zu 80 % hing stark von der Bakterienart und der zur Verfügung stehenden C-Quelle ab. Außerdem verdeutlichen die Ergebnisse, dass die Glykolyse der zugrundliegende Stoffwechselweg für einen Einbau von H aus dem Umgebungswasser in die C-gebundene H-Fraktion der Organismen ist. (iii) Unter natürlichen Abbaubedingungen unterschied sich der Einbau in die C-gebundene H-Fraktion der Laubstreu stark in Abhängigkeit von der Baumart (*F. sylvatica*: 48 %, *T. platyphyllos*: 18 %). Weder unter Labor- noch unter natürlichen Bedingungen hing der H-Einbau von der Zersetzbarkeit der Streu oder der mikrobiellen Aktivität während des Streuabbaus ab. Stattdessen wird vermutet, dass mikrobielle Transformationsprozesse während der Zersetzung der OM für den Einbau von Umgebungswasser-H in die C-gebundene H-Fraktion der Laubstreu verantwortlich sind.

Meine Arbeit liefert detaillierte Erkenntnisse über den Einbau von Umgebungswasser-H in die C-gebundene H-Fraktion der Pflanzenstreu, der ausgewaschenen TOM während des Streuabbaus sowie in den C-gebundenen H-Pool von Bakterien während des substanzspezifischen Metabolismus.

Während die geringen Einbauraten in die ausgewaschene TOM unter Laborbedingungen ohne den stetigen Eintrag externer Bestandteile zu erklären sind, weisen die hohen Einbauraten in die bakterielle Biomasse während des anabolen Metabolismus sowie eine beinahe vollständige Überprägung der δ^2H_n-Werte der ausgewaschenen TOM unter natürlichen Bedingungen auf die Bedeutung mikrobieller (Abbau-)Produkte als eine Quelle der SOM hin und tragen dadurch zu einer Erklärung für die enge Korrelation zwischen den δ^2H_n-Werten der SOM und den δ^2H-Werten des Niederschlages bei, da TOM eine SOM-Quelle für den Mineralboden ist.

Summary

Stable hydrogen (H) isotope ratios can be used to elucidate biogeochemical processes, serve as a paleo climate proxy, or identify soil organic matter (SOM) dynamics. However, there is little knowledge about the sources of SOM and bulk H dynamics during the decomposition of organic matter (OM).

The overarching aim of my thesis was to study the mechanisms responsible for the close correlation between the H isotope composition of long-term rainfall and the H isotope signature of the carbon (C)-bonded H pool (δ^2H_n values) in SOM. Here, the incorporation of ambient water-H during decomposition of OM is the main process suspected to shift δ^2H_n values of aboveground litter towards δ^2H_n values of SOM.

My objective was to study the incorporation of ambient water-H into the C-bonded H pool of bacteria, leaf litter and the total leached OM (TOM) and to assess the influence of the individual compounds with regards to the sources of SOM. To this end, we (i) investigated the incorporation of ambient water-H into leaf litter and leached OM during four weeks of leaf litter (*Fagus sylvatica* L. and *Acer pseudoplatanus* L.) decomposition and quantified the apparent H isotope fractionation in a leaf litter incubation experiment, (ii) studied the incorporation of ambient water-H into the bulk bacterial biomass during substrate-specific metabolism using two model organisms (*Bacillus atrophaeus* and *Escherichia Coli*) and quantified the associated apparent H isotope fractionation under laboratory conditions and (iii) investigated the incorporation of ambient water-H into the C-bonded H fraction of leaf litter and leached OM during 20 weeks of litter (*F. sylvatica* and *Tilia platyphyllos* SCOPOLI*)* decomposition under field conditions.

In the laboratory, the incorporation into leaf litter, total leached OM (TOM) and bacteria was traced via labeling experiments in which ambient waters with δ^2H values that differ from natural abundance levels were used. For the field experiment, we produced ^2H enriched leaf litter in the greenhouse. Afterwards, leaf litter was placed in litterbags to determine the incorporation into leaf litter and leached TOM during decomposition by the exchange of ^2H with isotopically lighter ambient water-H under natural conditions. As central method we used the steam equilibration procedure followed by TC/EA-IRMS measurement to account for the exchangeable H fraction (H_{ex}) of bulk OM and δ^2H_n values were determined by mass balance calculations.

(i) During four weeks of incubation, leaf litter experienced an incorporation of isotopically labeled water-H of 3-5 % of the total C-bonded H pool while the incorporation of ambient water-H into the C-bonded H pool of the leached TOM in solution was 8-9 %. (ii) The incorporation into the C-bonded H pool of bulk bacterial biomass up to 80 % strongly depended on bacterium species and the available C-source. Furthermore, the results illustrate the glycolysis pathway as a mechanism underlying the incorporation of ambient water-H into the C-bonded H pool of bacteria. (iii) Under natural conditions the incorporation of ambient water-H into the C-bonded H fraction of leaf litter

strongly depended on tree species (*F. sylvatica*: 48 %, *T. platyphyllos*: 18 %). Additionally, neither under laboratory conditions nor under field conditions the incorporation depended on the decomposability of leaf litter or microbial activity during decomposition. Rather we suspect ongoing microbial transformation processes during the microbial processing of OM as the driving factor for the observed incorporation of ambient water-H into the C-bonded H fraction of leaf litter.

My work provides profound insights into the incorporation of ambient water-H into the C-bonded H fraction of leaf litter and leached TOM during leaf litter decomposition and into the C-bonded H pool of bacteria during substrate-specific metabolism. While the observed small incorporation into leached TOM under laboratory conditions can be explained by the absence of additional inputs of external compounds, high incorporation rates into bulk bacterial biomass during anabolic metabolism together with an almost overprinting of δ^2H_n values of leached TOM under natural conditions highlight the importance of microbial (decomposition) products as a source of SOM and provide a partial explanation for the close correlation between δ^2H_n values of SOM and δ^2H values of long-term rainfall.

Table of Contents

List of Figures

Section B

Section C

Section D

Section E

List of Tables

Section B

Section C

Section D

Section A

General Introduction

1. Stable hydrogen isotopes as environmental tracer

The decomposition of organic matter (OM) is a crucial component of the global carbon (C) cycle (Berg and McClaugherty, 2014). With respect to longer residence times of C, soil organic matter (SOM) is the largest terrestrial C reservoir (Angst et al., 2021) which stores more C compared to the atmosphere and vegetation (Ciais et al., 2013; Schmidt et al., 2011; Eswaran et al., 1993). However, there is little knowledge about the sources of SOM (Lehmann and Kleber, 2015; Paul et al., 2016; Angst et al., 2021).

Hydrogen (H) is the most abundant element in the universe (Suess and Urey, 1956). Accordingly, H is present in most minerals of the earth crust and the major constituent of OM (Schimmelmann et al., 2006). The pool of H in the OM is commonly differentiated into an exchangeable H fraction (H_{ex}), e.g., O-, N-, S-bonded H, that equilibrates with air humidity and does not inherit a robust isotope signal (Sauer et al., 2009; Savin and Hsieh, 1998; Schimmelmann, 1991; Wassenaar and Hobson, 2000) and a nonexchangeable H fraction (H_n) (C-bonded H) that preserves its δ^2H values (δ^2H_n values) and does not exchange with water-H at temperatures usually occurring in soil environments at the earth surface (Savin and Hsieh, 1998; Schimmelmann et al., 2006; Sessions et al., 2004; Sheppard and Gilg, 1996). Via the steam equilibration device, it is possible to account for H_{ex} of bulk OM and consequently calculate the corresponding H_n values (Ruppenthal et al., 2010). With regards to biochemical processes, hydrogen is involved into life processes acting as ion or in the form of water (acid-base and redox reactions, water splitting in photosynthesis, biosynthesis of carbohydrates, amino acids and lipids) (Berg et al., 2012). The large mass difference of 100 % of the two stable isotopes ^{1}H (protium) and ^{2}H (deuterium), characterized by different zero-point energy levels, causes a different behavior of the two stable H isotopes during (bio-)chemical reactions. Hence, the ratio of ^{2}H to ^{1}H (expressed as the δ^2H value, compared to the H isotopic composition of the international reference standard "Vienna Standard Mean Ocean Water" (VSMOW)) and the resulting isotope fractionation can be used for a wide range of applications in environmental sciences. In more detail, stable H isotope ratios can be used to elucidate biogeochemical processes, identify SOM sources, serve as a paleo climate proxy (Kreuzer-Martin et al., 2004; Ruppenthal et al., 2013, 2015; Schimmelmann et al., 2006; Sessions, 2016).

The H contained in the OM derives from water (Berg et al., 2012), while on a global scale, the H isotopic composition of rainfall shows a characteristic spatial pattern of decreasing δ^2H values with increasing latitude, elevation, continentality and rainfall amount (Gleixner and Mügler, 2007). Therefore, δ^2H values of precipitation are a result of the temperature-dependent equilibrium H isotope fractionation between liquid water which is characterized by an enrichment of ^{2}H and water vapor (typically depleted in ^{2}H) during condensation and showing a strong correlation with mean annual temperatures (Bowen and Revenaugh, 2003; Craig, 1961; Dansgaard, 1964). In order to make reliable assertions about the composition of stable H isotope ratios of a sample, the exchangeable H fraction

has to be separated from C-bonded H by equilibration with water vapor of known H isotopic composition (Ruppenthal et al., 2010; Sauer et al., 2009; Wassenaar and Hobson, 2000), whereas afterwards δ^2H_n values are determined by mass balance calculations (Ruppenthal et al., 2010).

2. Stable hydrogen isotopes in soil organic matter

SOM dynamics are driven by environmental and biological controls (Schmidt et al., 2011). Therefore, δ^2H values are a promising indicator of OM transformation processes (Schimmelmann et al., 2006). However, up to date there is little knowledge about the composition and formation of SOM. Along a 2500-km climosequence in Argentina, it was shown that the H isotope signature of the C-bonded H pool in SOM was driven by the local long-term rainfall H isotope composition (Ruppenthal et al., 2015). Starting from soil water to root water uptake, there is no H isotopic fractionation (Hayes, 2001; Yakir, 1992). Subsequently, the transpiration in plants in response to air humidity and mixing with water vapor is associated with a ^2H enrichment in leaf water relative to source water taken up by roots (Craig and Gordon, 1965; Dongmann et al., 1974). Hence, the enrichment increases with increasing aridity (Cernusak et al., 2016). Afterwards, the photosynthetic H isotope fractionation causes δ^2H_n values to be lower than δ^2H values of precipitation (Cormier et al., 2018; Hayes, 2001; Yakir, 1992). Assuming that there is a constant ^2H fractionation factor during photosynthesis, assimilates become enriched in ^2H producing H-isotopically heavier leaf tissue under arid than under humid conditions (Hayes, 2001; Roden et al., 2000; Sanchez-Bragado et al., 2019). While this process is well described for cellulose in compound-specific studies (Epstein et al., 1977; Yapp and Epstein, 1982), studies about the aridity effect on δ^2H_n values of bulk OM are rare (Leaney et al., 1985; Rundel et al., 1979; Ziegler et al., 1976). However, during the transport of assimilates through the plant and further processing during biosynthesis reactions, the leaf water signal eventually gets lost. The resulting biosynthesized compounds reflect the H isotopic signal of the ambient cell water which might more closely resemble that of soil water (Roden et al., 2000; Yakir, 1992; Yakir and Deniro, 1990). For example, this has been shown for n-alkanes from terrestrial plants (Sachse et al., 2012) and tree-ring cellulose (Gray and Song, 1984), which might already show an H isotopic composition that is closer to soil water and thus related with that of mean local precipitation. Along a 2500-km climosequence in Argentina, it was shown that the aridity effect was present in leaves, together with an increase in δ^2H_n values in the order shoots < litter < roots < SOM (Ruppenthal et al., 2015). Together with a close correlation of δ^2H_n values of SOM with δ^2H values of the local long-term rainfall, the existing aridity signals in the C-bonded H pool of aboveground plant biomass were absent in that of SOM (Ruppenthal et al., 2015). From these findings, the authors concluded that the belowground root biomass (also showing a strong correlation of δ^2H_n values on δ^2H values of local long term precipitation) made a major contribution to SOM (Ruppenthal et al., 2015).

An alternative explanation for the close correlation between δ^2H_n values of SOM and local precipitation shown by Ruppenthal et al. (2015) including the leveling of the aridity signal of aboveground OM, requires the exchange of the C-bonded H pool with ambient water during the microbial decomposition and processing of SOM. This process is different from the rapid exchange between H in air moisture and ambient soil water and the exchangeable H pool (e.g. the H in hydroxyl groups) in SOM, because microbial activity affects the C-bonded H as well. However, the results of Ruppenthal et al. (2015) provide strong indications that there is an incorporation of ambient water into the C-bonded H fraction of SOM once heterotrophic organisms are involved in decomposition of OM.
In general soil organisms play a key function for biogeochemical cycling in ecosystems (Bardgett et al., 2008; Wallenstein and Hall, 2012). Here, it is generally assumed that during glycolysis, a metabolic reaction chain shared by nearly all organisms on earth (Berg et al., 2012), ambient water-H is incorporated into the C-bonded H fraction including the *de novo* formation of C-H bonds (Gerlt, 1999; Knowles and Albery, 1977; Rieder and Rose, 1959; Whitman, 1999; Yakir, 1992). Microbial studies corroborated that C-H bonds are regularly broken and reattached during microbial metabolism (Horita and Vass, 2003; Kreuzer-Martin et al., 2003; Kreuzer-Martin et al., 2004). As a result, the reported H incorporation into bacterial biomass up to 30 % of total H (Kreuzer-Martin et al., 2003; Kreuzer-Martin et al., 2004; Kreuzer-Martin and Jarman, 2007) and <5 to >70 % into bacterial amino acids (Fogel et al., 2016) illustrate the controversial results of the reported studies. The quantification of the incorporation into bulk bacterial biomass requires distinguishing between exchangeable and nonexchangeable (C-bonded) H and the contribution of microbial biomass is assumed to be 50-80 % (Liang and Balser, 2011; Simpson et al., 2007) to SOM. For this reason, the incorporation of ambient water-H into the bacterial biomass during metabolism may can be used to explain the close correlation of δ^2H_n values of SOM on δ^2H values of the local precipitation suggested by Ruppenthal et al. (2015) by the input of bacterial products and necromass to SOM. However, with regards to the importance of SOM in various ecosystems (Schmidt et al., 2011), mechanistic evidence relating the sources and the formation of SOM is lacking so far.

3. Stable hydrogen isotopes during the decomposition of organic matter

Plant litter enters the SOM pool during decomposition and recalcitrant compounds like lignin are accumulated (Berg and McClaugherty, 2014; Wickings et al., 2012) while cellulose is rather lost than accumulated in SOM (Preston et al., 2009). Because there are compound-specific δ^2H_n values, the preferential decomposition of organic compounds with distinct δ^2H_n values could systematically change the δ^2H_n values of litter-derived SOM during decomposition (DeBond et al., 2013). Nevertheless, this process would not necessarily drive the δ^2H_n values of SOM derived from aboveground litter towards that of soil water and therefore is an unlikely explanation for the loss of the

aridity signal in aboveground biomass. Consequently, to shedding more light on processes involved in the breakdown and rearrangement of C compounds during decomposition, the suggested incorporation of ambient water-H into the C-bonded H pool needs to be traced in labeling experiments using isotopic labeling that differs from natural abundance levels. With regards to this, the transferability of results from biochemical laboratory experiments on incorporation of ambient water into C-H bonds during heterotrophic activity to the C-bonded H fraction in the plant/litter/SOM systems has not yet been tested. In more detail, during the fifth step of the glycolysis, a H atom from ambient water is newly bound to the C_2 position of the glyceraldehyde-3-phosphate (GAP) molecule. As a result, the microbial metabolism is associated with an incorporation of ambient water-H into C-bonded H of the microbial metabolites in the range of 20 to 50 % during up to four days (Horita and Vass, 2003; Kreuzer-Martin et al., 2003; Kreuzer-Martin et al., 2004). Furthermore, the role of the glycolysis for the incorporation of ambient water-H into the C-bonded H pool of bulk bacteria biomass during metabolism has not been studied yet. In these short-term studies, particular microbial species were grown under optimum conditions (temperature, pH, availability of nutrients and C sources). In a one-year incubation, Paul et al. (2016) showed that more than 70 % of C-bonded H in lipids originated from ^{2}H-labeled ambient water. However, lipids, proteins, amino acids and other microbial cell compounds might not be representative for the variety of compounds present in natural OM. Additionally, the examined compounds consist of both C-bonded H as well as exchangeable O-, N- and S-bonded H that rapidly exchange with ambient water air moisture (Schimmelmann, 1991; Wassenaar and Hobson, 2000). Therefore, the quantification of incorporation of ambient water-H into bulk bacterial biomass requires distinguishing between exchangeable and C-bonded H, which can be reached by steam equilibration (Ruppenthal et al., 2013; Wassenaar and Hobson, 2000). Because the decomposition of OM is associated which heterotrophic activity, ambient water-H should be incorporated into the C-bonded H fraction of OM associated with a positive H isotope fractionation effect in the product relative to the reactant (Ruppenthal et al., 2015). Therein, faster decomposition associated with a high microbial activity should result in more pronounced microbial H incorporation into the C-bonded H pool. Furthermore, litter decomposition rates vary widely among species (Cornelissen, 1996; Wardle et al., 2006) and plant litter properties have a marked influence on decomposition rates (Fogel and Cromack Jr., 1977; Gartner and Cardon, 2004; Meentemeyer, 1978). Additionally, during microbial decomposition not only the solid phase of leaf litter is affected by transformation processes, but also new compounds like sugars and proteins, which are partly water-soluble, are synthesized. Leached total organic matter (TOM) in solution consists of a complex mixture of aromatic and alipathic C-rich compounds of different sizes and chemical structure (Dilling and Kaiser, 2002; Pagano et al., 2014). Degradation products such as amino acids as well as microbial metabolites are released into soil solution during the decomposition process (Habermehl et al., 2008; Mambelli et al., 2011; Martin et al., 1974; Voroney et al., 1989). Since degradation products and microbial metabolites underwent biosynthesis reactions potentially associated with the incorporation

of ambient water-H into the C-bonded H pool, δ^2H_n values of leached TOM might more closely resemble δ^2H values of ambient water than δ^2H_n values of the solid-state organic matter during decomposition.

In summary, there is a lack of knowledge concerning (i) the incorporation of ambient water-H into the C-bonded H fraction of microorganisms, leaf litter and leached OM and (ii) the associated H fractionation during the incorporation of ambient water-H into the C-bonded H fraction of OM during decomposition.

4. Objectives and structure of the thesis

Our overarching objective is to unravel the mechanisms responsible for the close correlation between δ^2H values of rainfall and δ^2H_n values of SOM. Here, the incorporation of ambient water-H during decomposition of OM is the main process suspected to shift δ^2H_n values of aboveground litter towards δ^2H_n values of SOM. Therefore, our research would improve the mechanistic understanding of the bacterial metabolism and transformation of OM during decomposition. Because our results will yield an estimate of the C-H bonds having been broken enzymatically, we could also contribute to the understanding of the breakdown and rearrangement of C compounds during decomposition and the influence of microbial products which forms part of the emerging view on SOM. Superior, for all sections of the thesis, the steam equilibration device with waters of varying H isotopic composition was applied to determine the contribution of exchangeable H to total H concentrations in OM (Ruppenthal et al., 2013).

Section B investigated the incorporation of ambient water-H into leaf litter and leached OM during decomposition under laboratory conditions. Therein the incorporation into the C-bonded H pool of leaf litter and leached TOM of *Fagus sylvatica* LINNÉ and *Acer pseudoplatanus* L. were incubated with waters differing in δ^2H values over four weeks. The results show small incorporation rates into the C-bonded H pool of bulk leaf litter and leached TOM for the first time and highlight the microbial input to the leached TOM.

In **Section C** the incorporation of ambient water-H into bulk bacterial biomass during substrate-specific metabolism using two model organisms *Escherichia coli* (gram-negative) and *Bacillus atrophaeus* (gram-positive) incubated in growing media using waters differing in δ^2H values supplemented with either D-glucose (favorable) or D-lysine (unfavorable) as sole C source was studied. In addition, for a selection of previously published studies, incorporation rates and the associated H isotope fractionation was recalculated using calculations based on the suggested approach. The results of this study provide first insights into the substrate and species-specific incorporation of ambient water-H into the C-bonded H pool of bulk bacterial biomass and support the glycolysis pathway as the mechanism underlying the incorporation of ambient water-H into the

C-bonded H fraction of bacteria. Contrary, stressful conditions forcing bacteria into a catabolism dominated metabolism disable the incorporation of ambient water-H.

Section D demonstrates the incorporation of ambient water-H into the C-bonded H fraction of leaf litter and leached OM during decomposition under field conditions, which was never investigated so far. Since it is challenging to manipulate δ^2H values of precipitation under field conditions, before the experiment, ^{2}H labeled leaf litter of *F. sylvatica* and *Tilia platyphyllos* SCOPOLI was produced by the irrigation of trees with differently ^{2}H enriched waters in the greenhouse. Subsequently, leaves were packed into litterbags and spread out in the field. In contrast to **Section B** and **C** the incorporation of ambient water-H into OM was investigated via the subsequent depletion of the ^{2}H label of OM during 20 weeks of decomposition. The results highlight microbial transformation processes in the remaining leaf litter associated with an incorporation of ambient water-H into the C-bonded H fraction of the remaining leaf litter and suggest that δ^2H_n values of leached TOM are driven by the influence of external bacterial input into the leached TOM.

Section E includes the general conclusion of this research work with regards to the determined incorporation rates. Therefore, the focus is on the relevance of the individual compounds for SOM dynamics including their contribution to SOM to explain the close correlation of δ^2H_n values of SOM with δ^2H values of local precipitation reported by Ruppenthal et al. (2015).

5. References

Angst, G., Pokorný, J., Mueller, C.W., Prater, I., Preusser, S., Kandeler, E., Meador, T., Straková, P., Hájek, T., van Buiten, G., Angst, Š., 2021. Soil texture affects the coupling of litter decomposition and soil organic matter formation. Soil Biology and Biochemistry 159, 108302.

Bardgett, R.D., Freeman, C., Ostle, N.J., 2008. Microbial contributions to climate change through carbon cycle feedbacks. The ISME journal 2, 805–814.

Berg, B., McClaugherty, C., 2014. Plant Litter. Decomposition, Humus Formation, Carbon Sequestration. Springer, Berlin, Heidelberg.

Berg, J.M., Tymoczko, J.L., Stryer, L., 2012. Biochemistry. This edition is for use outside the USA and Canada, 7th ed. Freeman Palgrave Macmillan, New York, NY.

Bowen, G.J., Revenaugh, J., 2003. Interpolating the isotopic composition of modern meteoric precipitation. Water Resources Research 39, 23.

Cernusak, L.A., Barbour, M.M., Arndt, S.K., Cheesman, A.W., English, N.B., Feild, T.S., Helliker, B.R., Holloway-Phillips, M.M., Holtum, J.A.M., Kahmen, A., McInerney, F.A., Munksgaard, N.C., Simonin, K.A., Song, X., Stuart-Williams, H., West, J.B., Farquhar, G.D., 2016. Stable isotopes in leaf water of terrestrial plants. Plant, cell & environment 39, 1087–1102.

Ciais, P., Sabine, C., bala, G., Bopp, L., Brovkin, V., Canadell, J., Chhabra, A., DeFries, R., Galloway, J., Heimann, M., Le Jones, C.Q., Myneni, R.B., Piao, S., Thornton, P., 2013. Carbon and Other Biogeochemical Cycles. The Physical Science Basis. Contribution of Working Group I to the Fifth Assessment Report of the Intergovernmental Panel on Climate Change. Climate change 2013.

Cormier, M.-A., Werner, R.A., Sauer, P.E., Gröcke, D.R., Leuenberger, M.C., Wieloch, T., Schleucher, J., Kahmen, A., 2018. 2 H-fractionations during the biosynthesis of carbohydrates and lipids imprint a metabolic signal on the δ^2H values of plant organic compounds. The New phytologist 218, 479–491.

Cornelissen, J.H.C., 1996. An Experimental Comparison of Leaf Decomposition Rates in a Wide Range of Temperate Plant Species and Types. The Journal of Ecology 84, 573.

Craig, H., 1961. Isotopic Variations in Meteoric Waters. Science (New York, N.Y.) 133, 1702–1703.

Craig, H., Gordon, L.A., 1965. Isotopic oceanography: Deuterium and oxygen-18 variation in the ocean and the marin atmosphere. Proc. Symp. on Marine Geochemistry, The University of Rhode Island, 1965.

Dansgaard, W., 1964. Stable isotopes in precipitation. Tellus 16, 436–468.

DeBond, N., Fogel, M.L., Morrill, P.L., Benner, R., Bowden, R., Ziegler, S., 2013. Variable δD values among major biochemicals in plants: Implications for environmental studies. Geochimica et Cosmochimica Acta 111, 117–127.

Dilling, J., Kaiser, K., 2002. Estimation of the hydrophobic fraction of dissolved organic matter in water samples using UV photometry. Water research 36, 5037–5044.

Dongmann, G., Nürnberg, H.W., Förstel, H., Wagener, K., 1974. On the enrichment of H2 18-O in the leaves of transpiring plants. Radiation and environmental biophysics 11, 41–52.

Epstein, S., Thompson, P., Yapp, C.J., 1977. Oxygen and hydrogen isotopic ratios in plant cellulose. Science (New York, N.Y.) 198, 1209–1215.

Eswaran, H., van den Berg, E., Reich, P., 1993. Organic Carbon in Soils of the World. Soil Science Society of America Journal 57, 192–194.

Fogel, M.L., Griffin, P.L., Newsome, S.D., 2016. Hydrogen isotopes in individual amino acids reflect differentiated pools of hydrogen from food and water in Escherichia coli. Proceedings of the National Academy of Sciences of the United States of America 113.

Fogel, R., Cromack Jr., K., 1977. Effect of habitat and substrate quality on Douglas fir litter decomposition in western Oregon. Canadian Journal of Botany 55, 1632–1640.

Gartner, T.B., Cardon, Z.G., 2004. Decomposition dynamics in mixed-species leaf litter. Oikos 104, 230–246.

Gerlt, J.A., 1999. Stabilization of Reactive Intermediates and Transition States in Enzyme Active Sites by Hydrogen Bonding, in: Comprehensive Natural Products Chemistry. Elsevier, pp. 5–29.

Gleixner, G., Mügler, I., 2007. Compound-Specific Hydrogen Isotope Ratios of Biomarkers: Tracing Climatic Changes in the Past, in: Stable Isotopes as Indicators of Ecological Change. Elsevier, pp. 249–265.

Gray, J., Song, S.J., 1984. Climatic implications of the natural variations of D/H ratios in tree ring cellulose. Earth and Planetary Science Letters 70, 129–138.

Habermehl, G.G.K., Hammann, P.E., Krebs, H.C., Ternes, W., 2008. Naturstoffchemie. Springer Berlin Heidelberg, Berlin, Heidelberg.

Hayes, J.M., 2001. Fractionation of Carbon and Hydrogen Isotopes in Biosynthetic Processes. Reviews in Mineralogy and Geochemistry 43, 225–277.

Horita, J., Vass, A.A., 2003. Stable-Isotope Fingerprints of Biological Agents as Forensic Tools. Journal of Forensic Sciences 48.

Knowles, J.R., Albery, W.J., 1977. Perfection in enzyme catalysis: the energetics of triosephosphate isomerase. Accounts of Chemical Research 10, 105–111.

Kreuzer-Martin, H.W., Chesson, L.A., Lott, M.J., Dorigan, J.V., Ehleringer, J.R., 2004. Stable Isotope Ratios as a Tool in Microbial Forensics—Part 1. Microbial Isotopic Composition as a Function of Growth Medium. Journal of Forensic Sciences 49, 1–7.

Kreuzer-Martin, H.W., Jarman, K.H., 2007. Stable isotope ratios and forensic analysis of microorganisms. Applied and environmental microbiology 73, 3896–3908.

Kreuzer-Martin, H.W., Lott, M.J., Dorigan, J., Ehleringer, J.R., 2003. Microbe forensics: oxygen and hydrogen stable isotope ratios in Bacillus subtilis cells and spores. Proceedings of the National Academy of Sciences of the United States of America 100, 815–819.

Leaney, F.W., Osmond, C.B., Allison, G.B., Ziegler, H., 1985. Hydrogen-isotope composition of leaf water in C3 and C 4 plants: its relationship to the hydrogen-isotope composition of dry matter. Planta 164, 215–220.

Lehmann, J., Kleber, M., 2015. The contentious nature of soil organic matter. Nature 528, 60–68.

Liang, C., Balser, T.C., 2011. Microbial production of recalcitrant organic matter in global soils: implications for productivity and climate policy. Nature reviews. Microbiology 9.

Mambelli, S., Bird, J.A., Gleixner, G., Dawson, T.E., Torn, M.S., 2011. Relative contribution of foliar and fine root pine litter to the molecular composition of soil organic matter after in situ degradation. Organic Geochemistry.

Martin, J.P., Haidfr, K., Farmkr, W.J., Fustec-Mathon, E., 1974. Decomposition and distribution of residual activity of some ^{13}C-microbial polysaccharides and cells, glucose, cellulose and wheat straw in soil. Soil Biology and Biochemistry 6, 221–230.

Meentemeyer, V., 1978. Macroclimate and Lignin Control of Litter Decomposition Rates. Ecology 59, 465–472.

Pagano, T., Bida, M., Kenny, J., 2014. Trends in Levels of Allochthonous Dissolved Organic Carbon in Natural Water: A Review of Potential Mechanisms under a Changing Climate. Water 6, 2862–2897.

Paul, A., Hatté, C., Pastor, L., Thiry, Y., Siclet, F., Balesdent, J., 2016. Hydrogen dynamics in soil organic matter as determined by 13 C and 2 H labeling experiments. Biogeosciences 13, 6587–6598.

Preston, C.M., Nault, J.R., Trofymow, J.A., Smyth, C., 2009. Chemical Changes During 6 Years of Decomposition of 11 Litters in Some Canadian Forest Sites. Part 1. Elemental Composition, Tannins, Phenolics, and Proximate Fractions. Ecosystems 12, 1053–1077.

Rieder, S.V., Rose, I.A., 1959. The mechanism of the triosephosphate isomerase reaction. The Journal of biological chemistry 234, 1007–1010.

Roden, J.S., Lin, G., Ehleringer, J.R., 2000. A mechanistic model for interpretation of hydrogen and oxygen isotope ratios in tree-ring cellulose. Geochimica et Cosmochimica Acta 64, 21–35.

Rundel, P.W., Stichler, W., Zander, R.H., Ziegler, H., 1979. Carbon and hydrogen isotope ratios of bryophytes from arid and humid regions. Oecologia 44, 91–94.

Ruppenthal, M., Oelmann, Y., del Valle, H.F., Wilcke, W., 2015. Stable isotope ratios of nonexchangeable hydrogen in organic matter of soils and plants along a 2100-km climosequence in Argentina: New insights into soil organic matter sources and transformations? Geochimica et Cosmochimica Acta 152, 54–71.

Ruppenthal, M., Oelmann, Y., Wilcke, W., 2010. Isotope ratios of nonexchangeable hydrogen in soils from different climate zones. Geoderma 155, 231–241.

Ruppenthal, M., Oelmann, Y., Wilcke, W., 2013. Optimized demineralization technique for the measurement of stable isotope ratios of nonexchangeable H in soil organic matter. Environmental Science & Technology 47, 949–957.

Sachse, D., Billault, I., Bowen, G.J., Chikaraishi, Y., Dawson, T.E., Feakins, S.J., Freeman, K.H., Magill, C.R., McInerney, F.A., van der Meer, M.T.J., Polissar, P., Robins, R.J., Sachs, J.P., Schmidt, H.-L., Sessions, A.L., White, J.W.C., West, J.B., Kahmen, A., 2012. Molecular Paleohydrology: Interpreting the Hydrogen-Isotopic Composition of Lipid Biomarkers from Photosynthesizing Organisms. Annual Review of Earth and Planetary Sciences 40, 221–249.

Sanchez-Bragado, R., Serret, M.D., Marimon, R.M., Bort, J., Araus, J.L., 2019. The Hydrogen Isotope Composition δ^2H Reflects Plant Performance. Plant physiology 180, 793–812.

Sauer, P.E., Schimmelmann, A., Sessions, A.L., Topalov, K., 2009. Simplified batch equilibration for D/H determination of non-exchangeable hydrogen in solid organic material. Rapid communications in mass spectrometry 23, 949–956.

Savin, S.M., Hsieh, J.C.C., 1998. The hydrogen and oxygen isotope geochemistry of pedogenic clay minerals: principles and theoretical background. Geoderma 82, 227–253.

Schimmelmann, A., 1991. Determination of the concentration and stable isotopic composition of nonexchangeable hydrogen in organic matter. Analytical chemistry 63, 2456–2459.

Schimmelmann, A., Sessions, A.L., Mastalerz, M., 2006. Hydrogen isotopic (D/H) composition of organic matter during diagenesis and thermal maturation. Annual Review of Earth and Planetary Sciences 34, 501–533.

Schmidt, M.W.I., Torn, M.S., Abiven, S., Dittmar, T., Guggenberger, G., Janssens, I.A., Kleber, M., Kögel-Knabner, I., Lehmann, J., Manning, D.A.C., Nannipieri, P., Rasse, D.P., Weiner, S., Trumbore, S.E., 2011. Persistence of soil organic matter as an ecosystem property. Nature 478, 49–56.

Sessions, A.L., 2016. Factors controlling the deuterium contents of sedimentary hydrocarbons. Organic Geochemistry 96, 43–64.

Sessions, A.L., Sylva, S.P., Summons, R.E., Hayes, J.M., 2004. Isotopic exchange of carbon-bound hydrogen over geologic timescales 1 1Associate editor: J. Horita. Geochimica et Cosmochimica Acta 68, 1545–1559.

Sheppard, S.M.F., Gilg, H.A., 1996. Stable isotope geochemistry of clay minerals. Clay Minerals 31, 1–24.

Simpson, A.J., Song, G., Smith, E., Lam, B., Novotny, E.H., Hayes, M.H.B., 2007. Unraveling the structural components of soil humin by use of solution-state nuclear magnetic resonance spectroscopy. Environmental Science & Technology 41, 876–883.

Suess, H.E., Urey, H.C., 1956. Abundances of the Elements. Reviews of Modern Physics 28, 53–74.

Voroney, R.P., Paul, E.A., Anderson, D.W., 1989. Decomposition of wheat straw and stabilization of microbial products. Canadian journal of soil science, 63–77.

Wallenstein, M.D., Hall, E.K., 2012. A trait-based framework for predicting when and where microbial adaptation to climate change will affect ecosystem functioning. Biogeochemistry 109, 35–47.

Wardle, D., Yeates, G., Barker, G., Bonner, K., 2006. The influence of plant litter diversity on decomposer abundance and diversity. Soil Biology and Biochemistry 38, 1052–1062.

Wassenaar, L.I., Hobson, K.A., 2000. Improved Method for Determining the Stable-Hydrogen Isotopic Composition (δD) of Complex Organic Materials of Environmental Interest. Environmental Science & Technology 34, 2354–2360.

Whitman, C.P., 1999. Keto–Enol Tautomerism in Enzymatic Reactions, in: Comprehensive Natural Products Chemistry. Elsevier, pp. 31–50.

Wickings, K., Grandy, A.S., Reed, S.C., Cleveland, C.C., 2012. The origin of litter chemical complexity during decomposition. Ecology letters 15, 1180–1188.

Yakir, D., 1992. Variations in the natural abundance of oxygen-18 and deuterium in plant carbohydrates. Plant, Cell and Environment 15, 1005–1020.

Yakir, D., Deniro, M.J., 1990. Oxygen and Hydrogen Isotope Fractionation during Cellulose Metabolism in Lemna gibba L. Plant physiology 93, 325–332.

Yapp, C.J., Epstein, S., 1982. A reexamination of cellulose carbon-bound hydrogen δD measurements and some factors affecting plant-water D/H relationships. Geochimica et Cosmochimica Acta 46, 955–965.

Ziegler, H., Osmond, C.B., Stichler, W., Trimborn, P., 1976. Hydrogen isotope discrimination in higher plants: Correlations with photosynthetic pathway and environment. Planta 128, 85–92.

Section B

Incorporation of Hydrogen from Ambient Water into the C-bonded H Pool during Litter Decomposition

Arnim Kessler[1], Katharina Kreis[1], Stefan Merseburger[2], Wolfgang Wilcke[2] and Yvonne Oelmann[1]

[1] *Geoecology. University of Tübingen. Tübingen. Germany*

[2] *Institute of Geography and Geoecology. Karlsruhe Institute of Technology (KIT). Karlsruhe. Germany*

Author	Author number	Scientific Idea	Experimental Work	Data Analysis and Interpretation	Paper Writing
Arnim Kessler	1.	0 %	70 %	40 %	40 %
Katharina Kreis	2.	0 %	30 %	10 %	0 %
Stefan Merseburger	3.	0 %	0 %	0 %	5 %
Wolfgang Wilcke	4.	30 %	0 %	20 %	15 %
Yvonne Oelmann	5.	70 %	0 %	30 %	40 %

Title

Incorporation of Hydrogen from Ambient Water into the C-bonded H Pool during Litter Decomposition

Status of publication

Published in *Soil Biology and Biochemistry*

Soil Biology and Biochemistry **2021**, 162 (9), 108407

DOI: 10.1016/j.soilbio.2021.108407

1. Abstract

Aridity was observed to affect the C-bonded stable H isotope ratios (δ^2H_n values) of aboveground plant organic matter but not δ^2H_n values of associated soil organic matter (SOM). Instead, δ^2H_n values of SOM correlate spatially with long-term mean δ^2H values of local rainfall. To explain this discrepancy, we investigated if and to which degree C-bonded H was replaced by ambient water-H during leaf litter decomposition in laboratory microcosms.

In a four-week incubation of leaf litter (*Fagus sylvatica* L. - beech, *Acer pseudoplatanus* L. - maple) with two H-isotopically labeled waters (δ^2H_{iw}: +50 ‰, +250 ‰), we found a small incorporation of isotopically labeled H into the C-bonded H pool (<5 % of total C-bonded H) in beech litter. For the leached, more reactive total organic matter in solution (TOM), we estimated that 8-9 % of C-bonded H was replaced by the isotope label during incubation. We suggest that the small incorporation of H from ambient water can be attributed to microbial processes.

However, the small incorporation of H from ambient water during microbial processing would not be sufficient to overprint the aridity signal present in plant organic matter and shift δ^2H_n values of SOM towards those of long-term rainfall. This supports the suggestion, that SOM originates from belowground sources including roots and microorganisms, which inherently show δ^2H_n values related with those of long-term rainfall.

2. Introduction

Stable H isotope ratios in soil organic matter (SOM) can be used as a tool to identify SOM proveniences or they can serve as a proxy for rainfall δ^2H values and thus, for paleoclimate (Kreuzer-Martin et al., 2004; Schimmelmann et al., 2006, Sessions, 2016). Along a 2500-km climosequence in Argentina, it was shown that the H isotope signature of the C-bonded H pool (δ^2H_n values) in SOM was driven by the local long-term rainfall H isotope composition and that existing aridity signals in the C-bonded H pool of aboveground plant biomass were absent in that of SOM (Ruppenthal et al., 2015). It is known that C-bonded H in SOM preserves its inherited δ^2H_n value and does not exchange with water-H at temperatures usually occurring in soil environments at the earth surface (Schimmelmann et al., 2006; Sessions et al., 2004). Therefore, the finding of a close correlation between δ^2H_n values of SOM and rainfall was unexpected at first glance, because the leveling of the aridity signals would have required a fast exchange of the C-bonded H pool with ambient water.

There are two non-exclusive explanations for this discrepancy. The first one is related to plant-internal processes before plant litter enters the SOM pool. Transpiration in response to air humidity and mixing with water vapor causes that leaf water is enriched in ^2H compared to the source water taken up via roots (e.g. precipitation) (Craig and Gordon 1965; Dongmann et al. 1974). The transpirational

enrichment of leaf water increases with increasing aridity (Cernusak et al., 2016). Photosynthetic isotope fractionation causes that δ^2H_n values of leaves (organic matter) are lower than δ^2H values of precipitation (Cormier et al., 2018; Hayes, 2001; Yakir, 1992). Assuming a constant ^2H fractionation factor associated with photosynthesis, assimilates become enriched in ^2H producing H-isotopically heavier leaf tissue under arid than under humid conditions (Hayes, 2001; Roden et al., 2000; Sanchez-Bragado et al., 2019). While this process is well documented in compound-specific studies for cellulose (Epstein et al., 1977; Yapp and Epstein, 1982), studies about the aridity effect on δ^2H_n values of bulk organic matter are rare (Rundel et al., 1979; Leaney et al., 1985; Ziegler et al., 1976). However, during the transport of assimilates through the plant and the further processing during biosynthesis reactions, the leaf water signal eventually gets lost. The resulting biosynthesized compounds reflect the H isotopic signal of the ambient cell water which might more closely resemble that of soil water (Roden and Ehleringer, 2000; Yakir and DeNiro, 1990; Yakir, 1992). This has been shown for n-alkanes from terrestrial plants (Sachse et al., 2012) and tree-ring cellulose (Gray and Song et al., 1984), which might already show an H isotopic composition that is closer to soil water and thus related with that of mean local precipitation (Gori et al., 2013; Kimak et al., 2015). Along the climosequence in the study of Ruppenthal et al. (2015), the aridity effect was present in the leaves, but no longer observable in the roots likely because assimilates transported to the roots served as educts of biosynthesis reactions associated with the incorporation of root-water H, which is H-isotopically close to soil water. Simultaneously, there was a strong correlation of δ^2H_n values of roots on δ^2H_n values of SOM (Ruppenthal et al., 2015). From these findings, the authors concluded that the belowground root biomass made a major contribution to SOM (Ruppenthal et al., 2015).

The second explanation for the relationship between δ^2H values of SOM and rainfall, which could also take place subsequently to plant biosynthesis reactions described above, relates to processes occurring when plant litter enters the SOM pool. During decomposition of organic matter, recalcitrant compounds like lignin are accumulated (Berg and McClaugherty, 2014; Wickings et al., 2012) while cellulose is rather lost from than accumulated in SOM (Preston et al., 2009). Because there are compound-specific δ^2H_n values, the preferential decomposition of organic compounds with distinct δ^2H_n values could systematically change the δ^2H_n values of litter-derived SOM during decomposition (DeBond et al., 2013). However, this process would not necessarily drive the δ^2H_n values of SOM derived from aboveground litter towards that of soil water and therefore is an unlikely explanation for the loss of the aridity signal in aboveground biomass. An alternative explanation would be that ambient water-H was rapidly incorporated into SOM by its microbial processing. This process is different from the rapid exchange between H in air moisture and ambient soil water and the exchangeable H pool (e.g., the H in hydroxyl groups) in SOM because it affects the C-bonded H as well. Common methods to measure δ^2H_n values account for the exchangeable H pool e.g., by steam equilibration (Ruppenthal et al., 2010; Wassenaar and Hobson, 2000) and use mass balance calculations to determine the nonexchangeable, C-bonded H pool. These methods can only distinguish

between readily exchangeable H mainly by physico-chemical equilibration and C-bonded H but they cannot reveal the history of H incorporated into the C-bonded H pool by enzymatic metabolic processes inside organism cells. Therefore, the incorporation needs to be traced in labeling experiments in which ambient water with δ^2H values that differ from natural abundance levels are used. Based on this approach, several studies corroborated that C-H bonds are regularly broken and reattached during microbial metabolism (Horita and Vass, 2003; Kreuzer-Martin et al., 2003, 2004). The microbial metabolism is associated with an incorporation of ambient water-H into C-bonded H of the microbial metabolites in the range of 20 to 50 % during up to four days (Horita and Vass, 2003; Kreuzer-Martin et al., 2003, 2004). In these short-term studies, particular microbial species were grown under optimum conditions (temperature, pH, availability of nutrients and C sources). In a one-year incubation, Paul et al. (2016) showed that more than 70 % of C-bonded H in lipids originated from ^2H-labeled ambient water. However, lipids, proteins, amino acids and other microbial cell compounds might not be representative for the variety of compounds present in natural organic matter. Therefore, the extent of incorporation of ambient water-H into the C-bonded H pool during decomposition of SOM by the associated microbial community yet awaits to be shown.

The extent of incorporation of ambient water-H into C-bonded H by metabolic processes inside cells might be related with the properties of the organic matter that drive decomposition rates. Faster decomposition associated with a high microbial activity should result in more pronounced microbial H incorporation into the C-bonded H pool. Litter decomposition rates vary widely among species (Cornelissen, 1996; Wardle et al., 1997) and plant litter properties have a marked influence on decomposition rates (Fogel and Cromack, 1977; Gartner and Cardon, 2004; Meentemeyer, 1978; Millar et al., 1936; Mindermann, 1968). Different studies reported tree species-specific trends of mass loss during decomposition: *Quercus rubur* LINNÉ, *Sorbus aucuparia* L. and *Acer pseudoplatanus* L. showed faster decomposition rates than *Picea abies* L., *Pinus sylvestris* L. and *Fagus sylvatica* L. (Angst et al., 2019; Don and Kalbitz, 2005; Joly et al., 2016; Zech et al., 2011).

During microbial decomposition not only the solid phase of leaf litter is affected by transformation processes but also new compounds like sugars and proteins which are partly water-soluble are synthesized. Leached total organic matter (TOM) in solution consists of a complex mixture of aromatic and alipathic, C-rich compounds of different sizes and chemical structure (Dilling and Kaiser, 2002; Pagano et al., 2014). Degradation products such as amino acids as well as microbial metabolites are released into soil solution during the decomposition process (Habermehl et al., 2008; Mambelli et al., 2011; Martin et al., 1974; Voroney and Paul, 1989). Since degradation products and microbial metabolites underwent biosynthesis reactions potentially associated with the incorporation of ambient water-H into the C-bonded H pool, δ^2H_n values of leached TOM might more closely resemble δ^2H values of ambient water than δ^2H_n values of the solid-state organic matter during decomposition.

Our objective was to determine, whether there is microbially-mediated incorporation of ambient water-H into organic matter during decomposition of aboveground plant litter. We hypothesized that (1) isotopically labeled (^{2}H enriched) ambient water-H is measurably incorporated into the C-bonded H pool of leaf litter (*F. sylvatica* and *A. pseudoplatanus*) during decomposition in a short period of time of four weeks. Furthermore, (2) the incorporation of ambient water-H into the C-bonded H pool is higher in leached TOM than the remaining solid-state leaf litter. Finally, we postulated that (3) the incorporation of ambient water-H into leaf litter and leached TOM depends on the litter quality of the two tree species (*A. pseudoplatanus* > *F. sylvatica*).

3. Material and Methods

3.1. Study sites, sampling and sample processing before incubation

In May 2018, we sampled leaf litter of *F. sylvatica* (beech) and *A. pseudoplatanus* (maple) from two forest sites in the Schönbuch which covers an area of 156 km² in southern Germany. In 2018, mean annual temperature recorded at a weather station in proximity to the sites was 11.4 °C and mean annual precipitation was 506 mm (WetterKontor GmbH, 2021). The beech site (9.1087, 48.5616; WGS84) is located in the Stadtwald Tübingen and is characterized by mainly *F. sylvatica* trees with a minor contribution of *Quercus robur* L. (oak). The maple site (9.0577, 48.5764; WGS84) is dominated by old maple trees with a few oak trees in patches. The parent material of the soils is loess resulting in Cambisols (beech site) and Luvisols (maple site, IUSS Working Group WRB, 2014). At each site, we sampled the Oi horizon in three plots of 10 m x 10 m (100 m²). In the laboratory, sampled beech and maple leaf litter samples were cleaned from leaf litter material of the accompanying vegetation, from adhering soil, fruits and macrofauna and manually homogenized. Then, leaf litter was dried for 48 h at 40 °C. Aliquots of all leaf samples were taken as t_0 samples just before incubating them.

3.2. Incubation and sample processing after incubation

For incubation, we used HDPE plastic containers with a volume of two liters and equipped with a screw cap (VWR chemicals, Germany). To collect leachates, a short tube (PVC) with a plug was inserted at the lower side (Fig. B-1). Ten g of dry leaf litter samples were placed into each container. Leaf litter samples were incubated for four weeks. We used two water labels (δ^2H ca. +50 ‰ and +250 ‰) which were produced by mixing deionized water (δ^2H = -75 ‰) with the corresponding volume of deuterated water (> 99.99 % ^{2}H, Deuterium Oxide, Campro Scientific, Germany) according to an isotopic mass balance calculation (Faghihi et al., 2015). The δ^2H values of the labels were, however, not measured. In total, there were 48 incubation containers: two leaf litter types x two water labels x four time intervals (one, two, three, and four weeks) x three replicates. Twice per week,

400 mL of ^{2}H-enriched water was percolated through the respective incubation containers within one hour while the leached TOM was collected by draining the water via the previously installed tube at the bottom of the incubation containers without filtration (Fig. B-1).

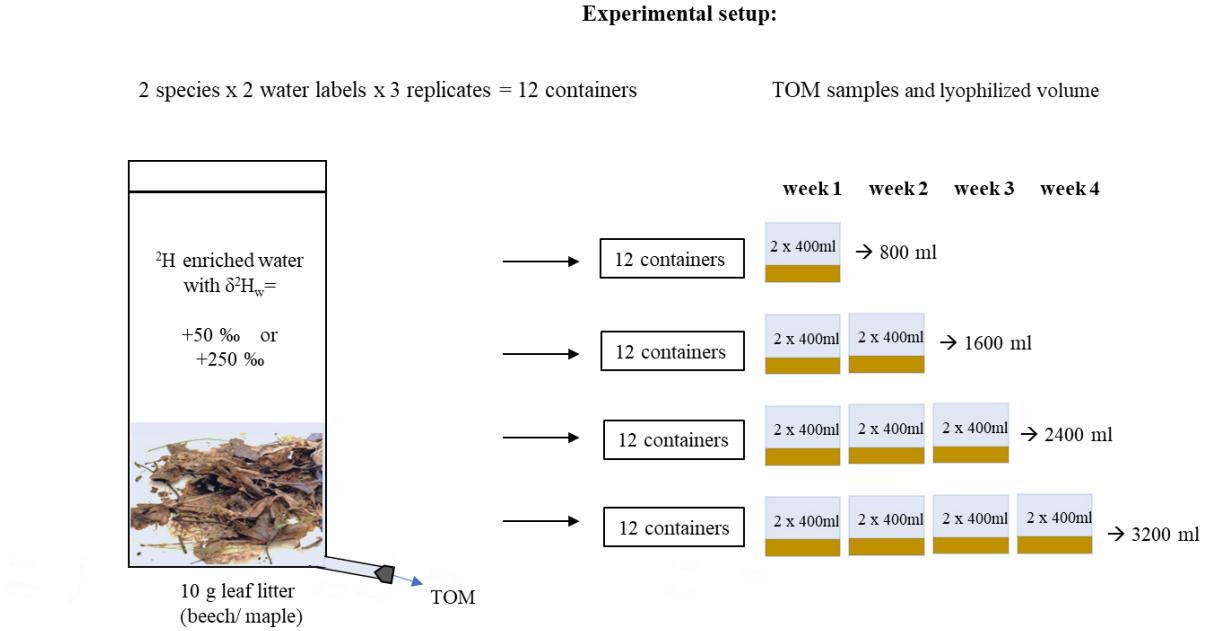

Fig. B-1: Experimental setup of the incubation experiment and the sampling design. Two litter types (beech/maple) were incubated with 400 mL of ^{2}H enriched water twice a week in three replicates, resulting in 12 containers per time interval.

After draining the water, leached TOM samples were immediately frozen at -20 °C. TOM samples of the two percolating events within one week were defrosted, combined per container, frozen again and subsequently lyophilized (LyoCube 4-8 LSCplus, Martinchrist, Germany) which yielded a solid sample. For the first week, we used the combined TOM samples of week one. For the other time intervals (two to four weeks) we again combined the weekly leached TOM (container-wise) according to the incubation intervals (week one + week two for the two-week interval etc.). Leached TOM was ground (Pulverisette 5, Fritsch GmbH, Germany). For solid leaf litter samples, each week one set (two leaf litter types x two water labels x three replicates = 12) of solid litter samples was sacrificed, dried for 48 h at 40 °C, weighed and ground (Pulverisette 5, Fritsch GmbH, Germany).

3.3. Steam equilibration

To account for the exchangeable pool of H (H_{ex}) that does not carry a robust isotope signal of the leaf litter and the leached TOM, we used the equilibration device of Ruppenthal et al. (2013) which was modified from Wassenaar and Hobson (2000). The equilibration device consists of a stainless steel vacuum vessel which was loaded with samples in tin capsules (0.025 mL, 2.9 x 6 mm, IVA

Analysentechnik GmbH+Co KG, Germany) held upright by a brass sample holder (Fig. B-S1). For the steam equilibration, we used three waters of measured δ^2H_w values (AWI = -268 ‰, ^{2}H-enriched = +113 ‰ and deionized water= -75 ‰) resulting in three aliquots of one and the same sample that were each equilibrated with a different water. This approach guarantees the full exchange of the isotopically exchangeable H with the equilibrium water-H (Ruppenthal et al., 2010).

Equilibration water (3.5 mL; corresponding to a ratio of equilibration water H to exchangeable sample H of at least 100:1) was injected into the evacuated vessel through a silicone rubber septum. Equilibration took place by disconnecting the vessel from the rest of the vacuum line with the help of quick connectors (Swagelok Company, USA), and placing it in a fan-assisted heating oven at 120 °C overnight. The next morning, the vacuum vessel was reconnected to the vacuum line, the equilibration water vapor was evacuated and the residual heat of the heavy stainless-steel vessel was used to simultaneously dry the samples for approx. 2 h. Once the vessel had cooled down, it was repressurized back to ambient pressure with dried Ar gas (purity grade 5.0). Flushing the device with dried argon gas was supposed to avoid isotopic reequilibration of equilibrated samples with ambient moisture. While the Ar continuously flew into the vessel, the equilibrated samples were sealed airtight with end cutting pliers and transferred to the Thermal Conversion/Elemental Analyzer-Isotope Ratio Mass Spectrometer (TC/EA-IRMS) autosampler for δ^2H analysis. The time between removing a sample from the argon-filled vessel and sealing it never exceeded 30 s, thus minimizing the risk of reequilibration with ambient moisture. To test the seal of tin capsules when using end cutting pliers, we monitored the weight loss of three sealed capsules containing acetone at room temperature over a period of one month. We did not detect any measurable weight loss that would otherwise have indicated that evaporated acetone escaped from the capsules. Therefore, we inferred that there was no exchange between Ar and ambient air in the capsules containing the equilibrated leaf litter and leached TOM samples.

3.4. Chemical analyses

After the steam equilibration, stable hydrogen isotope ratios of leaf litter and leached TOM samples were measured with a TC/EA-IRMS device (vario PYRO Cube and IsoPrime 100, Elementar Analysesysteme GmbH, Germany). Samples were pyrolyzed in the EA reactor at 1450 °C. The glassy carbon tube of the EA was packed with glassy carbon granules and a glassy carbon cup was placed on the granules to collect the molten tin and sample ash residues. Blank tin capsules did not show a measurable H_2 blank. The correction factor for H_3^+ ions produced in the ion source was determined before each batch of 120 samples using the automated procedure of the IRMS software (Ion Vantage, Elementar, Germany). The H_3^+-correction factor varied between 7.2 and 7.8 ppm nA^{-1}. For calibration of measured δ^2H values before each batch of samples, three certified international laboratory standards (VSMOW2, USGS46 and GISP) were used. The certified H isotope reference materials VSMOW2

(certified as 0±0.4 ‰) or USGS46 (certified as -235.8±0.7 ‰) were included as duplicate or triplicate measurements to determine precision and accuracy of our measurement and yielded δ^2H values of -0.4±4.6 ‰ (n = 15) and -237.3±2.3 ‰ (n = 15), respectively. The reproducibility of an internal laboratory standard (PE foil) was -67.7±1.7 ‰ (n = 30). Additionally, we measured C and N concentrations of initial leaf litter (before incubation), the remaining leaf litter (after each incubation interval) and leached TOM. For the analyses, 5-10 mg of each sample was weighed in and subsequently analyzed with the vario EL III Element Analyzer (Elementar Analysesysteme GmbH, Germany).

3.5. Calculations and statistical evaluation

The mass loss of leaf litter expressed as the lost fraction of the initial C stock (%) was calculated as the difference in litter C mass before (t_0) and after (t_i) incubation and related to litter C mass before incubation (t_0; Eq. 1). Litter C mass is the product of litter mass (M litter) and C concentration (CC litter) at each point in time (Eq. 1).

$$C\,mass\,loss[\%] = \frac{(M\ litter\,t_0[g] \times CC\,litter\,t_0[mg\,g^{-1}]) - (M\,litter\,t_i[g] \times CC\,litter\,t_i[mg\,g^{-1}])}{(M\ litter\,t_0[g] \times CC\,litter\,t_0[mg\,g^{-1}])} \times 100 \qquad (1)$$

The relative C mass loss comprises gaseous (respired CO_2) and dissolved (dissolved organic C) loss. Similar to relative C mass loss, we related the dissolved C mass at a given point in time (t_i) to C mass before incubation (t_0) to yield the relative leached, dissolved C mass loss (in %, Eq. 2). Dissolved C mass loss was calculated as the product of the mass of leached TOM and the corresponding C concentration at the respective points in time (Fig. S2).

$$Dissolved\,C\,mass\,loss[\%] = \frac{(M\,TOM\ t_i[g] \times CC\,TOM\ t_i[mg\,g^{-1}])}{(M\,litter\,t_i[g] \times CC\,litter\,t_i[mg\,g^{-1}])} \times 100 \qquad (2)$$

The contribution of respired C can then be calculated as the difference between the total C mass loss and the dissolved C mass loss. The proportion of C-bonded H with the respective δ^2H_n value of each sample was calculated with a mass balance approach adopted by Ruppenthal et al. (2010). The total H (H_t) pool is composed of an exchangeable H pool (H_{ex}) that isotopically exchanges with water and a C-bonded H pool (H_n) with respective δ^2H_{ex} and δ^2H_n values. Hence, δ^2H values of the total pool (δ^2H_t values) measured in the laboratory for total sample H can be expressed as shown in Eq. (1) (Feng et al., 1993; Filot et al., 2006; Schimmelmann, 1991; Wassenaar and Hobson, 2000):

$$\delta^2 H_t = (1 - x_e)\delta^2 H_n + x_e \delta^2 H_{ex} \quad (3)$$

χ_e represents the H pool that isotopically exchanged during equilibration. For different organic compounds, this pool varies from 0.0 for simple hydrocarbons up to 0.4 (i.e. 40 wt.% of H_t) for complex compounds like cellulose, kerogen or humic acid (Feng et al., 1993; Filot et al., 2006; Schimmelmann, 1991; Wassenaar and Hobson, 2000). In SOM, the fraction of isotopically exchangeable H varies substantially and depends on litter quality input and the degree of humification. If the exchangeable H pool of a sample reaches isotopic equilibrium with the equilibration water, the δ^2H_{ex} value is related to the δ^2H value of the equilibration water (δ^2H_w) with the equilibrium fractionation factor ($\alpha_{ex\text{-}w}$, Eq. 4) (Ruppenthal et al., 2010).

$$\alpha_{ex-w} = \frac{\delta^2 H_{ex} + 1000}{\delta^2 H_w + 1000} \quad (4)$$

The equilibrium fractionation factor $\alpha_{ex\text{-}w}$ depends on the chemical composition of the analyzed samples and the equilibration temperature (Feng et al., 1993; Filot et al., 2006; Schimmelmann, 1991; Wassenaar and Hobson, 2000). However, for chemically complex organic substances, direct experimental determination of $\alpha_{ex\text{-}w}$ is difficult because it would be necessary to asses $\alpha_{ex\text{-}w}$ values through δ^2H values of isotopically equilibrated samples with those of samples with chemically removed H (Wassenaar and Hobson, 2000). Past studies used an approximation of $\alpha_{ex\text{-}w}$ for substances like cellulose, humic acid, kerogen, keratin or collagen (Filot et al. 2006; Sauer et al., 2009; Schimmelmann et al., 1999; Wassenaar and Hobson, 2000). Here, for $\alpha_{ex\text{-}w}$, a provisional value of 1.08 was assigned, which is based on the cellulose equilibrium isotopic fractionation factor between isotopically exchangeable H and water-H at 114 °C, which has been experimentally determined (Schimmelmann, 1991). Via a sensitivity analysis over a $\alpha_{ex\text{-}w}$ range of 1.06 to 1.10, Schimmelmann et al. (1999) and Wassenaar and Hobson (2000) showed, that the use of provisional $\alpha_{ex\text{-}w}$ value is admissible while the isotopic shift, which is caused by the equilibration procedure is a function of isotopically exchangeable H and χ_e. Therefore, in our study, we used a $\alpha_{ex\text{-}w}$ value of 1.08.

If χ_e is constant among aliquots, a plot of δ^2H_t versus δ^2H_w should result in a straight line, defined by Eq. 5, which is obtained by solving Eq. 4 for δ^2H_{ex} and substituting into Eq. 3 (Ruppenthal et al., 2010).

$$\delta^2 H_t = x_e \alpha_{ex-w} \delta^2 H_w + (1 - x_e)\delta^2 H_n + 1000 x_e (\alpha_{ex-w} - 1) \quad (5)$$

When all of isotopically exchangeable H is in equilibrium with the water-H, the δ^2H_n value from Eq. 3 is equivalent to δ^2H value of the C-bonded H in the sample. Therefore, δ^2H_n can be calculated by rearranging Eq. 5 to Eq. 6 (Ruppenthal et al., 2010).

$$\delta^2 H_n = \frac{\delta^2 H_t - 1000 x_e (\alpha_{ex-w} - 1) - x_e \alpha_{ex-w} \delta^2 H_w}{(1 - x_e)} \quad (6)$$

Uncertainty in the isotopic sample equilibration and errors concerning the determination of δ^2H_n values can be caused by different physical conditions during equilibration e.g., temperature fluctuations. To increase the reliability of the regression analysis of δ^2H_t values on δ^2H_w values of equilibrated samples and an increase of the accuracy of δ^2H_n determinations, we used three isotopically distinct waters for equilibration (Ruppenthal et al., 2010).

To unambiguously differentiate the exchange processes with ^2H-labeled liquid water, air moisture or vapor in the exchangeable H pool, we term the metabolic incorporation of H from ambient water inside cells into the C-bonded H pool by microbial metabolism "incorporation" henceforward. If the δ^2H_w is manipulated, it is possible to trace this incorporation in microbes and in the microbial metabolites after cell lysis. In case of the incubation of natural organic matter with water, the incorporation refers to the mixture of microorganisms (living and dead) and microbially cycled degradation products. The incorporation will shift δ^2H_n values towards the δ^2H_w values of the incubation waters (δ^2H_{iw}). However, the incorporation will be associated with an isotope fractionation factor. If aliquots of the same sample are incubated with waters differing in δ^2H_{iw} values, the fractionation factor can be assumed as identical and thus, the shift only depends on the δ^2H_{iw} value. Consequently, the slope of the regression of the δ^2H_n values on the δ^2H_{iw} values indicates the extent of incorporation of ambient water-H into the C-bonded H pool. In case of no incorporation, there would be no shift in δ^2H_n values and accordingly, a slope of 0 would result. In case of incorporation of the complete C-bonded H pool, a 1:1 relationship between δ^2H_n and δ^2H_{iw} values would result (slope = 1). Commonly, the slope expressed as percentage (i.e., 1 equals 100 %) is used to depict the extent of ambient water-derived H (Luo and Sternberg, 1992; Yakir and DeNiro, 1990). We calculated incorporation for those cases only where two criteria were met namely that (i) δ^2H_n values in the 250 ‰ label increased relative to the initial δ^2H_n values and that (ii) δ^2H_n values differed significantly between the two incubation waters for a given sample. Our incorporation refers to the time interval until leaf litter or leached TOM sampling. Therefore e.g., the incorporation rate of week 4 includes all time intervals from one to four weeks. To determine the net apparent isotope fractionation of ^2H (ε^2H_n) between TOM and leaf litter, we calculated the apparent H isotope fractionation factor based on Eq. 7 according to Coplen (2011):

$$\varepsilon^2 H_{n\ TOM/leaf\ litter} = \frac{\delta^2 H_{n\ TOM} + 1000}{\delta^2 H_{n\ leaf\ litter} + 1000} - 1 \quad (7)$$

All statistical analyses were conducted with SPSS 11.5 (SPSS Inc., USA) and/or Microsoft Excel 2010 (Microsoft Corp., USA) software. Prior to statistical analyses, prerequisites were checked (normal distribution: Shapiro-Wilk test; homogeneity of variances: Levene's test). If normal distribution of residues or variance homogeneity was violated, data were transformed. To approach normal data distribution, data were $\log_{10}$-transformed. We used the Huynh-Feldt- or Greenhose-Geisser-correction according to Girden (1992) in case of heteroscedasticity. Significant differences between tree species or water labels during the temporal course of the incubation were analyzed using repeated measure analysis of variance (rmANOVA) while *t-tests* were *used to* determine differences between the means of the labeled water or tree species.

4. Results

4.1. Litter mass loss

Tree species had significant effects on C:N ratios before and after incubation ($p < 0.001$). Initial leaf litter of beech and maple showed mean C:N ratios of 36.7 ± standard deviation of 0.9 and 30.4±1.8, respectively. C:N ratios after incubation of leaf litter were 36.1±0.9 (beech) and 28.9±1.9 (maple). Conversely, C:N ratios of leached TOM were larger for maple (16.1±1) than for beech (10.2±1.3; $p \leq 0.003$). The mass loss of leaf litter expressed as the lost fraction of the initial C stock was significantly larger for maple than for beech and significantly increased with time (Table B-1; Fig. B-2). After the four-week incubation, approximately one-fourth (maple) and one-fifth (beech) of the initial C stock in the leaf litter was lost (Fig. B-2). The mass loss comprised loss by leaching (TOM) and in gaseous form (respired CO_2). Loss via leached TOM accounted for less than 5 % of the initial C stock and consequently, loss by respired CO_2 (data not shown) represented the majority of the mass loss (Fig. B-2).

Similar to the solid phase, the mass loss by leaching was significantly larger for maple than for beech and increased with time (Table B-1; Fig. B-2). Additionally, the temporal trend of the mass loss by leaching depended on tree species (significant interaction of time x tree species in Table B-1). In general, the larger C mass loss including dissolved C mass loss of maple litter as compared to beech litter was in line with our expectation.

Table B-1: Repeated measure ANOVA results for effects of time, water label (water) and tree species on the mass losses of solid state leaf litter (relative mass loss) and via leached total organic matter in solution (TOM) expressed as the lost fraction of the initial C stock and $\delta^2H_{n\ leaf\ litter}$ values. Non-significant interactions between factors are not displayed. Significant effects are displayed in bold.

Factors	DF	F	P
Relative mass loss			
Time	**3**	**38.60**	**<0.001**
Water	1	3.45	0.100
Tree species	**1**	**11.43**	**0.010**
Mass loss leached TOM			
Time	**3**	**59.25**	**<0.001**
Water	1	0.03	0.862
Tree species	**1**	**66.32**	**<0.001**
Time × Tree species	**3**	**3.16**	**0.043**
$\delta^2H_{n\ leaf\ litter}$			
Time	**3**	**5.46**	**0.016**
Water	**1**	**27.15**	**0.001**
Tree species	**1**	**136.69**	**<0.001**

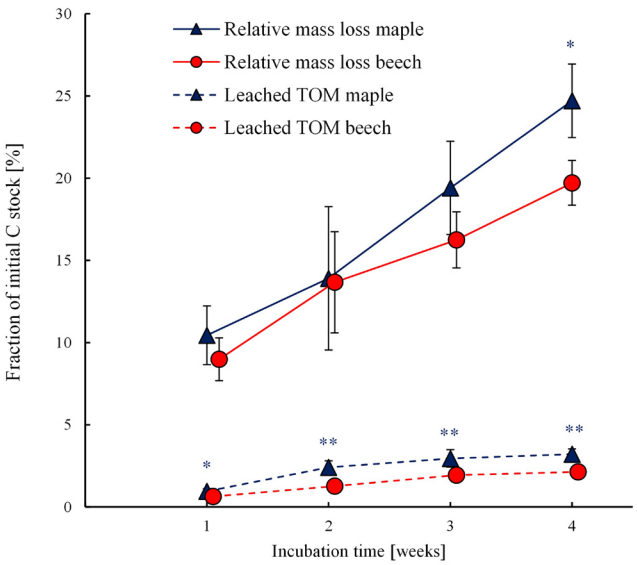

Fig. B-2: Fraction of the initial C stock in leaf litter lost in total (relative mass loss) and via leaching (leached TOM) for beech and maple during the course of the four-week incubation. Error bars show the standard deviations for each time step (n = 6). To ease readability, the sampling times have been shifted slightly. Asterisks indicate significant differences between tree species at a given incubation interval (* p <0.05; ** p <0.01; *** p <0.001).

4.2. Carbon-bonded stable hydrogen isotope ratios of leaf litter

The beech litter had significantly higher $\delta^2H_{n\ leaf\ litter}$ values than that of maple irrespective of incubation time and water label (Table B-1; Fig. B-3a). The $\delta^2H_{n\ leaf\ litter}$ values of both tree species increased with time (Table B-1; Fig. B-3a). The temporal trend was pronounced for the 250 ‰ label but negligible for the 50 ‰ water label (Fig. B-3a). Overall, the water labels produced the intended differences: the $\delta^2H_{n\ leaf\ litter}$ values after incubation with the 250 ‰ label were significantly higher than after incubation with the 50 ‰ label (Table B-1; Fig. B-3a). The analysis of individual time points, however, revealed that the effect of the water labels was more consistent for beech than for maple (asterisks in Fig. B-3a). There were significant δ^2H_n differences between the two sets of leaf litter samples incubated with the two differently labeled waters of 5.3–9.9 ‰ for three out of four intervals for beech and 10.5 ‰ (week 4) for maple. We found that 3 to 5 % of H in the C-bonded pool of beech and maple leaf litter experienced an incorporation of ambient water-H (Fig. B-4). Expressed as weekly rates, the average H incorporation rate was 1.2±0.3 %. The individual $\delta^2H_{n\ leaf\ litter}$ values are provided in Table B-S1.

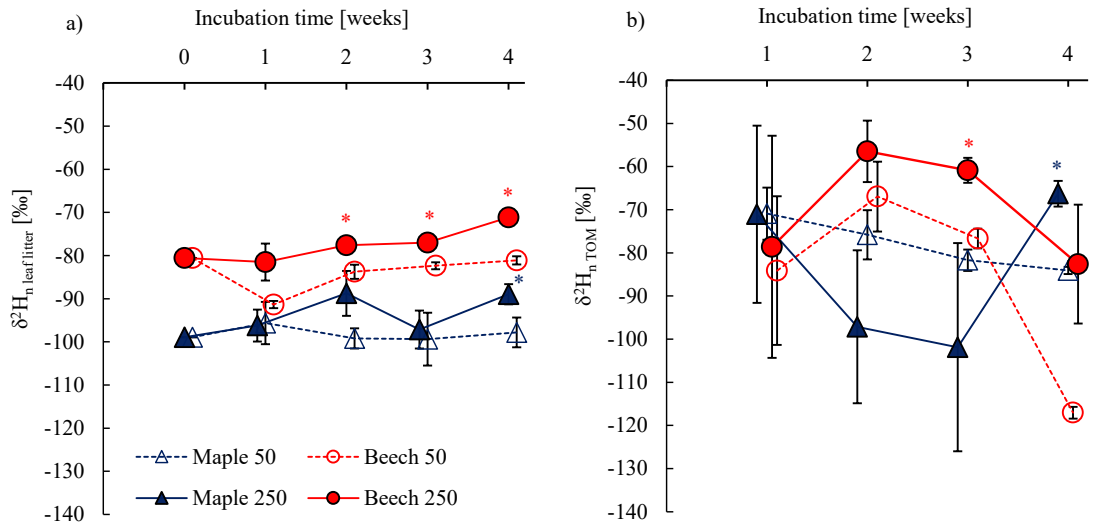

Fig. B-3: $\delta^2H_{n\ leaf\ litter}$ values (a) and $\delta^2H_{n\ TOM}$ values (b) differentiated according to the type of isotopically labelled incubation water (δ^2H_{iW}: +50 ‰, +250 ‰) during the course of the incubation. Error bars show the standard deviation of $\delta^2H_{n\ leaf\ litter}$ and $\delta^2H_{n\ TOM}$ values for each time step (n = 3). To ease readability, the sampling times have been shifted slightly along the x axis. Asterisks indicate that the two criteria (increase in δ^2H_n values, difference between the two water labels) allowed to calculate incorporation of ambient water-H into the C-bonded H pool.

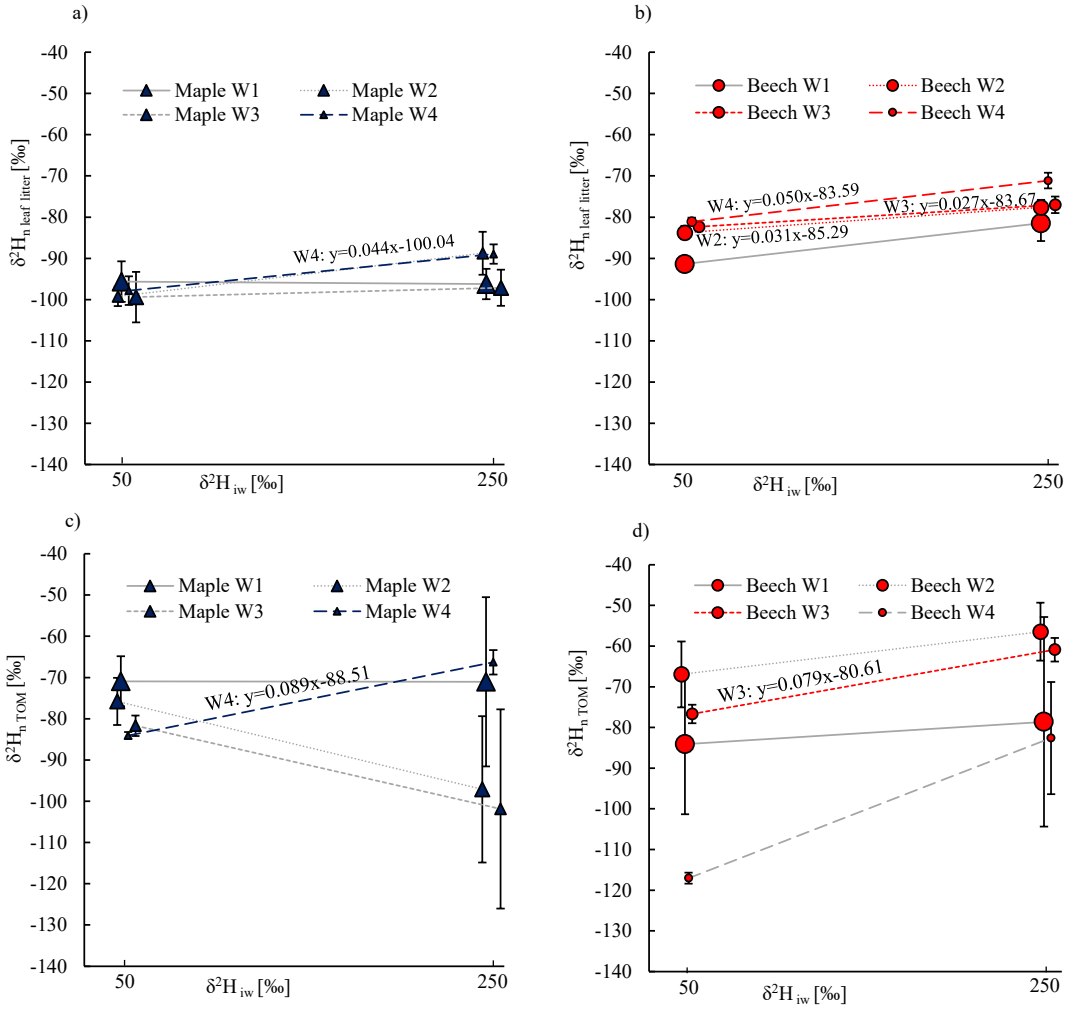

Fig. B-4: Regression of $\delta^2H_{n\ leaf\ litter}$ (a, b) and $\delta^2H_{n\ TOM}$ (c, d) values on δ^2H_{iW} values (+50 ‰, +250 ‰) of maple (a, c) and beech (b, d) for the four different incubation intervals (W1 to W4). The slopes of the regression equations (1 equals 100 %) depict the incorporation of H from isotopically labeled water into the C-bonded H pool (Yakir and DeNiro, 1990; Luo and Sternberg, 1992; Kreuzer-Martin et al., 2003). The linear functions are given above each line except for cases without a significant difference between the two labels (see Fig. 3a, b) and with negative slopes (i.e., δ^2H_n values of the +250 ‰ label were more negative than those of the +50 ‰ label). In these cases, regression lines are displayed in grey. Error bars show the standard deviation of $\delta^2H_{n\ leaf\ litter}$ values for each time step (n = 3). To ease readability, the sampling times have been shifted slightly.

4.3. Carbon-bonded stable hydrogen isotope ratios of leached organic compounds

In general, δ^2H_n values of leached TOM ($\delta^2H_{n\ TOM}$) were not significantly different or higher than the $\delta^2H_{n\ leaf\ litter}$ values (Fig. B-3 and Fig. B-S3). The only exception was the microcosm with leaf litter of beech and the 50 ‰ label after four weeks of incubation where the net apparent isotope fractionation ε^2H_n was significantly negative. After one week of incubation, leached TOM was characterized by

similar $\delta^2H_{n\ TOM}$ values irrespective of tree species and water label (Fig. B-3b). Thereafter, $\delta^2H_{n\ TOM}$ values varied without tree-species effects or a clear temporal pattern (Table B-S2; Fig. B-3b). Nevertheless, $\delta^2H_{n\ TOM}$ values were significantly higher in the samples that had been incubated with the 250 ‰ label than in those that had been incubated with the 50 ‰ label after three weeks (beech: difference of 15.8 ‰) and four weeks (beech: 34.4 ‰ and maple: 17.8 ‰; Fig. 3b). Identical to the calculation of incorporation that we applied for solid-state leaf litter, we used the slope approach for leached TOM. In some cases, we did either not detect a significant difference in $\delta^2H_{n\ TOM}$ values between the samples incubated with the two water labels or $\delta^2H_{n\ TOM}$ values of the sample incubated with the 250 ‰ label were smaller than those incubated with the 50 ‰ label (Fig. B-3b). For these cases, we could not calculate an incorporation (no regression equation in Fig. B-4). For the remaining two other cases, the incorporation of ambient water-H into the C-bonded H pool in leached TOM ranged between 8 and 9 % (Fig. B-4) which is equal to 2.6 and 2.2 % per week. The incorporation of ambient water-H into the C-bonded H pool tended to be larger for leached TOM than for leaf litter (beech: week 3; maple: week 4; Fig. B-4). The individual $\delta^2H_{n\ TOM}$ values are presented in Table B-S1.

5. Discussion

5.1. ^{2}H incorporation into the C-bonded H pool of the leaf litter

The fact that the $\delta^2H_{n\ leaf\ litter}$ values of beech and maple only increased with time during the incubation with the 250 ‰ label but not with the 50 ‰ label (Fig. B-3) illustrates that a strong label is required to detect the small incorporation of ambient water-H into the C-bonded H pool. Therefore, in a natural setting the incorporation of soil-water H (-150 to +20 ‰; Sprenger et al., 2016) during decomposition of litter or SOM likely hardly produces a detectable shift in δ^2H_n values. This increase in $\delta^2H_{n\ leaf\ litter}$ values could, however, also be caused by the accumulation of ^{2}H-enriched compounds during leaf litter decomposition, besides by incorporation of isotopically labeled, ^{2}H-enriched ambient water into the C-bonded H pool of litter. A compound that is known to accumulate during litter decomposition is lignin (Berg and McClaugherty, 2014; Wickings et al., 2012). However, δ^2H values in methoxyl groups of lignin were lower than δ^2H values of wood and cellulose (Gori et al., 2013). Similarly, lignin was shown to be depleted in ^{2}H relative to bulk organic matter and accordingly, lignin accumulation resulted in increasingly ^{2}H-depleted δ^2H values of bulk organic matter with progressing decomposition (DeBond et al., 2013). This is the opposite of what we observed and thus, lignin accumulation cannot serve as an explanation of our results. For cellulose, biosynthesis favors the accumulation of ^{2}H (Cormier et al., 2018) and in line, cellulose was shown to be H-isotopically heavier than bulk OM (DeBond et al., 2013). However, cellulose is lost during decomposition (Preston et al., 2009). Therefore, we did not find evidence that the accumulation of certain compounds could serve as an

explanation of the observed increase in the $\delta^2H_{n\ leaf\ litter}$ values of decomposed leaf litter during incubation with the 250 ‰ label.

The alternative explanation, i.e., incorporation of ^2H-enriched ambient water into the C-bonded H pool would require that the difference between the two water labels increases with progressing incubation as well since the large difference in δ^2H values between the two labeled waters would add up at each subsequent incubation interval. However, we found that the differences in $\delta^2H_{n\ leaf\ litter}$ values of beech and maple leaf litter did not change significantly with time (no interaction between time and label in Table B-1). Furthermore, the calculated percentage of incorporation of ambient water-H into the C-bonded H pool in leaf litter was small (<5 %) and is in contrast with the much higher incorporation (20 to 50 %) reported for microbial culture studies (Fogel et al., 2016; Kreuzer-Martin et al., 2004, 2006). We attribute the small extent of incorporation in our study to that facts that (i) leaf litter is less decomposable than the substrates (e.g., sugars and proteins) used in the microbial culture studies (Fogel et al., 2016; Kreuzer-Martin et al., 2004, 2006), which is also supported by an incomplete consumption of the leaf litter (up to 81 % of initial C stock was left after incubation) in our study, (ii) conditions in our study as opposed to media with optimized nutrient availability and pH in microbial culture studies were not optimum, and (iii) the incorporation into microbial metabolites like lipids or amino acids plays a small role during incubation of organic matter which usually comprises little reactive compounds that may not experience any H incorporation at all (e.g., lignin; Kalbitz et al., 2006). Our results do not fully support Hypothesis 1, because indications of an incorporation of ^2H-enriched ambient water into decomposing litter during the four weeks of litter incubation were weak and the calculated incorporation was small.

5.2. ^2H incorporation into leached TOM

The finding that $\delta^2H_{n\ TOM}$ values of leached TOM from our microcosms were either not significantly different from or significantly higher than those of the leaf litter during the entire incubation as reflected by the net apparent fractionation (Fig. B-S3) indicates that TOM leaching cannot have contributed to the slight increase in the $\delta^2H_{n\ leaf\ litter}$ values of the incubation with the 250 ‰ label. To explain net apparent fractionation between leached TOM and leaf litter that is either close to zero or positive (Fig. B-S3), again two processes acting simultaneously can be considered: (i) preferential leaching of H-isotopically heavy compounds and/or (ii) the potentially successive incorporation of isotopically labeled, ^2H-enriched ambient water into the C-bonded H pool of leached TOM. Typically, water-soluble and easily decomposable compounds like carbohydrates, proteins and amino acids are leached (Berg and McClaugherty et al., 2014; Habermehl et al., 2008; Nykvist, 1963). While we are not aware of studies on δ^2H_n values of proteins, C-bonded H in carbohydrates from photosynthesis and in amino acids seems to be depleted in ^2H (Sanchez-Bragado et al., 2019; Schmidt et al. 2007). In line, results of a field study on decomposition of beech and linden litter showed that $\delta^2H_{n\ TOM}$ values were,

on average, depleted in ^{2}H by $\varepsilon^2H_{n\ \mathrm{TOM/leaf\ litter}}$ = -42.9 ‰ relative to the source leaf litter ($\delta^2H_{n\ \mathrm{TOM}}$: -149.9 ± standard error 3.5 ‰; $\delta^2H_{n\ \mathrm{leaf\ litter}}$: -111.8±1.1 ‰; n = 36; own results). Therefore, it is reasonable to assume that leached TOM comprised a non-labeled proportion that was depleted in ^{2}H in our laboratory study as well. Thus, the net apparent ^{2}H accumulation from leaf litter to leached TOM (Fig. B-S3), must be attributable to the incorporation of isotopically labeled, ^{2}H-enriched ambient water into the C-bonded H pool of leached TOM, which overruled the fractionation caused by the selective dissolution of H-isotopically light compounds in TOM.

The incorporation of ambient water-H into leached TOM in our incubation (8 to 9 %; Fig. B-4) was still less than reported in the literature on microbial assays (Horita and Vass, 2003; Kreuzer-Martin et al., 2003, 2004). It can be assumed that the remaining leaf litter represents the more recalcitrant left-over while the less stable and polar decomposition products and microbial metabolites likely were leached in our experimental set up (Berg and Ågren, 1984; Habermehl et al., 2008; Krishna and Mohan, 2017; Mambelli et al., 2011; Martin et al., 1974; Voroney and Paul, 1989). These leached decomposition products and microbial metabolites experienced an incorporation of ambient water-H via the glycolysis-gluconeogenesis metabolic pathway inside microbial cells during leaf litter decomposition (Horita and Vass, 2003; Kreuzer-Martin et al., 2003; Ruppenthal et al., 2015). As expected in Hypothesis 2, the calculated incorporation of the ^{2}H-labeled ambient water-H into the C-bonded H pool tended to be larger for leached TOM (whole incubation period covered in week 4: 9 %, Fig. B-4) than for the remaining increasingly decomposed leaf litter (< 5 %, Fig. B-4). However, further experiments on δ^2H_n values of leached TOM and on the H-isotopic differentiation between litter- and microbially derived compounds are needed to confirm this conclusion.

Because of the contribution of ^{2}H-depleted compounds originating from the leaf litter to leached TOM, our estimates of H incorporation from ambient water into the C-bonded pool of TOM must be regarded as conservative and are likely too low. Our results illustrate, that there can be a small incorporation of H from ambient water into SOM and more so into leached TOM in a short time.

5.3. Influence of the tree species

The $\delta^2H_{n\ \mathrm{leaf\ litter}}$ values differed between the tree species and this difference was maintained during the four-week incubation (Fig. B-3). The observed difference might be related to initial differences in the chemical composition of the two tree species. Kalbitz et al. (2006) showed that beech litter had higher cellulose concentrations than maple litter irrespective of decomposition stage which could explain the higher $\delta^2H_{n\ \mathrm{leaf\ litter}}$ values of beech than maple (DeBond et al., 2013). However, we cannot rule out that the differences between $\delta^2H_{n\ \mathrm{leaf\ litter}}$ values of tree species might also be attributable to site-specific differences in δ^2H values of source water, to different ^{2}H-enrichment of leaf water related to different humidity or to a species-specific variation in isotope fractionation (Arosio et al., 2020).

We observed an increased loss of the initial C stock after four weeks of incubation and a higher mass loss in solution for maple than for beech (Fig. B-2). These facts, together with mostly non-detectable incorporation of ambient water-H into the C-bonded H pool of leached TOM of maple (Fig. B-4) contradicts our expectation that C loss and incorporation are coupled. In line with Joly et al. (2016), we regarded the degree to which the initial C stock was lost as an indicator of microbial activity. Accordingly, the higher the microbial activity is, the more metabolically active the microorganisms are, and the more intensively the glycolysis-gluconeogenesis pathway should operate. Maple is supposed to be more favorable for microbial activity than beech leaf litter (Angst et al., 2019; Don and Kalbitz, 2005; Joly et al., 2016; Zech et al., 2011). Consequently, mass loss and the incorporation of ambient water-H into the C-bonded H pool should be larger for leached TOM of maple than of beech. The fact that the incorporation of ambient water-H into the C-bonded H pool of leached TOM of maple was not as pronounced as expected based on mass loss might be related to the composition of leached TOM. If the mixture between the two TOM origins (leachate from leaf litter without the ^{2}H label or microbial metabolites bearing the ^{2}H label) depended on tree species, this would be reflected by the tree-specific estimates of incorporation. For example, a larger contribution of non-labeled leached TOM of a given tree species will result in a dilution of the ^{2}H enrichment of leached TOM and thus, in a reduced estimate of incorporation. The results suggest that such dilution effects might have occurred in our study. Because of faster decomposition of maple than beech litter, maple showed a higher mass loss (Fig. B-2). In line, Joly et al. (2016) found that the amount of leached organic matter of leaves of *A. pseudoplatanus* (85.5 mg g^{-1}) was 287 % larger than for leaves of *F. sylvatica* (22.1 mg g^{-1}).

Similarly, Don and Kalbitz (2005) reported that a significantly higher amount of TOM was leached from maple than beech leaves. Neither these authors nor we distinguished between litter- and microbially derived TOM. Nevertheless, the C:N ratios in our study support a substantial contribution of (non-isotopically labeled) litter-derived leached TOM for maple because the C:N ratios of leached TOM from maple leaf litter were significantly larger than the C:N ratios of leached TOM from beech leaf litter. Therefore, the C:N ratios of TOM leached from beech leaf litter matched better with those reported for microbial origin. Holland and Coleman (1987) showed that bacterial C:N ratios are in the range of 5-10 and Jenkinson et al. (1988) reported that the C:N ratio of the living soil microbial biomass is relatively constant at around 7. By contrast, C:N ratios >15 in case of leached TOM from maple leaf litter indicated a mixture of litter- and microbially derived TOM. Thus, we probably underestimated the incorporation of ambient water-H into the C-bonded H pool of leached TOM because of the dilution effect particularly for maple. Therefore, our initial expectation of a coupling between C loss and incorporation of ambient water-H into the C-bonded H pool might still hold true. Consequently, we can neither support nor reject our Hypothesis 3.

6. Conclusions

During the four-week incubation, we found an incorporation of ambient water-H into the C-bonded H pool ranging from 3 to 9 % of the C-bonded H pool. The incorporation of ambient water-H into the C-bonded H pool was smaller than the incorporation reported in previous studies that did not use natural OM along with the attached microbial community but microbial cultures. Our low incorporation rate cannot explain the loss of the H-isotopic aridity signal during processing of aboveground litter to SOM along the Argentinean climosequence of Ruppenthal et al. (2015). Our findings therefore support the alternative explanation that SOM originates more from root litter and microbial biomass, for which the glycolysis-gluconeogenesis pathway already resulted in an equilibration with the ambient soil water, than from aboveground litter. The incorporation of ambient water-H into the C-bonded pool tended to be larger for leached TOM than for the solid phase litter. The reason for the incorporation of ambient water-H into the C-bonded H-pool of leached TOM likely is the higher contribution of microbially cycled compounds to TOM than to the solid-phase litter.

Although maple litter in our study was more quickly decomposed than beech litter, the incorporation of ambient water-H into the C-bonded H pool was more pronounced for litter and for leached TOM of beech. This finding was likely caused by the underestimated H-incorporation from ambient water into the C-bonded H pool for maple because of the dilution of ^{2}H-enriched microbially derived TOM in solution by ^{2}H-depleted, litter-derived leached TOM. A larger dilution effect for maple than for beech is supported by a higher C:N ratio in leached TOM of maple than expected for microbial origin.

Future research should focus on the mechanistic understanding of the production of leached TOM and the contribution of microbially derived compounds to TOM in solution. Although our findings cannot explain the reason why aridity effects on $\delta^{2}H_{n}$ values disappeared between plant litter and SOM, they have implications for studies of the paleoenvironment. Over centuries to millennia, even small incorporation rates might add up and thus, the C-bonded H pool is suggested to show a stable $\delta^{2}H_{n}$ value only if the organic compounds are preserved from microbial activity such as in fossilized sediments but hardly in subsoils. Moreover, the finding that ambient water-H is mainly incorporated into fresh microbial components of leached TOM might open up new ways to assess the relative age of leached TOM and its fractions in that a higher incorporation of ambient water-H into TOM in solution is indicative of a higher contribution of fresh microbial compounds. However, if the difference in the natural abundance δ^{2}H values of ambient water and the C-bonded H pool in leached TOM was not as large as in our incubation with the 250 ‰ label, in-situ experiments with highly ^{2}H-enriched water might be needed to determine the size of the microbially derived contribution to the TOM in solution.

7. Acknowledgements

We thank Genoveva Tscholl and Sabine Flaiz for advice and assistance in EA-IRMS analyses. We thank two anonymous reviewers for their valuable input. The study was funded by the German Science Foundation (DFG, OE516/11-1).

8. References

Angst, Š., Harantová, L., Baldrian, P., Angst, G., Cajthaml, T., Straková, P., Blahut, J., Veselá, H., Frouz, J., 2019. Tree species identity alters decomposition of understory litter and associated microbial communities: a case study. Biology and Fertility of Soils 55, 525–538.

Arosio, T., Ziehmer-Wenz, M.M., Nicolussi, K., Schlüchter, C., Leuenberger, M., 2020. Larch Cellulose Shows Significantly Depleted Hydrogen Isotope Values with Respect to Evergreen Conifers in Contrast to Oxygen and Carbon Isotopes. Frontiers in Earth Science 8, 490.

Berg, B., Ågren, G.I., 1984. Decomposition of needle litter and its organic chemical components: theory and field experiments. Long-term decomposition in a Scots pine forest. III. Canadian Journal of Botany 62, 2880–2888.

Berg, B., McClaugherty, C., 2014. Plant Litter. Springer Berlin Heidelberg, Berlin, Heidelberg.

Cernusak, L.A., Barbour, M.M., Arndt, S.K., Cheesman, A.W., English, N.B., Feild, T.S., Helliker, B.R., Holloway-Phillips, M.M., Holtum, J.A.M., Kahmen, A., McInerney, F.A., Munksgaard, N.C., Simonin, K.A., Song, X., Stuart-Williams, H., West, J.B., Farquhar, G.D., 2016. Stable isotopes in leaf water of terrestrial plants. Plant, cell & environment 39, 1087–1102.

Coplen, T.B., 2011. Guidelines and recommended terms for expression of stable-isotope-ratio and gas-ratio measurement results. Rapid communications in mass spectrometry 25, 2538–2560.

Cormier, M.-A., Werner, R.A., Sauer, P.E., Gröcke, D.R., Leuenberger, M.C., Wieloch, T., Schleucher, J., Kahmen, A., 2018. ^{2}H-fractionations during the biosynthesis of carbohydrates and lipids imprint a metabolic signal on the δ^{2}H values of plant organic compounds. New Phytologist 218, 479–491.

Cornelissen, J.H.C., 1996. An Experimental Comparison of Leaf Decomposition Rates in a Wide Range of Temperate Plant Species and Types. The Journal of Ecology 84, 573.

Craig, H., Gordon, L.A., 1965. Deuterium and oxygen 18 variations in the ocean and the marine atmosphere, Stable Isotopes in Oceanographic Studies and Paleotemperatures. Consiglio Nazionale delle Ricerche Laboratorio di Geologia Nucleare, Pisa.

DeBond, N., Fogel, M.L., Morrill, P.L., Benner, R., Bowden, R., Ziegler, S., 2013. Variable δD values among major biochemicals in plants: Implications for environmental studies. Geochimica et Cosmochimica Acta 111, 117–127.

Dilling, J., Kaiser, K., 2002. Estimation of the hydrophobic fraction of dissolved organic matter in water samples using UV photometry. Water Research 36, 5037–5044.

Don, A., Kalbitz, K., 2005. Amounts and degradability of dissolved organic carbon from foliar litter at different decomposition stages. Soil Biology and Biochemistry 37, 2171–2179.

Dongmann, G., Nürnberg, H.W., Förstel, H., Wagener, K., 1974. On the enrichment of H218O in the leaves of transpiring plants. Radiation and Environmental Biophysics 11, 41–52.

Epstein, S., Thompson, P., Yapp, C.J., 1977. Oxygen and hydrogen isotopic ratios in plant cellulose. Science (New York, N.Y.) 198, 1209–1215.

Faghihi, V., Meijer, H.A.J., Gröning, M., 2015. A thoroughly validated spreadsheet for calculating isotopic abundances (^{2}H, ^{17}O, ^{18}O) for mixtures of waters with different isotopic compositions. Rapid Communications in Mass Spectrometry 29, 1351–1356.

Feng, X., Krishnamurthy, R.V., Epstein, S., 1993. Determination of ratios of nonexchangeable hydrogen in cellulose: A method based on the cellulose-water exchange reaction. Geochimica et Cosmochimica Acta 57, 4249–4256.

Filot, M.S., Leuenberger, M., Pazdur, A., Boettger, T., 2006. Rapid online equilibration method to determine the D/H ratios of non-exchangeable hydrogen in cellulose. Rapid communications in mass spectrometry 20, 3337–3344.

Fogel, R., Cromack Jr., K., 1977. Effect of habitat and substrate quality on Douglas fir litter decomposition in western Oregon. Canadian Journal of Botany 55, 1632–1640.

Fogel, M.L., Griffin, P.L., Newsome, S.D., 2016. Hydrogen isotopes in individual amino acids reflect differentiated pools of hydrogen from food and water in Escherichia coli. Proceedings of the National Academy of Sciences of the United States of America.

Gartner, T.B., Cardon, Z.G., 2004. Decomposition dynamics in mixed-species leaf litter. Oikos 104, 230–246.

Girden, E., 1992. ANOVA. SAGE Publications, Inc, 2455 Teller Road, Thousand Oaks California 91320 United States of America.

Gray, J., Song, S.J., 1984. Climatic implications of the natural variations of D/H ratios in tree ring cellulose. Earth and Planetary Science Letters 70, 129–138.

Gori, Y., Wehrens, R., Greule, M., Keppler, F., Ziller, L., La Porta, N., Camin, F., 2013. Carbon, hydrogen and oxygen stable isotope ratios of whole wood, cellulose and lignin methoxyl groups of Picea abies as climate proxies. Rapid Communications in Mass Spectrometry 27, 265–275.

Habermehl, G.G.K., Hammann, P.E., Krebs, H.C., Ternes, W., 2008. Naturstoffchemie. Springer Berlin Heidelberg, Berlin, Heidelberg.

Hayes, J.M., 2001. Fractionation of Carbon and Hydrogen Isotopes in Biosynthetic Processes. Reviews in Mineralogy and Geochemistry 43, 225–277.

Holland, E.A., Coleman, D.C., 1987. Litter Placement Effects on Microbial and Organic Matter Dynamics in an Agroecosystem. Ecology 68, 425–433.

Horita, J., Vass, A.A., 2003. Stable-Isotope Fingerprints of Biological Agents as Forensic Tools. Journal of Forensic Sciences 48.

IUSS Working Group WRB, 2014. World reference base for soil resources 2014. International soil classification system for naming soils and creating legends for soil maps. FAO, Rome.

Jenkinson, D.S., 1988. Determination of microbial biomass carbonand nitrogen in soil. J. R. Wilson, ed. Advancesin nitrogen cycling in agricultural ecosystems, 388-386.

Joly, F.-X., Fromin, N., Kiikkilä, O., Hättenschwiler, S., 2016. Diversity of leaf litter leachates from temperate forest trees and its consequences for soil microbial activity. Biogeochemistry 129, 373–388.

Kalbitz, K., Kaiser, K., Bargholz, J., Dardenne, P., 2006. Lignin degradation controls the production of dissolved organic matter in decomposing foliar litter. European Journal of Soil Science 57, 504–516.

Kimak, A., Kern, Z., Leuenberger, M., 2015. Qualitative Distinction of Autotrophic and Heterotrophic Processes at the Leaf Level by Means of Triple Stable Isotope (C-O-H) Patterns. Frontiers in Plant Science 6, 1008.

Klotzbücher, T., Kaiser, K., Guggenberger, G., Gatzek, C., Kalbitz, K., 2011. A new conceptual model for the fate of lignin in decomposing plant litter. Ecology 92, 1052-1062.

Kreuzer-Martin, H.W., Chesson, L.A., Lott, M.J., Dorigan, J.V., Ehleringer, J.R., 2004. Stable Isotope Ratios as a Tool in Microbial Forensics—Part 1. Microbial Isotopic Composition as a Function of Growth Medium. Journal of Forensic Sciences 49, 1–7.

Kreuzer-Martin, H.W., Lott, M.J., Dorigan, J., Ehleringer, J.R., 2003. Microbe forensics: oxygen and hydrogen stable isotope ratios in Bacillus subtilis cells and spores. Proceedings of the National Academy of Sciences of the United States of America 100, 815–819.

Kreuzer-Martin, H.W., Lott, M.J., Ehleringer, J.R., Hegg, E.L., 2006. Metabolic processes account for the majority of the intracellular water in log-phase Escherichia coli cells as revealed by hydrogen isotopes. Biochemistry 45, 13622–13630.

Krishna, M.P., Mohan, M., 2017. Litter decomposition in forest ecosystems: a review. Energy, Ecology and Environment 2, 236–249.

Leaney, F.W., Osmond, C.B., Allison, G.B., Ziegler, H., 1985. Hydrogen-isotope composition of leaf water in C3 and C 4 plants: its relationship to the hydrogen-isotope composition of dry matter. Planta 164, 215–220.

Luo, Y.-H., Sternberg, L.D.S.L., 1992. Hydrogen and Oxygen Isotopic Fractionation During Heterotrophic Cellulose Synthesis. Journal of Experimental Botany 43, 47–50.

Mambelli, S., Bird, J.A., Gleixner, G., Dawson, T.E., Torn, M.S., 2011. Relative contribution of foliar and fine root pine litter to the molecular composition of soil organic matter after in situ degradation. Organic Geochemistry.

Martin, J.P., Haidfr, K., Farmkr, W.J., Fustec-Mathon, E., 1974. Decomposition and distribution of residual activity of some ^{13}C-microbial polysaccharides and cells, glucose, cellulose and wheat straw in soil. Soil Biology and Biochemistry 6, 221–230.

Meentemeyer, V., 1978. Macroclimate and Lignin Control of Litter Decomposition Rates. Ecology 59, 465–472.

Millar, H.C., Smith, F.B., Brown, P.E., 1936. The Rate of Decomposition of Various Plant Materials in Soils 1. Agronomy Journal 28, 914–923.

Minderman, G., 1968. Addition, Decomposition and Accumulation of Organic Matter in Forests. The Journal of Ecology 56, 355.

Nykvist, N., 1963. Leaching and decomposition of water-soluble organic substances from different types of leaf and needle litter. Studia forestalia Suecica (0039-3150).

Pagano, T., Bida, M., Kenny, J., 2014. Trends in Levels of Allochthonous Dissolved Organic Carbon in Natural Water: A Review of Potential Mechanisms under a Changing Climate. Water 6, 2862–2897.

Paul, A., Hatté, C., Pastor, L., Thiry, Y., Siclet, F., Balesdent, J., 2016. Hydrogen dynamics in soil organic matter as determined by ^{13}C and ^{2}H labeling experiments. Biogeosciences 13, 6587–6598.

Preston, C.M., Nault, J.R., Trofymow, J.A., 2009. Chemical changes during 6 years of decomposition of 11 litters in some Canadian forest sites. Part 2. C-13 abundance, solid-state C-13 NMR spectroscopy and the meaning of "Lignin". Ecosystems 12, 1078-1102.

Roden, J.S., Lin, G., Ehleringer, J.R., 2000. A mechanistic model for interpretation of hydrogen and oxygen isotope ratios in tree-ring cellulose. Geochimica et Cosmochimica Acta 64, 21–35.

Rundel, P.W., Stichler, W., Zander, R.H., Ziegler, H., 1979. Carbon and hydrogen isotope ratios of bryophytes from arid and humid regions. Oecologia 44, 91–94.

Ruppenthal, M., Oelmann, Y., del Valle, H.F., Wilcke, W., 2015. Stable isotope ratios of nonexchangeable hydrogen in organic matter of soils and plants along a 2100-km climosequence in Argentina: New insights into soil organic matter sources and transformations? Geochimica et Cosmochimica Acta 152, 54–71.

Ruppenthal, M., Oelmann, Y., Wilcke, W., 2013. Optimized demineralization technique for the measurement of stable isotope ratios of nonexchangeable H in soil organic matter. Environmental Science & Technology 47, 949-957.

Ruppenthal, M., Oelmann, Y., Wilcke, W., 2010. Isotope ratios of nonexchangeable hydrogen in soils from different climate zones. Geoderma 155, 231–241.

Sachse, D., Billault, I., Bowen, G.J., Chikaraishi, Y., Dawson, T.E., Feakins, S.J., Freeman, K.H., Magill, C.R., McInerney, F.A., van der Meer, M.T.J., Polissar, P., Robins, R.J., Sachs, J.P., Schmidt, H.-L., Sessions, A.L., White, J.W.C., West, J.B., Kahmen, A., 2012. Molecular Paleohydrology: Interpreting the Hydrogen-Isotopic Composition of Lipid Biomarkers from Photosynthesizing Organisms. Annual Review of Earth and Planetary Sciences 40, 221–249.

Sanchez-Bragado, R., Serret, M.D., Marimon, R.M., Bort, J., Araus, J.L., 2019. The Hydrogen Isotope Composition δ^2H Reflects Plant Performance. Plant physiology 180, 793–812.

Sauer, P.E., Schimmelmann, A., Sessions, A.L., Topalov, K., 2009. Simplified batch equilibration for D/H determination of non-exchangeable hydrogen in solid organic material. Rapid communications in mass spectrometry 23, 949–956.

Schimmelmann, A., 1991. Determination of the concentration and stable isotopic composition of nonexchangeable hydrogen in organic matter. Analytical chemistry 63, 2456–2459.

Schimmelmann, A., Sessions, A.L., Mastalerz, M., 2006. Hydrogen isotopic (D/H) composition of organic matter during thermal maturation. Annual Review of Earth and Planetary Sciences 34, 501–533.

Schimmelmann, A., Lewan, M.D., Wintsch, R.P., 1999. D/H isotope ratios of kerogen, bitumen, oil, and water in hydrous pyrolysis of source rocks containing kerogen types I, II, IIS, and III. Geochimica et Cosmochimica Acta 63, 3751–3766.

Schmidt, H.-L., Werner, R.A., Roßmann, A., Mosandl, A., Schreier, P., 2007. Quality Control: Part 6.2.2, Stable Isotope Ratio Analysis in Quality Control of Flavourings, in: Ziegler, H. (Ed.), Flavourings. Wiley-VCH Verlag GmbH & Co. KGaA, Weinheim, Germany, 602-663.

Sessions, A.L., 2016. Factors controlling the deuterium contents of sedimentary hydrocarbons. Organic Geochemistry 96, 43–64.

Sessions, A.L., Sylva, S.P., Summons, R.E., Hayes, J.M., 2004. Isotopic exchange of carbon-bound hydrogen over geologic timescales 1 1Associate editor: J. Horita. Geochimica et Cosmochimica Acta 68, 1545–1559.

Sprenger, M., Leistert, H., Gimbel, K., Weiler, M., 2016. Illuminating hydrological processes at the soil-vegetation-atmosphere interface with water stable isotopes. Reviews of Geophysics 54, 674-704.

Voroney, R.P., Paul, E.A., Anderson, D.W., 1989. Decomposition of wheat straw and stabilization of microbial products. Canadian journal of soil science, 63–77.

Wardle, D.A., Bonner, K.I., Nicholson, K.S., 1997. Biodiversity and Plant Litter: Experimental Evidence Which Does Not Support the View That Enhanced Species Richness Improves Ecosystem Function. Oikos 79, 247.

Wassenaar, L.I., Hobson, K.A., 2000. Improved Method for Determining the Stable-Hydrogen Isotopic Composition (δD) of Complex Organic Materials of Environmental Interest. Environmental Science & Technology 34, 2354–2360.

Wetterkontor GmbH, 2021. https://www.wetterkontor.de/de/wetter/deutschland/monatswerte-station.asp?id=10738, last accessed 12 Feb 2021.

Wickings, K., Grandy, A.S., Reed, S.C., Cleveland, C.C., 2012. The origin of litter chemical complexity during decomposition. Ecology Letters 15, 1180-1188.

Yakir, D., 1992. Variations in the natural abundance of oxygen-18 and deuterium in plant carbohydrates. Plant, Cell and Environment 15, 1005–1020.

Yakir, D., Deniro, M.J., 1990. Oxygen and Hydrogen Isotope Fractionation during Cellulose Metabolism in Lemna gibba L. Plant Physiology 93, 325–332.

Yapp, C.J., Epstein, S., 1982. A reexamination of cellulose carbon-bound hydrogen δD measurements and some factors affecting plant-water D/H relationships. Geochimica et Cosmochimica Acta 46, 955–965.

Zech, M., Pedentchouk, N., Buggle, B., Leiber, K., Kalbitz, K., Marković, S.B., Glaser, B., 2011. Effect of leaf litter degradation and seasonality on D/H isotope ratios of n-alkane biomarkers. Geochimica et Cosmochimica Acta 75, 4917–4928.

Ziegler, H., Osmond, C.B., Stichler, W., Trimborn, P., 1976. Hydrogen isotope discrimination in higher plants: Correlations with photosynthetic pathway and environment. Planta 128, 85–92.

Section C

Incorporation of Ambient Water-H into the C-bonded H Pool of Bacteria during Substrate-Specific Metabolism

Arnim Kessler[1], Stefan Merseburger[2], Andreas Kappler[3], Wolfgang Wilcke[2] and Yvonne Oelmann[1]

[1] *Geoecology. University of Tübingen. Tübingen. Germany*

[2] *Institute of Geography and Geoecology. Karlsruhe Institute of Technology (KIT). Karlsruhe. Germany*

[3] *Geomicrobiology. University of Tübingen. Tübingen. Germany*

Author	Author number	Scientific Idea	Experimental Work	Data Analysis and Interpretation	Paper Writing
Arnim Kessler	1.	20 %	100 %	50 %	50 %
Stefan Merseburger	2.	0 %	0 %	0 %	0 %
Andreas Kappler	3.	0 %	0 %	10 %	5 %
Wolfgang Wilcke	4.	20 %	0 %	10 %	10 %
Yvonne Oelmann	5.	60 %	0 %	30 %	35 %

Title

Incorporation of Ambient Water-H into the C-Bonded H Pool of Bacteria during Substrate-Specific Metabolism

Status of publication

Published in *ACS Earth and Space Chemistry*

ACS Earth and Space Chemistry **2022**, *6* (9), 2180–2189

DOI: 10.1021/acsearthspacechem.2c00085

1. Abstract

The stable isotope ratios of C-bonded H (δ^2H_n values) can be used to locate soil samples for forensic purposes because of their close correlation with the δ^2H values of precipitation. Post-sampling bacterial activity might change the δ^2H_n values via glycolysis. We tested to which degree C-bonded H is replaced by H from ambient water under favorable and unfavorable growing conditions. We provided two heterotrophic bacteria (*Bacillus atrophaeus*, *Escherichia coli*) with glucose (favorable) or lysine (unfavorable) under aerobic conditions. We assessed the H incorporation from ambient water via ^2H labeling. We found that the H incorporation into bacterial biomass in the glucose treatment was 79±5.9 % (*B. atrophaeus*) and 43±3.0 % (*E. coli*), likely as a consequence of glycolysis and conservation of the δ^2H value in the anabolic mode of the tricarboxylic acid (TCA) cycle. Differences between species were possibly related with different compositions of metabolite mixtures. The bacteria did hardly grow with lysine while respiration continued, and we found no H incorporation because the catabolic mode of the TCA cycle, which was active when the bacteria grew on lysine, is associated with CO_2 release and a complete cleavage of former C–^2H bonds. Our results support the glycolysis pathway as a mechanism underlying the incorporation of ambient water-H into the C-bonded H pool of bacteria. Stressful conditions forcing bacteria into a catabolism-dominated metabolism disable the incorporation of ambient water-H, and δ^2H_n values can be applied to identify the origin of soil samples in forensics.

Graphical abstract

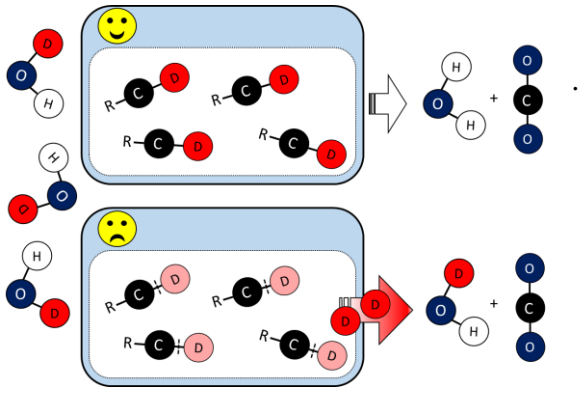

2. Introduction

Stable H isotope ratios (δ^2H values) of C-bonded H in compounds formed during young age and conserved for the whole life can help identify the region of birth of humans[1] or the natal origin of migrating animals.[2–4] The stable H isotope approach is based on the reliance of organisms on regional water sources with typical geographical patterns in δ^2H values.[5] Similarly, δ^2H values of C-bonded H

(δ^2H_n) of soil organic matter (SOM) that is built up from organic remains correlates closely with δ^2H values of precipitation.[6,7] Therefore, the origin of soil samples, which can be required e.g., evidenced in criminal cases, might be deducible from δ^2H_n values of SOM. However, not only dead organic remains with a preserved δ^2H_n value but also living microorganisms including bacteria are present in soil. Because of the short life cycle of bacteria of minutes to hours, no long-lived tissue exists in living bacterial cells and the δ^2H_n values can be quickly metabolically overprinted by the introduction of H atoms from ambient water.[8,9]

It is generally assumed that during glycolysis, a metabolic reaction chain shared by nearly all organisms on Earth,[10] ambient water-H is incorporated into the C-bonded H fraction which includes *de novo* formation of C-H bonds.[11–15] During the fifth step of the glycolysis, an H atom from ambient water is newly bound to the C_2 position of the glycerinealdehyde-3-phosphate (GAP) molecule. This H atom is eventually conserved in bacterial biomass if pyruvate as the end-product of glycolysis enters the anabolic mode of the tricarboxylic acid (TCA) cycle that generates biosynthesis products. Because many bacteria prefer glucose – the educt of the glycolysis – as a carbon source[16] for biosynthesis, an incorporation of ambient water-H was found if *Escherichia coli* or *Bacillus subtilis* were grown on glucose or growth substrates amended with glucose.[8,17] In these studies, the incorporation of ambient water-H was calculated for the bulk bacterial biomass.[8,17] Bulk bacterial biomass consists of both C-bonded H as well as O-, N-, and S-bonded H (exchangeable H; H_{ex}) that rapidly exchanges with ambient air moisture e.g., in the laboratory atmosphere.[18,19] Therefore, the calculation of incorporation of ambient water-H in previous studies on bacteria did not relate exclusively to C-bonded H. Accordingly, the calculated incorporation of ambient water-H up to 30 % of total H into bacterial biomass[8,9,20,21] and of <5 to >70 % into bacterial amino acids[17] contains uncertainties. The quantification of the incorporation of ambient water-H into bulk bacterial biomass requires to distinguish between exchangeable and nonexchangeable H. The H_{ex} can be tackled by steam equilibration[19,22], but this method has not been applied in microbiological studies so far.

Jointly, *de novo* formation of C-H bonds during glycolysis and the incorporation of ambient water-H during bacterial metabolism might suggest that H in the newly formed C-H bonds originates from cell water reflecting ambient water. However, the role of glycolysis for the incorporation of ambient water-H during bacterial metabolism has not been studied yet. Most bacterial species cannot grow on substrates that are not involved in glycolysis e.g., lysine – a ketogenic amino acid.[23–25]

However, as an adaption to stationary phase growth condition, *E. coli* was shown to continue metabolic activity including the gluconeogenesis/glycolysis pathways if provided with lysine.[25] Knorr et al.[25] showed that *E. coli* is able to degrade lysine catabolically. However, the used incubation medium was supplemented with glucose resulting in basic glycolytic activity and does not provide information about bacterial growth and incorporation of ambient water-H when lysine is the sole C-source. The incorporation of ambient water-H into biosynthesized compounds is associated with enzymatically mediated reactions which fractionate H and thus, produce kinetic isotope

fractionation.[26–28] As opposed to different isotope fractionation during the biosynthesis of individual bacterial lipids,[29–32] bulk bacterial biomass should be characterized by a consistent fractionation factor if glycolysis precedes the majority of biosynthesis products. For bacterial biomass and spores, a range of net apparent fractionation ($\varepsilon_{\text{biosynthesis product/water}}$) from +40 to +122 ‰ was reported.[20] However, this study did not compare different bacterial species.

We aimed to prove that ambient water-H is incorporated into C-bonded H during glycolysis. Moreover, we aimed to quantify the apparent H isotope fractionation by this H incorporation. We hypothesized that (i) there will be pronounced growth and a substantial incorporation of ambient water-H in the glucose treatment irrespective of the bacterium species; (ii) In the lysine treatment, *E. coli* will show metabolic activity and associated incorporation of ambient water-H into C-bonded H, whereas *B. atrophaeus* will die; and (iii), the isotope fractionation associated with the incorporation of ambient water-H into bulk bacterial biomass in the glucose treatment will be constant i.e., not depend on the bacterium species.

3. Material and Methods

3.1. Bacterial cultures and medium preparation

No unexpected or unusually high safety risks arose during the experiment. We used the gram-positive bacterium *Bacillus atrophaeus* (DSM 675) and the gram-negative bacterium *Escherichia coli* K-12 (MG 1655) (DSMZ, Braunschweig, Germany). Cultures were pre-grown in a Luria-Bertani (LB) medium at pH 7. Afterwards, *E. coli* and *B. atrophaeus* cultures were inoculated and incubated in Erlenmeyer-flasks at 28 °C and 32 °C, respectively. Cell cultures were harvested when reaching the mid-exponential growth phase which was identified by optical density (OD) measurements and their relation to growth functions. Cell suspensions were centrifuged (8 min) at 4000 *g* (Hermle Z300, Hermle Labortechnik, Germany); pellets were washed twice with 0.9 % NaCl. For the incubation, we transferred initial cells (grown on LB-medium) as necessary to reach an initial optical density (OD) of 0.1 in the incubation medium.

The incubation medium was a modified ^{2}H-labeled M9 minimal medium which is commonly used to provide a basic supply of phosphorus, nitrogen and sulfur.[33] The chemical composition of the medium is described in the supporting information (SI). As the only carbon and energy source, we used 2.5 g L^{-1} of either glucose or lysine (both Campro Scientific, Berlin, Germany). Three stock flasks per C source of the two growth media with varying H isotope ratios were prepared (δ^{2}H: +150 ‰, +250 ‰ and +500 ‰) by adding the appropriate amounts of sterile 99.99 % D_2O (Campro Scientific). For each incubation cycle, 100 mL of the corresponding stock media were filled in 250-mL flasks (Duran, Schott, Mainz, Germany), closed with gas washbottle tops (Duran) and autoclaved.

3.2. Incubation

The incubation experiment was carried out for 12 h (T1) and 24 h (T2). Two species of bacteria, two carbon sources, three incubation waters with different δ^2H values (δ^2H_{iW}) and two time intervals in triplicates resulted in an experimental setup of 72 incubation flasks. Additionally, an identical setup but without the addition of bacteria was considered as control treatment for the CO_2-production. Cell cultures of both bacteria were incubated at 20 °C. The gas wash bottles were sealed airtight at the top and aerated with carbon-free synthetic air through a tube on the one side, while the other side was connected with two tubes (Falcon, USA) filled with NaOH for monitoring CO_2 production. The processing of the samples is described in the SI.

3.3. Analyses

3.3.1. Optical-density, flow-cytometry, CO_2 and substrate-concentration measurements

All OD measurements to determine the bacterial biomass were performed at 600 nm (Specord 50 Plus, Analytic Jena, Germany). To guarantee identical initial cell numbers of the two cultures, cell numbers were determined via flow cytometry (Attune Nxt Flow Cytometer, Thermo) and OD was checked before each incubation cycle. Additionally, we calculated bacterial growth (BacG) for each time step as the difference in OD between the final (OD_{ti}) and initial OD (OD_{t0}) according to Equation 1:

$$BacG = OD_{ti} - OD_{t0} \quad (1)$$

For measurements of C mineralization, respired CO_2 was trapped in 1 M NaOH. Detailed information on the calculation of respiration rates is provided in the SI.

Glucose concentrations were determined by the glucose-6-phosphate dehydrogenase-based test kit for glucose (D-glucose UV-test 10 716 251 035. Food Analysis, Boehringer, Mannheim, Germany) using the manufacturer´s instructions (https://food.r-biopharm.com/wp-content/uploads/2012/06/roche_ifu_glucose_en_10716251035_2017-11.pdf) and NADPH measurements (Specord 50 Plus, Analytic Jena, Jena, Germany). Lysine concentrations were measured by HPLC at the Institute of Bio- and Geosciences, Jülich, Germany.

3.3.2. Steam equilibration and stable H isotope analysis

We used the steam equilibration device based on the design of Wassenaar and Hobson[19] and modified by Ruppenthal et al.[22] to determine $\delta^2H_{n\ bac}$ values of bulk bacterial biomass. Additionally, we measured the total δ^2H values (δ^2H_t) values of glucose ($\delta^2H_{glucose}$ = 91.6±6.3 ‰; n = 6) and lysine (δ^2H_{lysine} = 86.6±4.1 ‰; n = 6). Detailed information on the steam equilibration setup, stable H analysis and analytical quality are presented in the SI.

3.3.3. Calculations and statistical evaluation

To determine δ^2H values in bacterial biomass, which requires the elimination of the contribution of exchangeable H to δ^2H_t (i) and to quantify the incorporation of ambient water-H into bacterial biomass (ii) we used isotope labeling.[34]

We accounted for the exchangeable O-, N- and S-bonded H in the bacterial species (i) with a mass balance approach adopted from Ruppenthal et al.[6] The total H (H_t) pool consists of an H_{ex} fraction that isotopically exchanges with water vapor and a C-bonded H fraction (H_n) with respective δ^2H_{ex} and δ^2H_n values. Total δ^2H values (δ^2H_t) could be measured directly and this pool can be described by Eq. 2.[18,19,35–37]

$$\delta^2 H_t = (1 - x_e)\delta^2 H_n + x_e \delta^2 H_{ex} \quad (2)$$

x_e is the H fraction that isotopically exchanged during steam equilibration. With regard to different organic compounds, the exchangeable H fraction varies from 0.0 for simple hydrocarbons up to 0.4 (i.e., 40 wt.% of H_t) for complex compounds like cellulose, kerogen, or humic acid.[18,19,35,36] If the exchangeable H fraction of a sample is in isotopic equilibrium with the equilibration water, the δ^2H_{ex} value is related to the δ^2H value of the equilibration water (δ^2H_w) with the corresponding equilibrium fractionation factor ($\alpha_{ex\text{-}w}$, Eq. 3).[6]

$$\alpha_{ex-w} = \frac{\delta^2 H_{ex} + 1000}{\delta^2 H_w + 1000} \quad (3)$$

The equilibrium fractionation factor $\alpha_{ex\text{-}w}$ depends on the chemical composition of the analyzed samples and the equilibration temperature.[18,19,35,36] However, for chemically complex organic substances, direct experimental determination of $\alpha_{ex\text{-}w}$ is difficult because it would be necessary to assess $\alpha_{ex\text{-}w}$ values through δ^2H values of isotopically equilibrated samples with those of samples with chemically removed H.[19] Recent studies used an approximation of $\alpha_{ex\text{-}w}$ for substances like humic acid, kerogen, keratin or collagen.[18,19,38] Here, for $\alpha_{ex\text{-}w}$, a provisional value of 1.08 was assigned, which is based on the cellulose equilibrium isotopic fractionation factor between isotopically exchangeable H and water-H for 20 h at 114 °C, which has been experimentally determined.[18] Via a sensitivity analysis over a $\alpha_{ex\text{-}w}$ range of 1.06 to 1.10, Schimmelmann et al.[39] and Wassenaar and Hobson[19] showed, that the use of a provisional $\alpha_{ex\text{-}w}$ value is admissible while the isotopic shift which is caused by the equilibration procedure is a function of isotopically exchangeable H and x_e. Therefore, in our study, we used an $\alpha_{ex\text{-}w}$ value of 1.08.

If x_e is constant among aliquots, a plot of δ^2H_t versus δ^2H_w should result in a straight line, defined by Eq. 4, which is obtained by solving Eq. 3 for δ^2H_{ex} and substituting into Eq. 2.[6]

$$\delta^2 H_t = x_e \alpha_{ex-w} \delta^2 H_w + (1 - x_e) \delta^2 H_n + 1000 x_e (\alpha_{ex-w} - 1) \quad (4)$$

When all of isotopically exchangeable H is in equilibrium with the water-H, δ^2H_n from Eq. 2 is equivalent to δ^2H of the C-bonded H in the sample. Therefore, δ^2H_n can be calculated by rearranging Eq. 4 to Eq. 5.[6]

$$\delta^2 H_n = \frac{\delta^2 H_t - 1000 x_e (\alpha_{ex-w} - 1) - x_e \alpha_{ex-w} \delta^2 H_w}{(1 - x_e)} \quad (5)$$

For further information about the steam equilibration and the calculation of δ^2H_n values see Ruppenthal et al.[6]

To trace the incorporation of ambient water-H into the bacterial biomass (ii), we manipulated the H isotope signature of the water during the incubation of bacterial species (δ^2H_{iW}: 150 ‰, 250 ‰, 500 ‰). The incorporation of H from the incubation water will shift the H isotope signature of bacterial species ($\delta^2H_{n\ bac}$ values) towards the δ^2H_{iW} values and result in a straight line (see explanation for Eq. 4). Therefore Eq. 4 can be rewritten as Eq. 6:

$$\delta^2 H_{n\ bac\ ti} = x_{inc} \alpha_{inc-w} \delta^2 H_{iW} + (1 - x_{inc}) \delta^2 H_{n\ bac\ t0} + 1000 x_{inc} (\alpha_{inc-w} - 1) \quad (6)$$

with $\delta^2H_{n\ bac\ ti}$ values after incubation composed of a proportion that experienced incorporation $(x_{inc} \alpha_{inc-w} \delta^2 H_{iW} + 1000 x_{inc} (\alpha_{inc-w} - 1))$, a proportion that did not $((1 - x_{inc}) \delta^2 H_{n\ bac\ t0})$ and $\delta^2 H_{n\ bac\ t0}$ reflects the H isotope signature of the bacterial species before incubation. From a mathematical perspective, in the first term $x_{inc} \alpha_{inc-w}$ represents the slope of the linear regression of $\delta^2H_{n\ bac\ ti}$ on δ^2H_{iW} while the term $1000 x_{inc} (\alpha_{inc-w} - 1) + (1 - x_{inc}) \delta^2 H_{n\ bac\ t0}$ represents the y-axis intercept.[6] For the sake of simplicity, Horita and Vass[9] who used a similar approach for two bacterial species assumed no H isotope fractionation associated with the incorporation ($\alpha_{inc\text{-}w} = 1$). However, other studies on bacterial species reported a range of 1.04 to 1.12 for $\alpha_{inc\text{-}w}$ associated with incorporation.[20] Therefore, it seems advisable to account for $\alpha_{inc\text{-}w}$ in Eq. 6 which then contains two known variables ($\delta^2H_{n\ bac\ ti}$; $\delta^2H_{n\ bac\ t0}$) and two unknown variables (x_{inc} and $\alpha_{inc\text{-}w}$). We used the Levenberg-Marquardt algorithm as an iterative procedure to estimate the unknown variables.[40,41] As a start value we used $\alpha_{inc\text{-}w} = 0.66$ which is twice the lowest H isotope fractionation (2 times an ε of -170 ‰) reported for H isotope fractionation associated with the production of ^2H depleted photosynthates by autotrophic organisms.[42] For x_{inc}, we set the start value to 0.0001 representing hardly any incorporation. Theoretically, the maximum value for x_{inc} would be 1 (100 % incorporation)

which was neither exceeded nor reached in our calculations. Linear regressions and estimations of x_{inc} and $\alpha_{inc\text{-}w}$ were only calculated in case of a reliable incorporation as a prerequisite namely if there were (i) significant differences in $\delta^2H_{n\ bac\ ti}$ values among the three water label treatments and (ii) significantly positive slopes. For all samples in the lysine treatments the perquisites were not met. In all cases for which the prerequisites were met, there was a unique solution of the estimates for x_{inc} and $\alpha_{inc\text{-}w}$. In the same way, we calculated x_{inc} and $\alpha_{inc\text{-}w}$ based on published linear regressions of δ^2H_{bac} on δ^2H_{iW}.[8,9,20] To extract the exact values of the data points from the published figures, we used the WebPlotDigitizer software (Ankit Rohatgi, Version 4.5, USA). Information on statistical analyses are described in the SI.

4. Results

4.1. Substrate and species effects on bacterial performance

The interpretation of the ^2H incorporation requires the understanding of the bacterial performance during the incubation experiment. Therefore, we assessed a number of vital properties of the two studied bacterial species. Despite the hardly detectable lysine consumption, *B. atrophaeus* did show a small growth rate (Fig. C-1; means significantly different from zero, $p \leq 0.03$). By contrast, we observed a die-off of a proportion of *E. coli* in the lysine treatment (Fig. C-1; bacterial growth negative and significantly different from zero; $p \leq 0.003$). In the glucose treatment, *E. coli* consumed more substrate than *B. atrophaeus*, yet this difference was significant after 24 hours only (Fig. C-1a; significant time x bacterial species interaction in Table C-S1). In line, from 12 to 24 hours, the growth increase of *E. coli* was larger than that of *B. atrophaeus* in the glucose treatment (Fig. C-1b; significant time x bacterial species interaction in Table C-S1).

The ^2H concentration in the used incubation waters had no effect on the bacterial consumption of lysine or glucose, the bacterial growth (BacG) and the respiration ($p > 0.25$, Table C-S1). Lysine concentrations hardly changed with time in the incubations with both test organisms (*B. atrophaeus* and *E. coli*; Fig. C-1a; Table C-S1). In contrast, glucose concentrations decreased significantly with time in the incubations with both test organisms (Fig. C-1a; Table C-S1). The glucose consumption was reflected in increased total bacterial biomass production, growth and respiration in the glucose than in the lysine treatments (Figs. C-1b, C-2a, C-2b; Table C-S1). On average, total bacterial biomass production on glucose was 273 % higher than on lysine. In general, the effect of substrate on bacterial performance was more pronounced after 24 hours (Figs. C-1, C-2; Table C-S1) with the exception of respiration for which the substrate effect was similar between the sampling periods (non-significant time x substrate interactions in Table C-S1). Accordingly, respiration standardized to the bacterial biomass was significantly higher particularly after 24 hours in the lysine treatments

respiration for which the substrate effect was similar between the sampling periods (non-significant time x substrate interactions in Table C-S1). Accordingly, respiration standardized to the bacterial biomass was significantly higher particularly after 24 hours in the lysine treatments (*B. atrophaeus*: 4.3 ± standard deviation of 1.4 mg CO_2 $(10^3$ cells$)^{-1}$; *E. coli*: 1.0±0.24 mg CO_2 $(10^3$ cells$)^{-1}$ as compared to the glucose treatments (0.9±0.8 mg CO_2 $(10^3$ cells$)^{-1}$; Table B-S2). The substrate effects were consistent for both bacterial species (Figs. C-1, C-2; non-significant bacterial species x substrate interactions in Table C-S2).

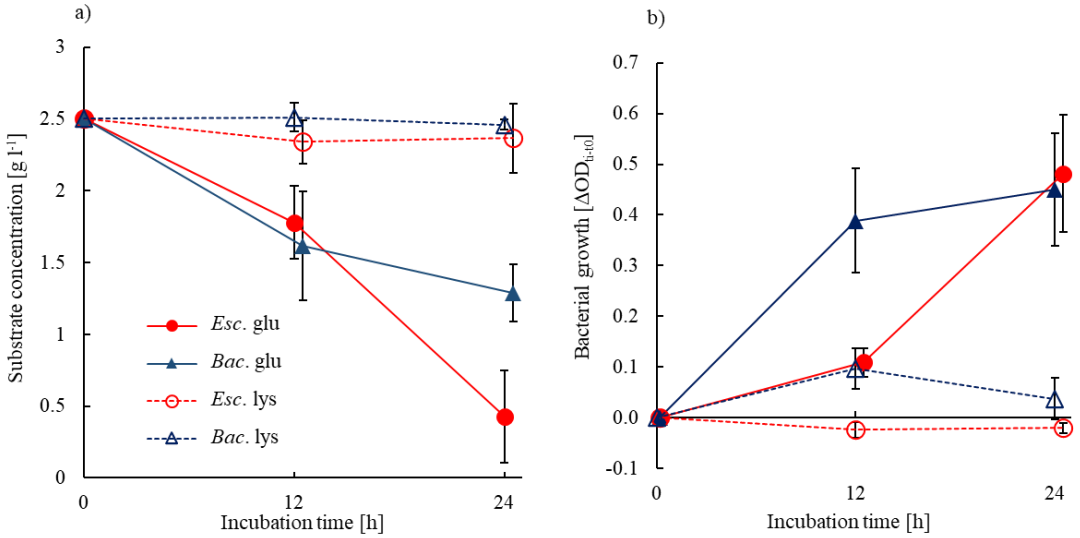

Fig. C-1: Remaining substrate concentrations in the incubation medium (a) and bacterial growth expressed as the differences in the optical density [OD] at 600 nm between time step t_i and t_0 (ΔOD_{ti-t0}) (b) for *B. atrophaeus* (*Bac.*) and *E. coli* (*Esc.*) and the corresponding substrate (glucose (glu) or lysine (lys)) after 12 h and 24 h of incubation. Error bars show the standard deviation of substrate concentrations and optical density differences for each time step (n = 9). To ease readability, the sampling times have been shifted slightly. Time, substrate, time x bacterial species, and time x substrate significantly ($p < 0.001$) influenced substrate consumption and bacterial growth in the statistical model (Table C-S1).

The amount of biomass production and respiration of *B. atrophaeus* were larger than those of *E. coli* particularly after 12 h (Fig. C-2; Table C-S1). After 24 h, we did not observe a significant difference in the total respiration between bacterial species for glucose anymore (Table C-S1, mean of 83.4±15.9 mg CO_2). For lysine this effect was still pronounced (55.6±6.8 mg CO_2 (*B. atrophaeus*) and 40.1±3.4 mg CO_2 (*E. coli*) respectively; Fig. C-2c, d; significant time x bacterial species interaction in Table C-S1). The same was true when respiration was standardized to bacterial biomass. There was a significant difference in respiration between bacterial species in the glucose treatment after 24 h ($p < 0.001$; *B. atrophaeus*: 1.7±0.4 mg CO_2 $(10^3$ cells$)^{-1}$, *E. coli*: 0.26 mg±0.04 mg CO_2 $(10^3$ cells$)^{-1}$; Table C-S2).

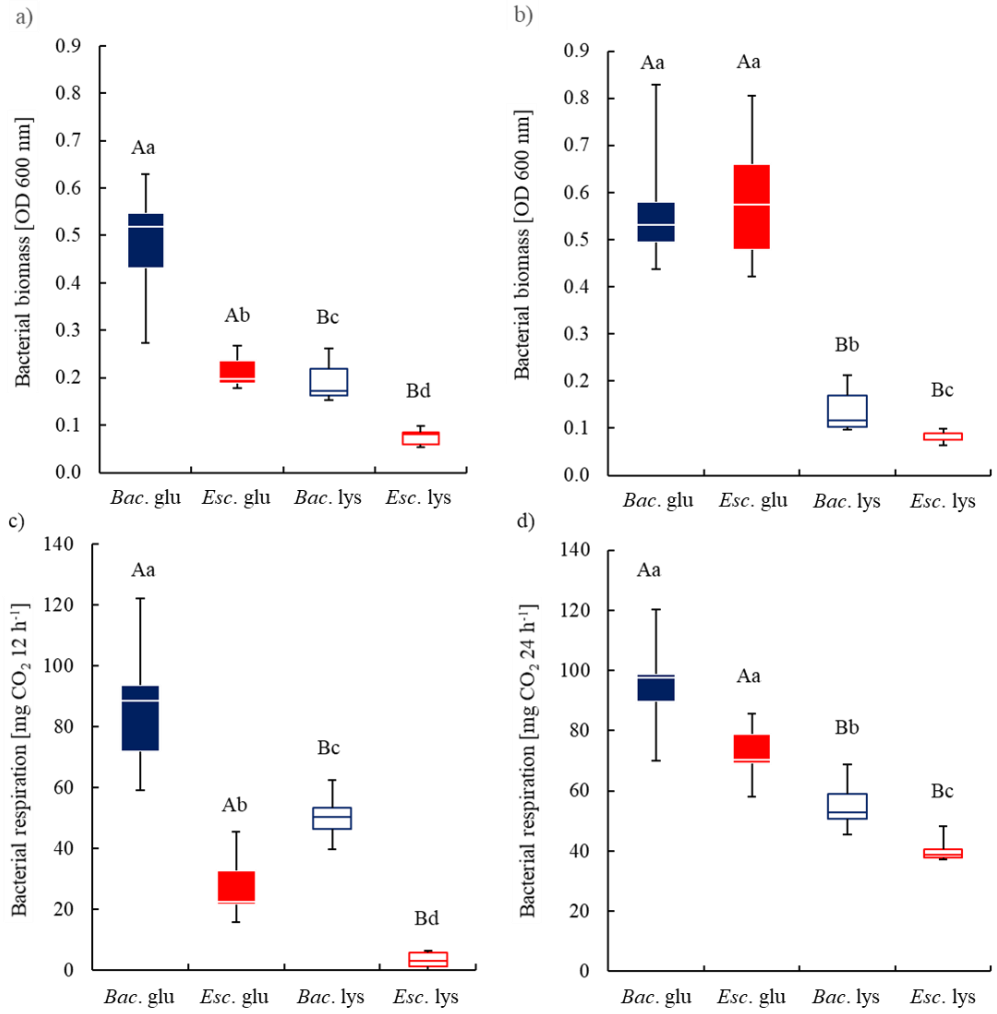

Fig. C-2: Bacterial biomass (Optical density [OD] at 600 nm; a, b) and bacterial respiration (c, d) of *B. atrophaeus* (*Bac.*) and *E. coli* (*Esc.*) and the corresponding substrate (glucose (glu) or lysine (lys)) after 12 h (a, c) and 24 h (b, d) of incubation. Upper-case letters indicate significant differences between substrates, while lower-case letters show significant differences between the two bacterial species. Error bars show the standard deviation of bacterial biomass and respiration for each treatment (n = 9). Please note that (a) and (b) served as a basis to calculate the difference in the optical density [OD] at 600 nm in Figure C-1b.

4.2. Substrate and species effects on δ^2H_n values of bacteria and H incorporation

Initial pre-cultures of *B. atrophaeus* grown on LB-medium showed a tendency of lower exchangeable H concentrations (19.1 %; n = 2) compared with *E. coli* (25.3 %; n = 2). After incubation in the M9 minimal medium with either glucose or lysine, *B. atrophaeus* had a significantly larger contribution of exchangeable H (23.4±6.0 %) than *E. coli* (19.4±3.4 %; Table C-S1 and C-S3).

The δ^2H_n values of the inocula of the bacterial species ranged between -119.8 ‰ and -115.7 ‰ (*B. atrophaeus* for the 12- and 24-hour incubations, respectively; n = 1 for each incubation duration) and between -163.0 ‰ and -168.8 ‰ (*E. coli* for the 12- and 24-hour incubations, respectively). Because these small, random differences were temporally propagated, we did not evaluate the effects of time and bacterial species on δ^2H_n values of the bacterial species ($\delta^2H_{n\ bac}$) during the incubation. Nevertheless, the effect of water can be assessed independently and this was different for the substrates (significant substrate x water interaction in Table C-S1).

$\delta^2H_{n\ bac}$ values in the lysine treatment did not increase with increasingly ^2H-enriched incubation waters for each bacterium species (mean and standard deviations of the $\delta^2H_{n\ bac}$ values for both incubation times: *B. atrophaeus* -110.8±9.4 ‰, *E. coli*: -90.2±12.4 ‰; Fig. C-3). Accordingly, the slope of the regression of $\delta^2H_{n\ bac}$ values on δ^2H_{iW} values did not differ significantly from zero (0.49 > p >0.07) and no incorporation from ambient water-H was detected for the lysine treatment (therefore not included in Table C-S1).

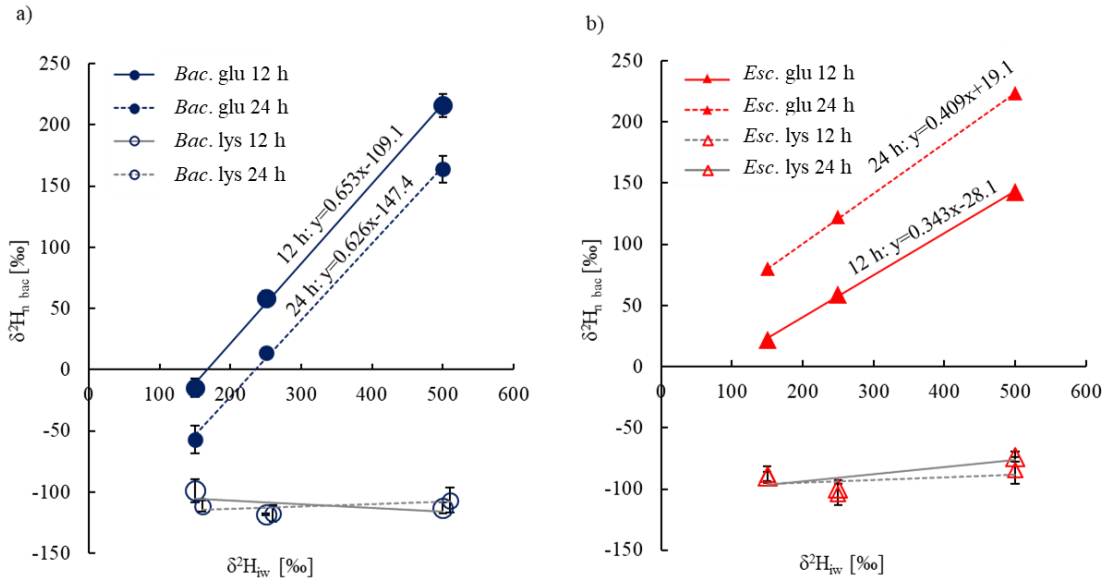

Fig. C-3: Regression of the $\delta^2H_{n\ bac}$ values of *B. atrophaeus* (*Bac.*) (a) and *E. coli* (*Esc.*) (b) on the δ^2H_{iw} values (+150 ‰, +250 ‰, +500 ‰) for glucose (glu) or lysine (lys) after 12 h (solid lines) and 24 h (dashed lines) of incubation. If the regression line of $\delta^2H_{n\ bac}$ values on δ^2H_{iW} values did not significantly differ from zero indicating that ^2H-enriched water labels did not result in more positive $\delta^2H_{n\ bac}$ values, lines were colored in grey and the regression equation was excluded. Error bars show the standard deviation of $\delta^2H_{n\ bac}$ values for each time step (n = 3).

Nevertheless, the $\delta^2H_{n\ bac}$ values during the incubation were enriched in ^2H as compared to initial $\delta^2H_{n\ bac}$ values ($\varepsilon_{ti/t0}$; *B. atrophaeus*: 7.9±10.7 ‰; *E. coli*: 90.8±14.6 ‰) and this difference significantly differed from zero (p ≤0.007; Fig. C-3). In contrast to the lysine treatment (Table C-S1; significant interaction substrate x water), $\delta^2H_{n\ bac}$ values in the glucose treatment differed significantly

among the three ^{2}H-enriched incubation water treatments for both bacterial species (Fig. C-3; Table C-S1).

Table C-1: Compilation of the results for bacterial species, analyzed compartment, culture medium with the means of calculated incorporation (x_{inc}) and the isotope fractionation (expressed both as $\alpha_{inc\text{-}w}$ and $\varepsilon_{BacBiom/w}$) of our incubation experiment and recalculated values for data of previously published studies according to Eq. 6 and 7.

source	bacterial species	compartment	culture medium	time [h]	x_{inc} [%]	$\alpha_{inc\text{-}w}$	$\varepsilon_{BacBiom/w}$ [‰]
This study	*B. atrophaeus*	Cells	M9 Minimal medium (MM) + Glucose	12	78.2±6.0	0.835±0.001	-165±1
			M9 MM + Glucose	24	79.4±5.7	0.789±0.004	-207±6
	E. coli	Cells	M9 MM + Glucose	12	42.4±2.7	0.809±0.004	-191±4
			M9 MM + Glucose	24	44.1±3.1	0.927±0.000	-72±1
Kreuzer-Martin et al.[20]	*B. subtilis*	Cells	Schaeffer's sporulation medium (SSM)	3	10.9	1.171	171
		Spores	SSM	48	35.6	0.785	-215
Kreuzer-Martin et al.[8]	*B. subtilis*	Spores	Difco SSM	48	26.9	1.041	41
		Spores	Oxoid SSM	48	34.8	0.832	-168
		Spores	Luria-Bertani	48	33.0	0.970	-30
		Spores	Difco SSM + Glucose	48	30.3	1.022	22
		Spores	Oxoid SSM + Glucose	48	33.1	0.996	-4
Horita and Vass[9]	*B. subtilis*	Cells	BBL Trypticase Soy Broth -TSB (Soybean-Casein Digest Medium)	96	26.3	0.974	-26
	E. agglomerans	Cells	BBL Trypticase Soy Broth -TSB	96	35.7	0.790	-210

Based on the regression, we estimated the incorporation of ambient water-H into the C-bonded H in bacterial biomass (x_{inc}) and the associated isotope fractionation ($\alpha_{inc\text{-}w}$, $\varepsilon_{BacBiom/w}$; Table C-1). x_{inc} did not change with time and was consistently larger for *B. atrophaeus* (mean of the two incubation periods 79.0±5.9 %) than for *E. coli* (43.2±3.0 %; Tables C-S1). The associated isotope fractionation was also different for the two bacterial species (Table C-S1). However, the species-specific effect changed with time (Table C-S1) and was related to the growth rates: if growth rates were small (after 12 hours for *E. coli* and after 24 h for *B. atrophaeus*) $\varepsilon_{BacBiom/w}$ was comparable between species while

it differed between species if growth rates were large (after 12 hours for *B. atrophaeus* and after 24 h for *E. coli*).

5. Discussion

5.1. Incorporation into C-bonded H in the glucose treatment

In the glucose treatment, substrate consumption, bacterial growth, bacterial biomass and respiration were significantly higher than in the lysine treatment (Figs. C-1, C-2). This is in line with the first part of hypothesis (i) and with positive effects of glucose on bacterial growth,[43,44] bacterial biomass[45] and bacterial respiration.[46,47] Growth involves endergonic, anabolic reactions during biosynthesis that are enabled by energy, namely by adenosine triphosphate (ATP).[48] The glycolysis pathway requires glucose as the reaction educt[49] and glucose degradation generates ATP because the net balance is the gain of two ATP molecules per molecule of glucose.[50] This positive net balance of ATP allows bacteria to build up cell compounds and thus can explain the positive effect of glucose on bacterial performance.

Along with the positive effect of glucose on bacterial performance, we found substantial incorporation (39 to 86 %) of ambient water-H into the C-bonded H pool of bacteria in the glucose treatment (Table C-1). This also supports the first part of hypothesis (i) and is higher than the incorporation of ambient water-H in previous bacterial studies ranging from 11 to 36 % (Table C-1). In these previous studies, a reequilibration of H_{ex} with vapor in ambient air after incubation and before H isotope measurements cannot be excluded but could hinder the detection of ^{2}H-enriched H and might have reduced the labeling efficiency. Therefore, incorporation of ambient water-H is underestimated if the exchangeable H is included.[8,9,17,20,21] In line with our results on the nonexchangeable, C-bonded H fraction, 70 % of H in lipids was derived from ambient water-H during decomposition of soil organic matter and this incorporation was mostly driven by bacterial biosynthesis.[51] As opposed to the situation described below for the lysine treatment, ^{2}H from ambient water was incorporated into C-bonded H during glycolysis and the resulting compounds were not oxidized completely but were retained in organismic tissue. This retention is possible via the anabolic mode of the TCA cycle. In anabolic processes, intermediates of the TCA are used for the synthesis of various compounds. For example, acetyl coenzyme A (CoA), which is generated e.g., from the pyruvate produced by the glycolysis pathway, is an important building block of metabolic intermediates in the central carbon metabolism[52] and precursor of many anabolic reactions.[53] The fact that the incorporation of ambient water-H into C-bonded H did not change over time (Table C-1) indicates that catabolic reactions (= loss of incorporated ^{2}H) and anabolic reactions (= preservation of incorporation of ^{2}H) keep pace with each other if glucose is available as a substrate.

In contrast to the last part of hypothesis (i), we found that the incorporation of ambient water-H significantly differed between the two bacterial species (Fig. C-3; Table C-1). This species-specific difference was constant with time (Table C-S1) although the species effect on bacterial performance was not (Figs. C-1, C-2). For example, *E. coli* grew and respired less than *B. atrophaeus* after 12 h, whereas growth and respiration of the two species did not differ after 24 h. Therefore, not the metabolism but the species seem to be relevant for the extent of incorporation of ambient water-H into bacterial biomass. Such species-specific differences in the extent of incorporation of ambient water-H might be related to different contributions of biosynthesis pathways and thus, ultimately to a species-specific chemical composition of bacterial biomass. For example, gram-positive and gram-negative bacteria differ in terms of the composition of the cell wall.[54] Peptidoglycan (PG) is the building block of cell walls composed of units of N-acetyl-glucosamine-N-acetyl-muramic acid crosslinked via pentapeptide chains.[55] Cells and spores of gram-positive bacteria such as *B. atrophaeus* are surrounded by a thick PG layer that accounts for up to 90 % of the bacterial dry weight.[56] By contrast, the PG layer contributes only 10 % in gram-negative bacteria such as *E. coli*.[56] N-acetyl-glucosamine is a derivate of glucose and N-acetyl-muramic acid is a glucose molecule with an acetylated amid at the C_2 position.[57,58] Their synthesis structurally binds acetyl-CoA. Therefore, a thicker layer of PG in *B. atrophaeus* would also reflect a higher glycolysis-related incorporation of ambient water-H than in *E. coli* – which is in line with our results. This reasoning is also corroborated by a larger proportion of H_{ex} in *B. atrophaeus* than in *E. coli* (Table C-S3) because of an increased contribution of O- and N-bonded H in hydroxyl, carboxyl, and amine groups in the PG layer. In summary, the pronounced effect of glucose corroborates glycolysis as the mechanism underlying the incorporation of ambient water-H into organismic tissue. However, the subsequent biosynthesis pathways likely determine the extent of incorporation which is species-specific.

5.2. H incorporation into C-bonded H in the lysine treatment

E. coli showed a partial die-off while *B. atrophaeus* maintained growth – yet at slow rates – if lysine was provided as a substrate (Fig. C-1). Irrespective of bacterial growth, both bacterial species maintained metabolism as indicated by respiration (Fig. C-2b) which is contrary to our expectation (first part of hypothesis ii). In case of carbon starvation of *E. coli*, lysine could be recycled in the stationary phase (cease of growth while metabolism continues) and catabolic reactions[25] that oxidize organic compounds to CO_2, e.g., in the TCA cycle, promote the energy regeneration. Knorr et al.[25] demonstrated the catabolic degradation during the central metabolic pathway of lysine to succinate in *E. coli* via intermediates of glutarate and *L*-2-hydroxyglutarate in wildtype *E. coli*. Compared with Knorr et al.[25] our incubation was not conducted under optimal conditions. More importantly, our M9 minimal medium was not supplemented with glucose as carbon and energy source. These results of Knorr et al.[25] suggest, that the bacteria need a readily available C source to metabolize lysine. The

addition of glucose therefore ensured basic glycolytic activity, which could explain that *E. coli* was not able to show bacterial growth in our experiment with lysine as the sole C-source.

Because *B. atrophaeus* is not able to use lysine as an energy source but also continued metabolic activity, a more likely explanation for the observed ongoing bacterial respiration without substrate consumption might be the bacterial consumption of dead cells. During starvation, cell membranes lose integrity[59] and *E. coli* recycles metabolites from dead cells which sustains the viability of the remaining culture.[60] For *Bacillus subtilis*, González-Pastor et al.[61] described that cells which entered the sporulation pathway act cooperatively by blocking sister cells to sporulate, causing the latter to lyse which allows others to keep on metabolizing and its siblings consequently are cannibalized. In line, we found an indication of sporulation for the extracted bacterial pellets of *B. atrophaeus* which showed a red color.[62] Therefore, in contrast to hypothesis (ii), not the metabolic pathways but the bacterial recycling decided about the bacterial performance of *E. coli* and *B atrophaeus* in the lysine treatment.

The lack of an incorporation of ambient water-H in the lysine treatment (Fig. C-3) in principle corroborates the second part of hypothesis (ii). However, this could have been simply attributable to the lacking lysine consumption and growth (Fig. C-1). Therefore, we cannot confirm that incorporation of ambient water-H does not take place for growth substrates that are not involved in glycolysis because this would have required an uptake of lysine by the bacterial species, which was not the case. Nevertheless, the lack of incorporation of ambient water-H in the lysine treatment is different from studies showing such an incorporation for any metabolically active bacteria.[8,9,17,20,21] Irrespective of the C source, the measured respiration rates suggest that the studied bacteria were metabolically active. The stressful conditions indicated by large respiration:cell number ratios[46,63,64] in the lysine treatment were more pronounced for *B. atrophaeus* than *E. coli* at both sampling times and even only showed up for *E. coli* after 24 h of incubation (Fig. C-S1). This stress likely forced the bacterial species to produce energy for basic metabolism in the absence of a suitable growth substrate. Yet, despite basic metabolic activity, we could not calculate H incorporation for the lysine treatment. Knowledge on reaction pathways of metabolic activity under sub-optimal growth conditions is scarce.[60,65] Nevertheless, although glycolysis as part of the basic metabolism might have involved the incorporation of ^{2}H from the isotopically labeled incubation waters in our study, the C-^{2}H bond in GAP can be broken again during subsequent oxidation steps in the TCA cycle. We speculate that a respiration-driven ^{2}H incorporation was no longer detectable because the former synthesized C-^{2}H bonds were completely oxidized to CO_2. In other words, the amphibolic TCA cycle worked in the catabolic mode that serves to generate energy. In summary, the incorporation of ambient water-H into the C-bonded H fraction was negligible in the studied bacteria under the specific stressful conditions of our lysine treatment.

Strikingly, although the complete conversion to CO_2 should have eradicated any isotope effect, a significant, label-independent ^{2}H enrichment of $\delta^{2}H_{n\ bac}$ values after incubation as compared to initial

$\delta^2H_{n\ bac}$ values for bacterial species was observed in the lysine treatment ($\varepsilon_{ti/t0}$; *B. atrophaeus*: 7.9±10.7 ‰; *E. coli*: 90.8±14.6 ‰). In general, a ^2H enrichment in bacteria growing on substrates involved in the TCA cycle was also reported for lipids[26,29] although the ^2H enrichment was less pronounced under stationary phase conditions.[29] The ^2H enrichment was attributed to positive isotope fractionation factors associated with the reduction of nicotinamide adenine dinucleotide phosphate ($NADP^+$) by dehydrogenase and transhydrogenase enzymes.[29,66] Because these reactions involve hydride transfers also from ambient water[15,26] – which we did not find – NADPH-related reactions cannot explain the ^2H enrichment of bacteria in our incubation. Alternatively, kinetic isotope fractionation associated with the complete conversion of R-C-^2H to H_2O and CO_2 might result in a ^2H enrichment in the remaining bacterial biomass – and a ^2H depletion in the produced H_2O. Similarly, during SOM decomposition ^{13}C enrichment in the remaining SOM and ^{13}C depletion in the produced CO_2 were reported.[67,68] Furthermore, a ^2H depletion in intracellular water due to metabolic activity of *E. coli* was also reported by Kreuzer-Martin et al.[69] Notably, the ^2H depletion was most pronounced under stressful (stationary phase) conditions[69] that also apply to our lysine treatment. In summary, the type of growth substrate and the resulting importance of catabolic reactions dictate whether the incorporation of ambient water-H will leave an imprint on the bacterial species.

5.3. Isotope fractionation associated with H incorporation into C-bonded H

In case of relatively small growth rates (*E. coli* after 12 h; *B. atrophaeus* after 24 h; Fig. C-1b), $\varepsilon_{BacBiom/w}$ was around -200 ‰ for both species (Table C-1). This is in line with hypothesis (iii). However, during pronounced growth (*E. coli* after 24 h; *B. atrophaeus* after 12 h; Fig. C-1b), $\varepsilon_{BacBiom/w}$ was less negative and differed between the two studied bacterium species (Tables S1). This is contrary to our expectation and to the postulation of species-independent H isotope fractionation factors.[26] Furthermore, several studies suggested that heterotrophic metabolism results in an enrichment in ^2H in the synthesized product relative to ambient water,[7,15,29] which is the opposite of what we found. Nevertheless, other studies confirm that $\varepsilon_{BacBiom/w}$ can be as low as -215 ‰[20] (Table C-1). In conjunction with our findings related to the importance of reactions involved in metabolism (Section C 5.1) we propose that the highly variable $\varepsilon_{BacBiom/w}$ values are a result of different growth-induced- net apparent fractionation factors. In agreement, different H isotope fractionation during lipid synthesis in bacteria in stationary and exponential growth phases were reported.[29] In more detail, Wijker et al.[26] argued that not only ^2H enrichment but also ^2H depletion is possible in bacterial lipids. They found ^2H depleted lipids in *E. coli* and attributed this to an imbalance between the demand for NADPH as reducing power for anabolic reactions and catabolic NADPH production.[26] The NADPH underproduction shifts the net apparent isotope fractionation from ^2H enrichment in NADPH as a reaction product towards ^2H depletion in NADH as the reaction educt.[26] Such an imbalanced NADPH

consumption and production was not only evident in *E. coli* but also in *B. subtilis*.[26] Consequently, our results suggest a species- independent H isotope fractionation. However, we cannot tease apart the effect of growth rates and metabolic fluxes from species because the two species varied in growth (Fig. C-1b) and metabolic rates. In summary, growth conditions and likely the related metabolic fluxes influence the isotope fractionation associated with the incorporation of ambient water-H into bacterial biomass.

Our results show that bacteria adjust δ^2H_n values to the H isotopic composition of ambient water during metabolism and therefore, δ^2H_n values of bacteria are not isotopically stable. On the one hand, the influence of metabolic flux rates under changing environmental conditions constrains the assignment of bacterial origins and thus, of soil samples based on H isotope ratios. Notably, under stressful conditions, the isotopic composition of water is not incorporated into bacterial biomass because bacteria switch to catabolic metabolism. Stressful conditions imply e.g., desiccation,[70] nutrient limitation,[71] and starvation,[72] especially starvation of glucose[73,74] leading to increased catabolic activity. Under these conditions, soil samples will preserve the imprint of ambient water on δ^2H_n values of SOM at the sample location. On the other hand, the H isotope approach opens up new opportunities to study growth conditions of bacteria under different environmental conditions together with different bacterial activities and metabolism. Furthermore, our results improve the understanding of microbial modification of δ^2H_n values in soil organic matter (SOM) and might moreover be useful to assess the microbial input to SOM.

6. Acknowledgements

We thank Lars Grimm, Ellen Röhm and Dr. Casey Bryce for the technical support in the microbiology laboratory and Sabine Flaiz for advice and assistance in EA-IRMS analyses. We also thank Prof. Dr. Jan Marienhagen and Sascha Sokolowsky (Institute of Bio- and Geosciences; Jülich) for lysine analysis. The study was funded by the German Research Foundation (DFG, OE516/11-1).

7. References

(1) Meier-Augenstein, W.; Hobson, K. A.; Wassenaar, L. I. Critique: measuring hydrogen stable isotope abundance of proteins to infer origins of wildlife, food and people. *Bioanalysis* **2013**, 5, 751−767.

(2) Hallworth, M. T.; Marra, P. P.; McFarland, K. P.; Zahendra, S.; Studds, C. E. Tracking dragons: stable isotopes reveal the annual cycle of a long-distance migratory insect. *Biol. Lett.* **2018**, 14, 20180741.

(3) Hobson, K. A.; Doward, K.; Kardynal, K. J.; Mcneil, J. N. Inferring origins of migrating insects using isoscapes: a case study using the true armyworm, *Mythimna unipuncta*, in North America. *Ecol. Entomol*. **2018**, 43, 332−341.

(4) Bowen, G. J.; Wassenaar, L. I.; Hobson, K. A. Global application of stable hydrogen and oxygen isotopes to wildlife forensics. *Oecologia* **2005**, 143, 337−348.

(5) West, J. B.; Bowen, G. J.; Dawson, T. E.; Tu, K. P. Isoscapes Springer Netherlands: Dordrecht, **2010**, DOI: 10.1007/978-90-481-3354-3.

(6) Ruppenthal, M.; Oelmann, Y.; Wilcke, W. Isotope ratios of nonexchangeable hydrogen in soils from different climate zones. *Geoderma* **2010**, 155, 231−241.

(7) Ruppenthal, M.; Oelmann, Y.; del Valle, H. F.; Wilcke, W. Stable isotope ratios of nonexchangeable hydrogen in organic matter of soils and plants along a 2100-km climosequence in Argentina: New insights into soil organic matter sources and transformations? *Geochim*. *Cosmochim*. *Acta* **2015**, 152, 54−71.

(8) Kreuzer-Martin, H. W.; Chesson, L. A.; Lott, M. J.; Dorigan, J. V.; Ehleringer, J. R. Stable isotope ratios as a tool in microbial forensics Part 1. Microbial isotopic composition as a function of growth medium. *J. Forensic Sci*. **2004**, 49, 1−7.

(9) Horita, J.; Vass, A. A. Stable-isotope fingerprints of biological agents as forensic tools. *J. Forensic Sci*. **2003**, 48, 2002170.

(10) Berg, J. M.; Tymoczko, J. L.; Stryer, L. Biochemistry 7th ed., Freeman Palgrave Macmillan: New York, NY 2012.

(11) Gerlt, J. A. Stabilization of Reactive Intermediates and Transition States in Enzyme Active Sites by Hydrogen Bonding. In: Comprehensive *Nat. Prod. Chem.*; 5−29. Elsevier, 1999.

(12) Knowles, J. R.; Albery, W. J. Perfection in enzyme catalysis: the energetics of triosephosphate isomerase. *Acc. Chem. Res*. **1977**, 10, 105−111.

(13) Rieder, S. V.; Rose, I. A. The mechanism of the triosephosphate isomerase reaction. *J. Biol. Chem*. **1959**, 234, 1007−1010.

(14) Whitman, C. P. Keto−Enol Tautomerism in Enzymatic Reactions. In: Comprehensive *Nat. Prod. Chem.*; 31−50. Elsevier,1999.

(15) Yakir, D. Variations in the natural abundance of oxygen-18 and deuterium in plant carbohydrates. *Plant, Cell Environ*. **1992**, 15, 1005−1020.

(16) Bren, A.; Park, J. O.; Towbin, B. D.; Dekel, E.; Rabinowitz, J. D.; Alon, U. Glucose becomes one of the worst carbon sources for *E. coli* on poor nitrogen sources due to suboptimal levels of cAMP. *Sci. Rep*. **2016**, 6, 24834.

(17) Fogel, M. L.; Griffin, P. L.; Newsome, S. D. Hydrogen isotopes in individual amino acids reflect differentiated pools of hydrogen from food and water in *Escherichia coli. Proc. Natl. Acad. Sci*. *U. S. A*. **2016**, 113, 4648−4653.

(18) Schimmelmann, A. Determination of the concentration and stable isotopic composition of nonexchangeable hydrogen in organic matter. *Anal. Chem*. **1991**, 63, 2456−2459.

(19) Wassenaar, L. I.; Hobson, K. A. Improved method for determining the stable-hydrogen isotopic composition (δD) of complex organic materials of environmental interest. *Environ. Sci. Technol.* **2000**, 34, 2354−2360.

(20) Kreuzer-Martin, H. W.; Lott, M. J.; Dorigan, J.; Ehleringer, J. R. Microbe forensics: oxygen and hydrogen stable isotope ratios in *Bacillus subtilis* cells and spores. *Proc. Natl. Acad. Sci. U. S. A*. **2003**, 100, 815−819.

(21) Kreuzer-Martin, H. W.; Jarman, K. H. Stable isotope ratios and forensic analysis of microorganisms. *Appl. Environ. Microbiol*. **2007**, 73, 3896−3908.

(22) Ruppenthal, M.; Oelmann, Y.; Wilcke, W. Optimized demineralization technique for the measurement of stable isotope ratios of nonexchangeable H in soil organic matter. *Environ. Sci. Technol.* **2013**, 47, 949−957.

(23) Neshich, I. A. P.; Kiyota, E.; Arruda, P. Genome-wide analysis of lysine catabolism in bacteria reveals new connections with osmotic stress resistance. *ISME J.* **2013**, 7, 2400−2410.

(24) Newsholme, P.; Stenson, L.; Sulvucci, M.; Sumayao, R.; Krause, M. Amino Acid Metabolism. In: *Compr. Biotech.* **2011**, 3−14.

(25) Knorr, S.; Sinn, M.; Galetskiy, D.; Williams, R. M.; Wang, C.; Müller, N.; Mayans, O.; Schleheck, D.; Hartig, J. S. Widespread bacterial lysine degradation proceeding via glutarate and L-2-hydroxyglutarate. *Nat. Commun.* **2018**, 9, 5071.

(26) Wijker, R. S.; Sessions, A. L.; Fuhrer, T.; Phan, M. 2H/1H variation in microbial lipids is controlled by NADPH metabolism. *Proc. Natl. Acad. Sci. U. S. A.* **2019**, 116, 12173−12182.

(27) Jackson, J. B.; Peake, S. J.; White, S. A. Structure and mechanism of proton-translocating transhydrogenase. *FEBS Lett.* **1999**, 464, 1−8.

(28) O'Leary, M. H. Multiple isotope effects on enzyme-catalyzed reactions. *Annu. Rev. Biochem.* **1989**, 58, 377−401.

(29) Heinzelmann, S. M.; Villanueva, L.; Sinke-Schoen, D.; Sinninghe Damsté, J. S.; Schouten, S.; van der Meer, M. T. J. Impact of metabolism and growth phase on the hydrogen isotopic composition of microbial fatty acids. *Front. Microbiol.* **2015**, 6, 408.

(30) Zhao, W.; Fang, J.; Huang, X.; Zhang, Y.; Liu, W.; Wang, Y.; Zhang, L. Carbon and hydrogen isotope fractionation in lipid biosynthesis by *Sporosarcina* sp. DSK25. *Geochem. Perspect. Lett.* **2020**, 9−13.

(31) Sessions, A. L.; Burgoyne, T. W.; Schimmelmann, A.; Hayes, J. M. Fractionation of hydrogen isotopes in lipid biosynthesis. *Org. Geochem.* **1999**, 30, 1193−1200.

(32) Fang, J.; Li, C.; Zhang, L.; Davis, T.; Kato, C.; Bartlett, D. H. Hydrogen isotope fractionation in lipid biosynthesis by the piezophilic bacterium *Moritella japonica* DSK1. *Chem. Geol.* **2014**, 367, 34−38.

(33) Xiao, J.; Elf, J..; Li, G.; Ji, Y.; Xie, G. S. Imaging Gene Expression in Living Cells at the Single-Molecule Level. In: *Single Molecules*: A *Laboratory Manual.* **2008**.

(34) Kessler, A.; Kreis, K.; Merseburger, S.; Wilcke, W.; Oelmann, Y. Incorporation of hydrogen from ambient water into the C-bonded H pool during litter decomposition. *Soil Biol. Biochem.* **2021**, 162, 108407.

(35) Feng, X.; Krishnamurthy, R. V.; Epstein, S. Determination ofratios of nonexchangeable hydrogen in cellulose: A method based on the cellulose-water exchange reaction. *Geochim. Cosmochim. Acta* **1993**, 57, 4249−4256.

(36) Filot, M. S.; Leuenberger, M.; Pazdur, A.; Boettger, T. Rapid online equilibration method to determine the D/H ratios of non- exchangeable hydrogen in cellulose. *Rapid Commun. Mass Spectrom.: RCM* **2006**, 20, 3337−3344.

(37) Sessions, A. L.; Hayes, J. M. Calculation of hydrogen isotopic fractionations in biogeochemical systems. *Geochim. Cosmochim. Acta* **2005**, 69, 593−597.

(38) Sauer, P. E.; Schimmelmann, A.; Sessions, A. L.; Topalov, K. Simplified batch equilibration for D/H determination of non- exchangeable hydrogen in solid organic material. *Rapid Commun. Mass Spectrom.: RCM* **2009**, 23, 949−956.

(39) Schimmelmann, A.; Lewan, M. D.; Wintsch, R. P. D/H isotope ratios of kerogen, bitumen, oil, and water in hydrous pyrolysis of source rocks containing kerogen types I, II, IIS, and III. *Geochim. Cosmochim. Acta* **1999**, 63, 3751−3766.

(40) Levenberg, K. A method for the solution of certain non-linear problems in least squares. *Quart. Appl. Math.* **1944**, 2, 164−168.

(41) Marquardt, D. W. An Algorithm for Least-Squares Estimation of Nonlinear Parameters. *J. Soc. Ind. Appl. Math.* **1963**, 11, 431−441.

(42) Yakir, D.; Deniro, M. J. Oxygen and hydrogen isotope fractionation during cellulose metabolism in *Lemna gibba* L. *Plant Physiol.* **1990**, 93, 325−332.

(43) Blagodatskaya, E.; Kuzyakov, Y. Active microorganisms in soil: Critical review of estimation criteria and approaches. *Soil Biol. Biochem.* **2013**, 67, 192−211.

(44) Mau, R. L.; Liu, C. M.; Aziz, M.; Schwartz, E.; Dijkstra, P.; Marks, J. C.; Price, L. B.; Keim, P.; Hungate, B. A. Linking soil bacterial biodiversity and soil carbon stability. *ISME J.* **2015**, 9, 1477−1480.

(45) Sparling, G. P. Microcalorimetry and other methods to assess biomass and activity in soil. *Soil Biol. Biochem.* **1981**, 13, 93−98.

(46) Anderson, T.-H.; Domsch, K. H. Soil microbial biomass: The eco-physiological approach. *Soil Biol. Biochem.* **2010**, 42, 2039−2043.

(47) Ehlers, K.; Bakken, L. R.; Frostegård, Å.; Frossard, E.; Bünemann, E. K. Phosphorus limitation in a Ferralsol: Impact on microbial activity and cell internal P pools. *Soil Biol. Biochem*. **2010**, 42, 558−566.

(48) Repke, K. R. H. Reinstatement of the ATP high energy paradigm. *Mol. Cell. Biochem.* **1996**, 160-161, 95−99.

(49) Zhang, S.; Yang, W.; Chen, H.; Liu, B.; Lin, B.; Tao, Y. Metabolic engineering for efficient supply of acetyl-CoA from different carbon sources in *Escherichia coli. Microb. Cell Fact.* **2019**, 18, 130.

(50) Chaudhry, R.; Varacallo, M. StatPearls. *Biochemistry, Glycolysis, Treasure Island* (FL); 2021.

(51) Paul, A.; Hatté, C.; Pastor, L.; Thiry, Y.; Siclet, F.; Balesdent, J. Hydrogen dynamics in soil organic matter as determined by ^{13}C and ^{2}H labeling experiments. *Biogeosciences* **2016**, 13, 6587−6598.

(52) Kremer, K.; van Teeseling, M. C. F.; Schada von Borzyskowski, L.; Bernhardsgrütter, I.; van Spanning, R. J. M.; Gates, A. J.; Remus- Emsermann, M. N. P.; Thanbichler, M.; Erb, T. J. Dynamic metabolic rewiring enables efficient acetyl coenzyme A assimilation in *Paracoccus denitrificans*. *MBio* **2019**, 10.

(53) Martínez-Reyes, I.; Chandel, N. S. Mitochondrial TCA cycle metabolites control physiology and disease. *Nat. Commun*. **2020**, 11, 102.

(54) Madigan, M. T.; Martinko, J. M. *Brock biology of microorganisms*; 11th ed., Pearson Prentice Hall: Upper Saddle River, NJ 2006.

(55) Typas, A.; Banzhaf, M.; Gross, C. A.; Vollmer, W. From the regulation of peptidoglycan synthesis to bacterial growth and morphology. *Nat. Rev. Microbiol*. **2011**, 10, 123−136.

(56) Malanovic, N.; Lohner, K. Antimicrobial peptides targeting Gram-positive bacteria. *Pharmaceuticals* **2016**, 9, 59.

(57) Apostel, C.; Dippold, M.; Kuzyakov, Y. Biochemistry of hexose and pentose transformations in soil analyzed by position-specific labeling and ^{13}C-PLFA. *Soil Biol. Biochem*. **2015**, 80, 199−208.

(58) Gunina, A.; Dippold, M. A.; Glaser, B.; Kuzyakov, Y. Fate of low molecular weight organic substances in an arable soil: from microbial uptake to utilisation and stabilisation. Soil Biol. Biochem. 2014, 77, 304−313.

(59) Schink, S. J.; Biselli, E.; Ammar, C.; Gerland, U. Death Rate of E. coli during Starvation Is Set by Maintenance Cost and Biomass Recycling. *Cell Syst*. **2019**, 9, 64−73.

(60) Lempp, M.; Lubrano, P.; Bange, G.; Link, H. Metabolism of non-growing bacteria. *Biol. Chem*. **2020**, 401, 1479−1485.

(61) González-Pastor, J. E.; Hobbs, E. C.; Losick, R. Cannibalism by sporulating bacteria. *Science* **2003**, 301, 510−513.

(62) Moeller, R.; Horneck, G.; Facius, R.; Stackebrandt, E. Role of pigmentation in protecting *Bacillus* sp. endospores against environ- mental UV radiation. *FEMS Microbiol. Ecol*. **2005**, 51, 231−236.

(63) Killham, K. A physiological determination of the impact of environmental stress on the activity of microbial biomass. *Environ. Pollut., Ser. A* **1985**, 38, 283−294.

(64) Yin, Y.; Gu, J.; Wang, X.; Zhang, Y.; Zheng, W.; Chen, R.; Wang, X. Effects of rhamnolipid and Tween-80 on cellulase activities and metabolic functions of the bacterial community during chicken manure composting. *Bioresour. Technol.* **2019**, 288, 121507.

(65) Bergkessel, M.; Basta, D. W.; Newman, D. K. The physiology of growth arrest: uniting molecular and environmental microbiology. *Nat. Rev. Microbiol*. **2016**, 14, 549−562.

(66) Zhang, X.; Gillespie, A. L.; Sessions, A. L. Large D/H variations in bacterial lipids reflect central metabolic pathways. *Proc. Natl. Acad. Sci. U. S. A.* **2009**, 106, 12580−12586.

(67) Brüggemann, N.; Gessler, A.; Kayler, Z.; Keel, S. G.; Badeck, F.; Barthel, M.; Boeckx, P.; Buchmann, N.; Brugnoli, E.; Esperschü tz, J.; Gavrichkova, O.; Ghashghaie, J.; Gomez-Casanovas, N.; Keitel, C.; Knohl, A.; Kuptz, D.; Palacio, S.; Salmon, Y.; Uchida, Y.; Bahn, M. Carbon allocation and carbon isotope fluxes in the plant-soil- atmosphere continuum: a review. *Biogeosciences* **2011**, 8, 3457−3489.

(68) Werth, M.; Kuzyakov, Y. ^{13}C fractionation at the root−microorganisms−soil interface: A review and outlook for partitioning studies. *Soil Biol. Biochem*. **2010**, 42, 1372−1384.

(69) Kreuzer-Martin, H. W.; Lott, M. J.; Ehleringer, J. R.; Hegg, E. L. Metabolic processes account for the majority of the intracellular water in log-phase *Escherichia coli* cells as revealed by hydrogen isotopes. *Biochemistry* **2006**, 45, 13622−13630.

(70) Manzoni, S.; Schaeffer, S. M.; Katul, G.; Porporato, A.; Schimel, J. P. A theoretical analysis of microbial eco-physiological and diffusion limitations to carbon cycling in drying soils. *Soil Biol. Biochem.* **2014**, 73, 69−83.

(71) Shimizu, K. Regulation systems of bacteria such as *Escherichia coli* in response to nutrient limitation and environmental stresses. *Metabolites* **2014**, 4, 1−35.

(72) Chubukov, V.; Sauer, U. Environmental dependence of stationary-phase metabolism in *Bacillus subtilis* and *Escherichia coli*. *Appl. Environ. Microbiol*. **2014**, 80, 2901−2909.

(73) Death, A.; Ferenci, T. Between feast and famine: endogenous inducer synthesis in the adaptation of *Escherichia coli* to growth with limiting carbohydrates. *J. Bacteriol*. **1994**, 176, 5101−5107.

(74) Matin, A. Microbial regulatory mechanisms at low nutrient concentrations as studied in chemostat. *Strategies of Microbial Life in Extreme Environments*: Dahlem Konferenzen: Berlin, 1979.

Section D

Incorporation of Hydrogen from Ambient Water into the C-bonded H Fraction: An Organic Matter Delabeling Approach under Field Conditions

Arnim Kessler[1], Felix Schneider[1], Stefan Merseburger[2], Wolfgang Wilcke[2] and Yvonne Oelmann[1]

[1] *Geoecology. University of Tübingen. Tübingen. Germany*

[2] *Institute of Geography and Geoecology. Karlsruhe Institute of Technology (KIT). Karlsruhe. Germany*

Author	Author number	Scientific Idea	Experimental Work	Data Analysis and Interpretation	Paper Writing
Arnim Kessler	1.	0 %	80 %	50 %	50 %
Felix Schneider	2.	0 %	20 %	20 %	0 %
Stefan Merseburger	3.	0 %	0 %	0 %	0 %
Wolfgang Wilcke	4.	20 %	0 %	0 %	5 %
Yvonne Oelmann	5.	80 %	0 %	30 %	45 %

Title

Incorporation of Hydrogen from Ambient Water into the C-bonded H Faction:

An Organic Matter Delabeling Approach under Field Conditions

Status of publication

Manuscript in preparation

1. Abstract

The close correlation of C-bonded stable H isotope ratios (δ^2H_n values) in soil organic matter (SOM) with long-term mean δ^2H values of local rainfall arouses great interest with regards to the source of SOM. We performed a 20-weeks litterbag experiment with ^2H labelled and differently decomposable leaves (*Fagus sylvatica* L. - beech, *Tilia platyphyllos* SCOP. - lime). Our results show that during decomposition, ^2H enriched leaves exchange with ambient water and leaves get subsequently ^2H depleted resulting in an incorporation of ambient water-H into the C-bonded H fraction of 43-79 %. Although the incorporation rates strongly depended on litter type, C-mass loss was not the driving factor the observed incorporation in leaves. Leached organic matter (TOM) was also depleted in ^2H and did not depend on the H isotopic composition of leaves. Rather we suggest that the ^2H depletion and the incorporation of H from ambient water into leaves is driven by transformation processes during the microbial processing of OM and bacterial inputs together with constant tree species specific H isotope fractionation. For leached TOM we were not able to determine incorporation rates. However, we suspect that the leached TOM consists of leached compounds with a high proportion of external microorganisms carrying the site-specific δ^2H_n values. Our results highlight the importance of the microbial input and belowground plant biomass as the sources of SOM.

Graphical abstract

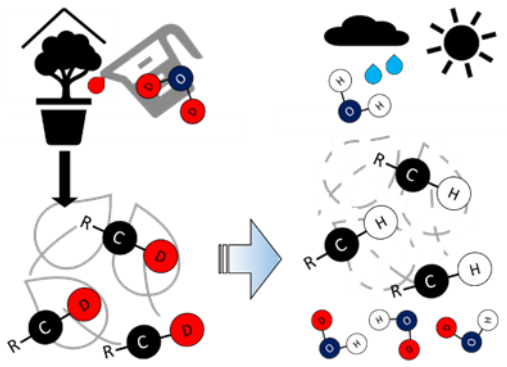

2. Introduction

Litter decomposition contributes to the formation of soil organic matter (SOM) and releases CO_2 in the atmosphere and thus, plays an important role as a sink and a source in the global carbon (C) cycle.[1–3] Stable isotope approaches were successfully applied to shed light on bulk C and nitrogen (N) dynamics during litter decomposition[4,5] while there is little knowledge about bulk hydrogen (H) dynamics during decomposition.

Laboratory studies revealed that ambient water-H is incorporated into C-H bonds of OM during decomposition.[6] This incorporation is due to the *de novo* formation of C-H bonds during glycolysis,[7–12]

a metabolic pathway, which is shared by nearly all organisms on earth.[13] Accordingly, up to 80 % of H in microbial biomass originates from ambient water-H incorporated during recent metabolic activity relying on easily available substrates such as glucose or complex nutrient mixtures.[12,14–16] Similarly, Paul et al.[17] used clearly defined, different ^{2}H enriched molecules to derive the incorporation of water during microbial biosynthesis. However, the H incorporation was much smaller (< 9 %) if natural leaf litter was provided as a substrate for microorganism metabolism under laboratory conditions with optimum temperature and water availability.[6] It remains to be tested whether ambient water-H incorporation into C-bonded H is detectable at all during decomposition under field conditions including temperature and water availability below optimum for metabolic activity of microorganisms. The quantification of ambient water-H incorporation into C-bonded H commonly relies on the recovery of ^{2}H-labeled ambient water in organic material such as microorganisms or litter.[6,12,14–16] As opposed to a constant H isotope ratio ($\delta^{2}H$) of ambient water in closed incubation systems in the laboratory, the $\delta^{2}H$ values of soil water can vary from -34 ‰ to -72 ‰ within weeks under field conditions of a temperate climate.[18] This variability combined with a loss of the ^{2}H label via evaporation and leaching renders mass balance calculations based on the ^{2}H labeling of ambient water under field conditions impossible. Alternatively, the decomposing material can be isotopically labeled. For example, ^{13}C- or ^{15}N-labeled litter were exposed to field conditions for up to 8 years.[19–21] In these studies, the temporal course of the C and N isotope signatures ($\delta^{13}C$, $\delta^{15}N$) in the litter and in mineral soil was used to infer leaf litter decomposition and SOM dynamics Similarly, Paul et al.[17] made use of ^{2}H- (and ^{13}C) labeled compounds to assess ambient water-H incorporation into C-bonded H in soil during decomposition. However, this study was carried out under laboratory conditions and not under field conditions. Additionally, they used three model compounds for glucid, lipid and protein families which only partly resemble the complexity of compounds present in litter and SOM. Therefore, a new approach based on ^{2}H-labeled natural litter needs to be developed to study H dynamics during litter decomposition under field conditions. Theoretically, the production of ^{2}H-labeled litter should be possible given that several studies reported increased $\delta^{2}H$ values of leaves if plants were irrigated with ^{2}H-enriched water.[22,23] The decrease in the isotope signature of C-bonded H ($\delta^{2}H_{n}$) of litter over time could inform about the extent of replacement of the ^{2}H label by isotopically lighter ambient water-H (delabeling) and thus, about ambient water-H incorporation during decomposition under field conditions.

After a given exposure time in the field, the litter will comprise a mixture of organic compounds initially present in the litter, metabolites produced during decomposition and microbial biomass[24–27] of which only the latter two experienced an incorporation of ambient water-H. By contrast, the water percolating through the litter will contain mainly metabolites and microbial detritus – particularly after the first flush of water-soluble compounds contained initially in the litter.[28,29] Therefore, organic compounds in litter leachates likely will be characterized by larger ambient water-H incorporation into C-bonded H as compared to those in the decomposed litter.

The ambient water-H incorporation during litter decomposition can be expected to be linked to metabolic activity including glycolysis in microorganisms.[6,30] Metabolic activity of microorganisms is increased in case of favorable, easily degradable substrates.[1,12,31] Therefore, litter containing higher concentrations of recalcitrant compounds and thus, higher C:N ratios, will be decomposed slower[32–34] which likely will be associated with a larger incorporation of ambient water-H into the C-bonded H fraction. Our aim was to develop a litter delabeling approach to quantify the incorporation of ambient water-H into C-bonded H of litter during decomposition under field conditions. To this end, we studied the replacement of ^2H in labeled leaf litter and in litter leachates by isotopically lighter ambient water-H during decomposition of rapidly decomposing *Tilia platyphyllos* SCOPOLI leaves and of more slowly decomposing *Fagus sylvatica* LINNÉ leaves. We hypothesized that (i) during decomposition of ^2H labeled leaves isotopically light ambient water-H will be incorporated into the C-bonded H fraction resulting in a decrease in δ^2H_n values of leaf litter over time. Furthermore, we expected that the decrease in δ^2H_n values will be more pronounced (ii) for organic matter in litter leachates than for the decomposed leaf litter and (iii) in case of the rapidly decomposing lime as compared to the slowly decomposing beech leaf litter.

3. Material and Methods

3.1. Production of ^2H-enriched leaves

We planted three to four years old trees of *T. platyphyllos* (lime) *and F. sylvativa* (beech) in flower pots in a greenhouse in spring 2018. The trees were watered twice a week with 800 mL of waters differing in the isotopic signature (δ^2H_W= +50 ‰ and δ^2H_W= +250 ‰) which were produced by mixing deionized water with the corresponding amount of deuterated water (> 99.99 % ^2H, Deuterium Oxide, Campro Scientific, Germany) according to isotopic mass balance calculation.[35] Furthermore, we included a control water treatment (C) without the addition of deuterated water and used tap water from the Laboratory of Soil Science and Geoecology at the University of Tübingen (δ^2H_W= -66.9 ± standard deviation of 1.7 ‰, n = 11). After a growing season of six months, all leaves were harvested directly from the trees to avoid pre-colonization of soil organisms. Afterwards, leaves of each tree individual were dried separately in a drying oven at 40 °C for 48 hours and subsequently merged to one composite sample containing three tree individuals within one water label treatment. 1 to 2 g of each replicate was stored as initial leaf sample whereas another aliquot of 1 to 2 g of dried leaves were filled into litterbags with a size of 10 x 10 cm^2. The litterbags were produced using a polyethylene (PE) net with a mesh size of 2 x 2 mm (Meyer Gartenbau, Germany) and sewed with a PE thread (Edeka, Germany).

3.2. Study sites, litterbag experiment and sample processing

The study sites are located close to the city of Tübingen, Germany (site 1: 9.0436, 48.5511; site 2: 9.0522°, 48.5537°; WGS84) in proximity of around 400m to each other. In 2019, mean annual temperature recorded at a weather station in proximity to the sites was 10.8 °C and mean annual precipitation was 660.7 mm.[36] The parent material of the soils is Knollenmergel resulting in Luvisols.[37] The vegetation of the first site consists exclusively of *F. sylvatica* trees while the second site is characterized by mainly *T. platyphyllos* trees with a few trees of *Quercus robur* L. and *Acer pseudoplatanus* L.. At each site, air temperature and soil surface temperature were monitored in 15 min intervals (TMS-4, TOMST s.r.o., Czech Republic). Additionally, the volume of precipitation was measured in biweekly intervals and precipitation samples were taken biweekly with HDPE Containers placed at a height of one metre with a collection opening diameter of 0.1 m (VWR chemicals, Germany). To study the decomposition of beech and lime leaves, litterbags with a size of 10 x 10 cm and a mesh size of 2 mm were placed into upwards opened HDPE containers (VWR chemicals) (= lysimeters) upright on the forest floor. To collect the leached total organic matter (TOM) of each container, a short tube (PVC) was inserted at one side of the containers and connected to a water flask (Duran, Germany) which were placed lower down in a watertight box (Fig. D-S1). To prevent external litter input, the containers were covered with a PE mesh with a mesh size of 2 x 2 cm. Therefore, litterbags were not in contact with material of the local organic layer. This simplification was necessary to facilitate the tracing of the H isotope label by avoiding dilution effects by site-specific OM on the litter/native OM mixture. Yet, microbial colonization of litterbags was enabled by leaching of the phyllosphere via the precipitation. For example, the phyllosphere and the OM in the canopy is characterized by microorganisms which are similar to the microbial biomass on the forest floor[38] while the microorganisms of the phillosphere are leached via the precipitation.[39] Litterbags of each litter type were placed at the "home" site forest stands (beech litter at beech site; lime litter at lime site) and at an "away" site (beech litter at lime site; lime litter at beech site). We did not observe any differences neither between the sites nor between the home/away contrast for each litter type (Table D-S1). Therefore, we combined the results of the two sites for data analyses resulting in n = 6 for each litter type and label treatment (Table D-S2). For leaf litter, there was a destructive sampling of a subset of the samples after four, 12 and 20 weeks. In total, 108 lysimeters were equipped with litterbags: three time steps two litter types x three label treatments x time intervals x six replicates. The experimental setup and sample processing is described in the SI in more detail. With exception of the first time step of four weeks, TOM samples were taken in biweekly intervals and immediately frozen at -20 °C. Afterwards, leached TOM samples were defrosted and bulked as follows: TOM samples of the leaf litter exposed in the field over four (TOM_{T1}) and 12 weeks (TOM_{T2}) were bulked over the respective decomposition period of leaf litter. Only the percolates of leaf litter exposed to decomposition over 20 weeks were bulked four-weekly (TOM_{T1-T5}) to investigate the temporal variability of TOM, resulting

in five time steps. Bulked TOM samples were frozen again and subsequently lyophilized (NaProFood GmbH, Germany). Afterwards the lyophilized TOM samples were ground (Pulverisette 5, Fritsch, Germany).

3.3. Steam-Equilibration and stable H analysis

To account for the exchangeable fraction of H (H_{ex}) that does not carry a robust isotope signal of the leaves and TOM, we used the equilibration device based on the design used by Wassenaar and Hobson[40] and modified by Ruppenthal et al.[41]. Detailed information on the steam equilibration setup and stable H analysis and analytical quality are presented in the SI.

3.4. Calculations and statistical evaluation

Leaf mass loss in litterbags that comprises gaseous (respired CO_2) and dissolved organic C, expressed as the lost fraction of initial C stock (%) was calculated according to Kessler et al.[6] If TOM only originate from degradation, there should be a close linkage between TOM mass and C-mass loss. However, if additional OM is entering the TOM, for example via the input of microorganisms from the phyllosphere[39] the mass of leached TOM and C-mass loss do not match. Thus, with respect to the ratio of leached TOM mass to C-mass loss over time, we estimate whether the source of leached TOM (degradation versus external input) has changed over time. Based on the calculations, we determined δ^2H_n values of initial leaves ($\delta^2H_{n\ leaves\ t0}$) and for each sampling time step ($\delta^2H_{n\ leaves\ ti}$). Consequently, δ^2H_n values of bulked TOM samples ($\delta^2H_{n\ TOM}$) were calculated in accordance with the corresponding litterbags. Here, δ^2H_n values of TOM $_{T1}$ ($\delta^2H_{n\ TOM\ T1}$) were calculated in accordance with leaf litter which was exposed to decomposition over four weeks in the field. $\delta^2H_{n\ TOM}$ of TOM $_{T2}$ ($\delta^2H_{n\ TOM\ T2}$) were analyzed from bulked TOM samples. Furthermore, in order to allow for a direct comparison between $\delta^2H_{n\ TOM}$ (biweekly sampling until final time step of 20 weeks ($\delta^2H_{n\ TOM\ b}$) and $\delta^2H_{n\ leaves}$ (sampled once at final time step of 20 weeks), we calculated $\delta^2H_{n\ TOM\ b}$ by the volume of leached TOM. To differentiate exchange processes with air moisture or vapour in the exchangeable H pool (accounted for methodologically, see Section D 2), the metabolic incorporation from ambient water-H into the C-bonded H pool is termed incorporation". If $\delta^2H_{n\ leaves\ t0}$ values are manipulated e.g. enriched in ^2H, it is possible to trace the incorporation of isotopically lighter ambient water-H. The incorporation of H from ambient water will shift the H isotope signature of leaves towards isotopically lighter δ^2H_W values. Commonly, ambient water is isotopically labelled.[12,14–16] For these studies, the slope of the regression of δ^2H_n values of organisms on δ^2H values of ambient water is used to calculate the incorporation of ambient water-H into the C-bonded H pool of organisms and the associated apparent H fractionation factor.[12] Because under field conditions it is challenging to manipulate the H isotopic composition of ambient water over a longer period of time, we used two leaf litter label treatments. Our reasoning is as follows: If there is no incorporation of ambient water-H into the

C-bonded H fraction, initial δ^2H_n values of leaves before decomposition ($\delta^2H_{n\ leaves\ t0}$) and δ^2H_n values of leaves at a given time step ($\delta^2H_{n\ leaves\ ti}$) should be equal, and the slope of the regression of the $\delta^2H_{n\ leaves\ ti}$ on $\delta^2H_{n\ leaves\ t0}$ of the two labels should be close to 1. Contrary to this, a complete incorporation of ambient water-H into the C-bonded H fraction should shift the initial, ^2H-enriched $\delta^2H_{n\ leaves\ t0}$ values towards the non-labeled control and thus, result in similar $\delta^2H_{n\ leaves\ ti}$ values of the label treatments and δ^2H_n values of the control treatment ($\delta^2H_{n\ leaves\ C}$). Therefore, $\delta^2H_{n\ leaves\ ti}$ will no longer be related to the initial label and the slope of the regression of $\delta^2H_{n\ leaves\ ti}$ on $\delta^2H_{n\ leaves\ t0}$ will be close to zero. Consequently, the slope can be used to infer the extent of incorporation of ambient water-H into the C-bonded H fraction. However, the corresponding H fractionation factor between the OM and water ($\alpha_{inc\text{-}w}$) also forms part of the slope.[12] We followed the approach that we used in a former experiment to quantify both the H incorporation (x_{inc}) and the associated H isotope fractionation factor $\alpha_{inc\text{-}w}$.[12] Because of the reversed relationship between the slope and the incorporation in (slope of 1 indicates no incorporation) as compared to our previous approach (slope of 1 reflects incorporation for the complete H pool), the incorporation x_{inc} was calculated as the deviation from 1 and expressed in percent in the current study. Linear regressions and estimations for the incorporation of ambient water-H into the C-bonded H fraction and $\alpha_{inc\text{-}w}$ require (i) an initial labeled δ^2H_n value of the corresponding sample. Furthermore, (ii) there should be an absence of a water treatment effect on the resulting δ^2H_n values which implies, that there was an incorporation of ambient water-H into the C-bonded H pool which results in the disappearance of the water treatment effect. In all cases where the requirements were met, the estimates for x_{inc} and $\alpha_{inc\text{-}w}$ are given by a unique solution. The incorporation relates to the complete time period until leaves or leached TOM were sampled. However, there was no initial labeled δ^2H_n value of leached TOM. Furthermore, δ^2H_n values of leached TOM consistently did not show an effect of the water label during leaf litter decomposition. As a result, we were not able to calculate an incorporation of ambient water-H into the C-bonded H pool of the leached TOM.

To determine the net apparent isotope fractionation factor of ^2H between $\delta^2H_{n\ leaves\ ti}$ and $\delta^2H_{n\ leaves\ t0}$ ($\varepsilon^2H_{n\ ti\text{-}t0}$) as well as between leached TOM and leaves ($\varepsilon^2H_{n\ TOM\text{-}leaves}$) we calculated the net apparent H isotope fractionation factor for each time step according to Coplen.[42] Information on statistical analyses are described in the SI.

4. Results

4.1. Climatic conditions and hydrogen isotope ratios of precipitation

Soil temperature constantly decreased from a maximum of 17.2 ± standard deviation of 0.2 °C in August to a minimum of 2.5±0.4 °C in January at the end of the experiment, which is typical for the

seasonal course (mean of 7.8±5.0 °C) (Fig. D-2). The sum of precipitation during the experiment was 219.6±42.3 mm and a maximum monthly precipitation of 75.5±20.3 mm was reached in October. This coincides with the period of leaf shedding which usually ends around late October or early November for beech and lime under these climate conditions.[43,44] On average, $\delta^2H_{n\ prec}$ values were -81.4±28.2 ‰ with a minimum of -143.1±1.9 ‰ at the time step with the lowest recorded amount of precipitation of 27.4±9.2 mm during November (Fig. D-2).

4.2. Leaf mass loss

The C:N ratio of leaves strongly depended on tree species ($p < 0.001$; Table. D-S2; Fig. D-1b): C:N ratios of beech were larger than for lime. During the experimental course, the initial C:N ratio of beech leaves were significantly higher (22.2±2.2) as compared to all subsequent sampling intervals of decomposing leaf litter (19.1±0.2). By contrast, C:N ratios of lime leaves were 14.8±2.2 over 20 weeks of leaf litter exposure under field conditions. The mass loss of leaves expressed as the proportional loss of the initial C stock of leaves significantly increased with time (Fig. D-1a; Table D-S2) and was significantly larger for lime than for beech throughout the experimental course (after 20 weeks: 88 % and 59 %, for lime and beech, respectively).

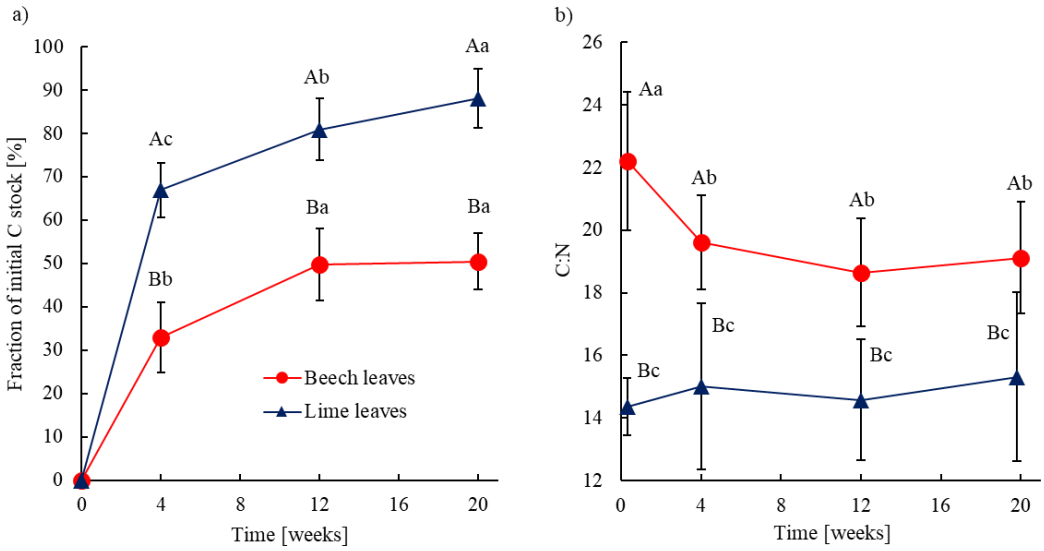

Fig. D-1: Fraction of the initial C stock in leaves lost in total (relative mass loss) (a) and (b) C:N ratio for beech and lime during 20 weeks of leaf litter decomposition under field conditions. Capital letters indicate significant differences between tree species while lowercase letters show significant differences between subsequent time steps. Error bars show the standard deviations for each time step (n = 18).

4.3. Carbon-bonded stable hydrogen isotope ratios in leaves

Initially, leaves of both tree species showed significantly different proportions of exchangeable H (Table D-S2; beech: 23.9±9.3 %; lime: 7.3±2.4 %). Within four weeks, the proportion of exchangeable H decreased (significant time effect) which was more pronounced in the leaves of beech compared to lime (significant interaction time x tree species, Table D-S2). Thereafter, the tree species effect was no longer evident, resulting in an average proportion of exchangeable H of 4.2±1.0 % after 20 weeks.

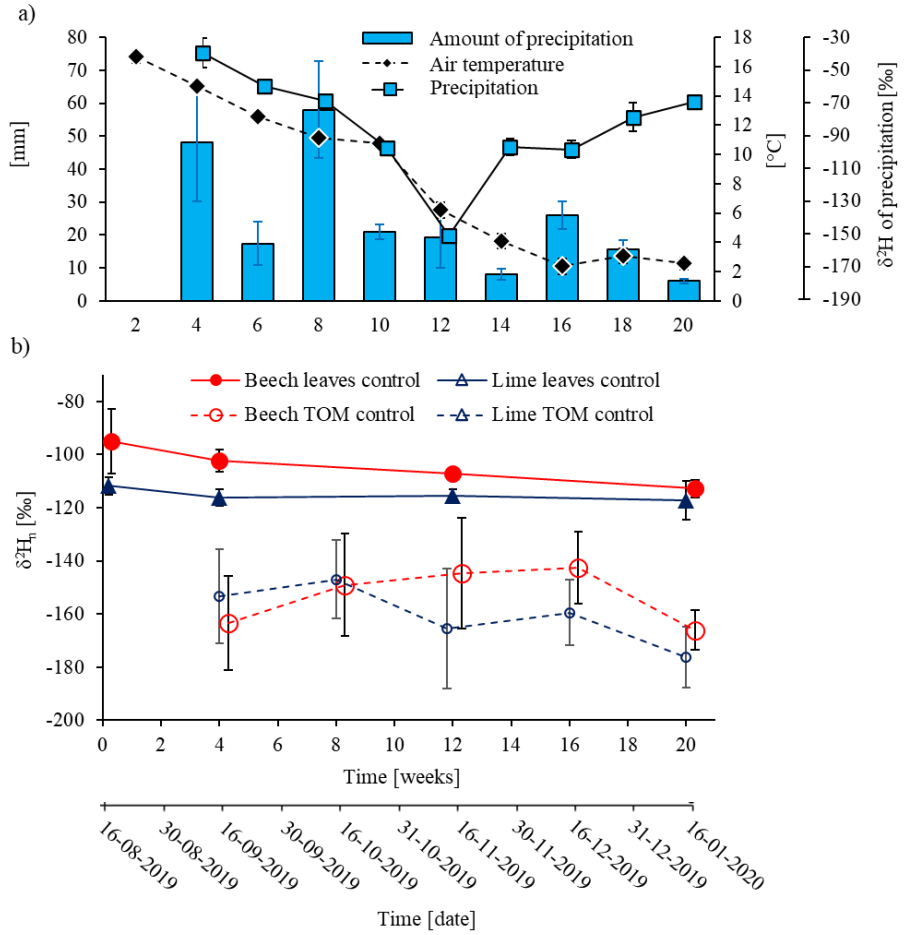

Fig. D-2: Mean amount of local precipitation, mean of air temperature, δ^2H values of local precipitation and δ^2H_n values of leaves and biweekly bulked TOM (with exception for the first time step after four weeks) of the control treatments (n = 6) for beech and lime during 20 weeks of decomposition. Error bars show the standard deviations for each time step. To ease readability, the sampling times have been shifted slightly.

The irrigation of tree saplings with waters differing in the H isotopic composition had a significant influence on initial $\delta^2H_{n\ leaf}$ values of tree species ($p = 0.003$) and depended on the corresponding water treatment ($p < 0.001$) with -95.1±12.2 ‰, -71.3±12.3 ‰, -55.3±8.1 ‰ (beech) and -111.7±3.3 ‰, -94.9±1.4 ‰, -72.4±8.9 ‰ (lime) for the control, +50 ‰ and +250 ‰ treatment, respectively (Fig. D-2 and Fig. D-3). Similarly, $\delta^2H_{n\ leaf}$ values during decomposition strongly depended on the

water label ($p < 0.001$) (Fig. D-S2 and Fig. D-S3; Table D-S2). Over time, $\delta^2H_{n\ leaf}$ values decreased in dependence of water label, most pronounced during the first four weeks of decomposition (significant interaction of time x leaf label, Fig. D-S2 and Fig. D-S3). $\delta^2H_{n\ leaf}$ values significantly decreased over time ($p < 0.004$). With regard to the temporal course of $\delta^2H_{n\ leaf}$ values we found no superior effect of tree species (significant interaction of time x tree species, Table D-S2) whereas $\delta^2H_{n\ leaf}$ values of beech showed a larger decrease over time as compared to lime (Fig. D-S2) which is shown by the significant interaction of time x tree species (Table D-S2).

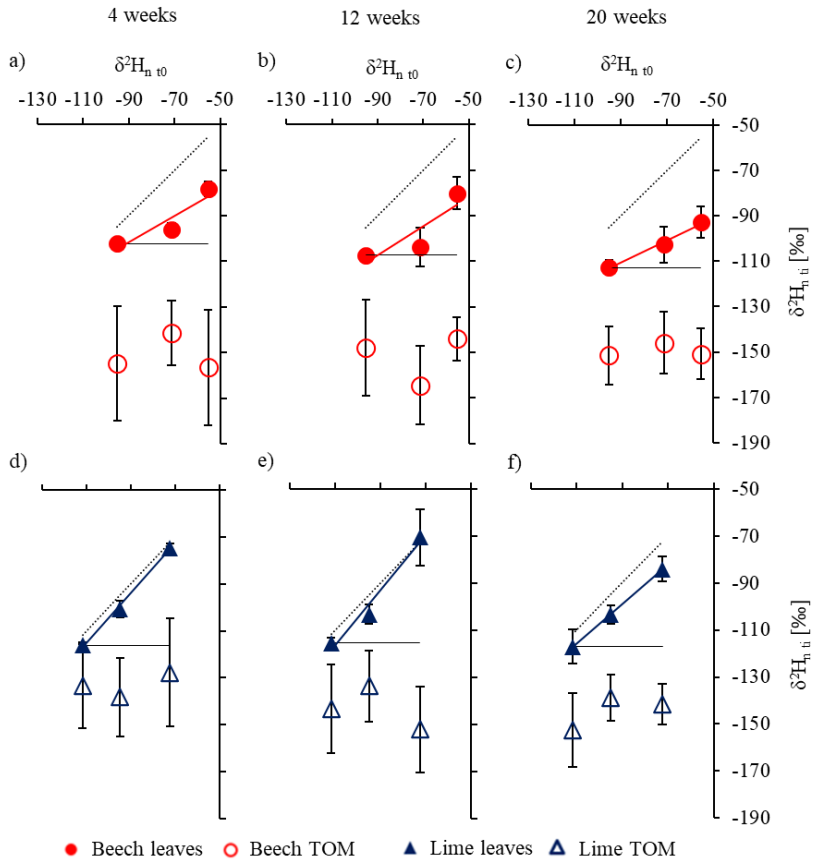

Fig. D-3: $\delta^2H_{n\ leaves}$ and $\delta^2H_{n\ TOM}$ values after each time step (t_i) depending on initial $\delta^2H_{n\ leaves}$ and $\delta^2H_{n\ TOM}$ values (t_0) for beech (a-c) and lime (d-f) after 4, 12 and 20 weeks of decomposition. The regression line of initial δ^2H_n values ($\delta^2H_{n\ t0}$) on δ^2H_n values at each time step ($\delta^2H_{n\ ti}$) are given for the decomposing leaves. Dotted lines visualize the 1:1 relationship between $\delta^2H_{n\ t0}$ and $\delta^2H_{n\ ti}$ values meaning that there is no change between $\delta^2H_{n\ t0}$ and $\delta^2H_{n\ ti}$ values and accordingly, no ambient water-H incorporation. By contrast, horizontal solid lines show the pattern that would emerge if all H was incorporated from ambient water and thus $\delta^2H_{n\ ti}$ values of initially ^{2}H-enriched leaves shifted towards the non-labelled control (slope = 0). Error bars show the standard deviation of $\delta^2H_{n\ leaves}$ and $\delta^2H_{n\ TOM}$ values for each leave litter type and time step (n = 6).

Although $\delta^2H_{n\ leaf}$ values of the control treatments strongly depended on tree species (beech: -107.5±5.4 ‰ and lime: beech: -116.2±4.9 ‰; $p < 0.001$) $\delta^2H_{n\ leaf}$ values of the control treatments did not differ between time steps ($p > 0.143$). Furthermore, for all leaf labels, $\delta^2H_{n\ leaf}$ values of beech deviated more from initial $\delta^2H_{n\ leaf}$ values compared to lime (significant interaction of tree species and leaf label) (Fig. D-S2 and Fig. D-S3). The regression of $\delta^2H_{n\ leaves\ ti}$ on $\delta^2H_{n\ leaves\ t0}$ values was significant for all sampling intervals and leaf litter types ($p < 0.001$) and yielded the following slopes: 0.58, 0.64, 0.50 (beech) and 1.06, 1.16, 0.84 (lime) after 4, 12, and 20 weeks, respectively (Fig. D-3; Table D-S3). Based on these regressions, after 20 weeks of decomposition, we found that 48 % of H in the C-bonded H fraction of beech and 15 % of lime leaves experienced an incorporation of ambient water-H. The incorporation was accompanied by an apparent H isotope fractionation of $\varepsilon_{leaves\ ti/leaves\ t0}$= -39 ‰ and -7 ‰ for beech and lime, respectively.

4.4. Carbon-bonded stable hydrogen isotope ratios in leached organic compounds

Irrespective of leaf litter type, M_{TOM} decreased with time from 106.9±63.2 mg after 4 weeks to 3.3±2.9 mg after 20 weeks of decomposition. The ratio of M_{TOM} to C-mass loss with 2.3±1.7 was constant over time and did not differ between leaf litter types. The proportion of exchangeable H of leached TOM slightly changed over time from 9.2±4.4 % after 4 weeks to 6.7±2.9 % after 20 weeks (Table D-S2) but did not depend on leaf litter type. Differences between $\delta^2H_{n\ TOM}$ were significantly lower compared to $\delta^2H_{n\ leaves}$ for the control treatments irrespective of water treatments and tree species but was mostly pronounced from the 16th week of decomposition (Fig. D-2 and Fig. D-3). $\delta^2H_{n\ TOM}$ values of both leaf litter types were different depending on the time considered (Table D-S2; Fig. D-S2 and Fig. D-S3). During decomposition under field conditions, leached TOM was characterized by similar $\delta^2H_{n\ TOM}$ values irrespective of label and leaf litter type (Table D-S2; Fig. D-2 and Fig. D-S3). H isotope fractionation between leaves and leached TOM ($\varepsilon^2H_{\ TOM/\ leaves}$) was constant over the course of the experiment (Fig. D-2; Table D-S3). After 4 weeks of decomposition, leached TOM of beech showed a more negative apparent fractionation compared to lime with an overall mean of -49.3±23.5 ‰ and -31.7±21.9 ‰ respectively. The slopes of the regressions of $\delta^2H_{n\ leaf\ t0}$ on $\delta^2H_{n\ TOM}$ did not differ significantly from zero ($p > 0.05$).

5. Discussion

5.1. Incorporation of ambient water-H into the C-bonded H fraction of leaves during decomposition under field conditions

The ^2H enrichment and thus, the isotopic labeling of tree leaves was successful since $\delta^2H_{n\ leaves}$ of initial leaves depended on δ^2H values of the waters used for irrigation in the greenhouse (Fig. D-3;

Table D-S2). Irrespective of tree species, $\delta^2H_{n\ leaves}$ values were significantly and increasingly enriched in ^2H with increasing δ^2H values of the irrigation water (Fig. D-3 and Fig. D-S2). This is in line with the incorporation of H from the source water during biosynthesis reactions in plants which include an increase in *n*-alkane δ^2H values.[22,23] However, differences in δ^2H values of irrigation water treatments ($\Delta^2H_{50\text{-}C}$ = 120 ‰, $\Delta^2H_{250\text{-}50}$ = 200 ‰) were not reflected in differences of initial $\delta^2H_{n\ leaf}$ values neither for lime ($\Delta^2H_{n\ 50\text{-}C}$ = 16.8 ‰, $\Delta^2H_{n\ 250\text{-}50}$ = 22.5 ‰) nor for beech ($\Delta^2H_{n\ 50\text{-}C}$ = 23.8 ‰, $\Delta^2H_{n\ 250\text{-}50}$ = 16.0 ‰). On the one hand, the transpirational exchange of leaf water between individual trees during leaf growth in the greenhouse might have reduced the initially large difference in δ^2H values among irrigation waters. Leaf water is in a constant exchange with water vapor of the atmosphere.[45] The result of the equilibrium exchange between ^2H enriched leaf water and ^2H depleted atmospheric vapor is, that δ^2H values of leaf water are less positive than the applied tracer[22] and therefore leaf tissue is ^2H depleted compared to δ^2H values of the irrigation water. Future studies should minimize such effects by placing a vapor barrier between tree individuals that receive differently ^2H-enriched irrigation water. On the other hand, there is a strong negative of approximately -170 ‰ during the photolysis of water that is the net effect of (i) a negative H isotope fractionation during the incorporation of H into NADPH[11,46] and (ii) a positive H isotope fractionation during the exchange of C-bonded H of photosynthates with cell water.[47,48] During the exposition of leaf litter in the field, $\delta^2H_{n\ leaf}$ values of the control treatments did not vary much (Fig. D-3). Since the irrigation water of the control treatment had δ^2H values similar to incident rainfall at the field sites (Fig. D-2), we can assume that $\delta^2H_{n\ leaf}$ values of the control treatment are in equilibrium with δ^2H values of the local precipitation. For beech, this is furthermore supported by a comparable δ^2H_n values (-95.1±12.1 ‰) as compared to freshly fallen beech litter which was collected approx. 6 km away from the experiment site (-80.5 ‰).[6]

By contrast, $\delta^2H_{n\ leaf}$ values of the label treatments significantly decreased during the exposition of leaf litter in the field (Fig. D-3, significant interaction of leaf label and time, Table D-S2) which is supported by the most pronounced decrease in $\delta^2H_{n\ leaf}$ values at the beginning (Fig. D-2) and the co-occurring most pronounced mass loss during decomposition (Fig. D-1). We can exclude the preferential leaching of ^2H-enriched compounds as an explanation because $\delta^2H_{n\ TOM}$ values were not enriched in ^2H and also showed no difference between the two labels (Fig. D-3). Alternatively, the incorporation of isotopically lighter ambient water-H can be inferred to the greatest C-mass loss rates during the first 12 weeks irrespective of tree species (Fig. D-1a). There is an overlapping substrate usage by bacteria and fungi during early stages of decomposition.[49] While fungi mobilize compounds that could otherwise not be metabolized by bacteria,[50] a higher glycolytic activity in bacteria compared to fungi seemed to be reasonable.

While decomposition in early stages occurs simultaneously by bacteria and fungi,[51] shift from bacterial to fungal mediated decomposition, driven by less soluble C compound availability have been

observed especially during early stages of decomposition of a few months[52] to breakdown more complex C-compounds.[53]

The use of two labels enabled us to quantify the incorporation of ambient water-H into the C-bonded H fraction during decomposition under field conditions. To this end, we used the regression between $\delta^2H_{n\ leaves\ ti}$ values after exposure in the field on the initial $\delta^2H_{n\ leaves\ ti}$. After 20 weeks of litter decomposition, the calculated percentage of incorporation of ambient water-H into the C-bonded H pool ranged between 15 % and 48 %. This incorporation is larger as compared to our laboratory incubation experiment showing an incorporation of <5 % into leaf litter.[6] However, in the mentioned study, leaf litter decomposition was only studied over four weeks of incubation associated with much lower C-mass losses of 32 % to initial C stock compared to 70 % (in this study, Fig. D-1a). While Paul et al.[17] showed that 47 to 69 % H of the added compounds was mineralized within the first weeks, 70 % of C-bonded H of the defined compounds underwent exchange with water-H, which can be explained by a longer duration of the laboratory incubation experiment and model substances that do not represent realistic ecological conditions. In summary our results confirm our first hypothesis that the incorporation of isotopically light ambient water-H into the formerly ^2H labeled C-bonded H fraction of leaf litter is detectable during decomposition under field conditions.

5.2. Incorporation of ambient water-H into the C-bonded H fraction of leached organic matter during decomposition under field conditions

The calculation of the incorporation of ambient water-H into the C-bonded H pool of leached TOM turned out to be difficult because there were no differences in $\delta^2H_{n\ TOM}$ values neither among labels nor between label treatments and control at any sampling interval (Fig. D-2 and Fig. D-3; Table D-S2). Therefore, there is no initial ^2H-enriched TOM that is successively delabeled, which is contrary to the pattern of what we observed for leaf litter. Nevertheless, the slopes of $\delta^2H_{n\ TOM\ ti}$ values on $\delta^2H_{n\ leaves\ t0}$ values close to zero at all sampling intervals (Fig. D-3). As a possible explanation, we suspect an incorporation of ambient water-H that affects the complete C-bonded H pool of leached TOM. However, in a previous laboratory experiment under optimum temperature and moisture conditions, we found a much less incorporation into leached TOM[6] and the variability in δ^2H values of rainwater is not reflected in the corresponding $\delta^2H_{n\ TOM}$ values. Therefore, the possible explanations are not likely to explain the observed pattern of $\delta^2H_{n\ TOM}$ values. Instead, we assume that the leached TOM consists of microbial metabolites synthesized at the time when they were leached, and older compounds carrying the H isotopic signature of precipitation, while δ^2H_n values are integrated over an extended period. Additionally, we assume that there is an external input into leached TOM via throughfall. This might also comprise microorganisms and their remains originating from the canopy and results in a homogenization, because leached microorganisms differ in age and metabolic activities at different points in time. This assumption is supported by relatively long turnover rates of

microbial C of about one year[54] resulting in incomplete exchange processes and incorporation rates. Furthermore, there is an increase of organic C from throughfall to percolates and leached OM concentrations increase from rainwater through the passage of the forest canopy.[55] Here, Vance and Nadkarni[38] highlighted, that the microbial biomass in the canopy humus is similar to that of the forest floor while DOM concentrations are driven by the microbial activity.[56,57]

The decomposition of dead OM in the canopy of trees can also contribute to DOC in throughfall[58] and can contribute up to 30 % to TOC.[59] Because C-mass loss and the volume of rainfall decreased over the experimental period from 32.9 to 0.7 % (beech) and 66.8 to 7.2 % (lime) of initial C stock and 48.2 to 5.9 mm respectively, it was difficult to separate the origin of leached TOM. Furthermore, the influence of leaching from the canopy decreased also because of leaf shedding towards the end of the litter exposure in the field after 12 weeks. Accordingly, both the C-mass loss from leaf litter and the mass of leached TOM decreased with ongoing experimental duration and results in a relatively constant ratio of 2.3±1.7 over time (Table S-4). Augusti et al.[60] showed, that the hydrogen isotopic signature of formerly bonded H gets imprinted by the surrounding water during C-H breakdown which could explain the delabeling of leached TOM, while the H isotopic composition of the former C-H bonds is found in the surrounding water. Otherwise during leaf litter incubation, we have shown, that the incorporation of ambient water-H in leached compounds is only 5-8 %.[6] However, it has to be kept in mind, that the C mass loss in that experiment was also lower (20-25 %) than in our current study.

Our results suggest that TOM consists of a mixture of decomposed OM which probably underwent H incorporation and ancient compounds, so that the resulting $\delta^2H_{n\ TOM}$ values are accumulated and δ^2H values of precipitation are integrated in the C-bonded H fraction of TOM over a longer time period. Here, we suggest external bacterial input originating from leaves into TOM, carrying the local specific δ^2H_n values and compounds that experienced incorporation.

Contrary to our hypothesis, our results suggest, that the ^2H depletion is not mainly driven by an incorporation of ambient water-H into the C-bonded H fraction of TOM. Instead, because $\delta^2H_{n\ TOM}$ values did not reflect δ^2H values of precipitation we suggest that $\delta^2H_{n\ TOM}$ values can be explained by a TOM input from the canopy that comprises microorganisms showing the site-specific H isotopic composition with a large incorporation of ambient water-H. Therefore, we have to reject hypothesis two. However, further experiments are needed to shed light on the chemical composition of leached TOM under field conditions.

5.3. Tree species effects on ambient water-H incorporation during decomposition of leaf litter under field conditions

We found a higher incorporation of ambient water-H into the C-bonded H fraction in beech leaves as compared to lime leaves (Fig. D-3) even though leaves of lime were decomposed faster as compared to beech leaves (Fig. D-1). Furthermore, $\delta^2H_{n\ leaf\ ti}$ values of lime did not differ from the initial

$\delta^2H_{n\ leaf\ t0}$ values after four and 12 weeks (slope close to 1; Fig. D-3; Table S3) although these were the time intervals with the fastest decomposition (69 to 65 %, respectively, of C in lime leaves had been decomposed already; Fig. D-1a). These findings are contrary to our expectation that decomposability is directly linked to an incorporation of ambient water-H into the C-bonded H fraction and a simultaneous delabeling. The microbial community and the metabolism of certain groups might be a key to understand these counterintuitive results. Firstly, the determined incorporation rates into leaves can be explained by tree species specific colonizable surfaces for the microbial community. Due to the lower mass loss of beech, the microbial biomass on the surface of leaves in the litterbags have a larger living habitat compared to lime leaves that highlights the microbial contribution to the analyzed leaf samples. Additionally, the microbial habitat of lime successively declined with ongoing decomposition and bacteria sticking to the leaf surfaces get leached. Accordingly, it is known that the surface area of beech litter increases during litter decomposition.[61] Because of the larger incorporation of ambient water-H in microorganisms[12] the colonizable surface controlling the microbial biomass might be decisive for the extent of ambient water-H incorporation. As a result, the microbial community composition and its metabolism affect the H incorporation into leaves. We have shown that C:N ratios of beech were larger than for lime. The larger C:N ratios of beech leaves are an indicator for less degradable and resistant compounds.[62] Furthermore, higher C:N ratios of beech leaves (Fig. D-1b) suggest preceding fungal decomposition[49] and gram-positive bacteria are adapted to more biochemically complex litter input and decompose complex substrates but have slow growth rates[63] with a mean residence time (MRT) of litter-derived C in PLFAs of 26-44 days.[49] Generally, fungi are able to decompose complex and recalcitrant compounds cometabolically,[52,64,65] while the source material is chemically transformed (together with a change in the C:N ratio) but not mineralized. Moreover, the source material gets easier available for bacteria for successive decomposition which is accompanied by H incorporation. Moore et al.[66] highlighted 2-3 turnover times for bacterial biomass during one growing season, while fungi only regenerated about 75 % over the same time while the transformation of complex litter material can also increase their stability.[24,67,68] The microbial community which is dominated by gram-positive bacteria can explain the larger incorporation of ambient water-H into leaves of beech. We have shown that there is a larger incorporation of ambient water-H into the bulk biomass of gram-positive bacteria compared to gram-negative bacteria.[12] With regards to substrate-specific metabolism, we have shown, that the incorporation of ambient water-H into the C-bonded H pool of bulk bacteria is more pronounced for Gram-positive bacteria (79 %) than for Gram-negative bacteria (43 %).[12] Therefore, with regards to leaves of beech, a larger contribution of gram-positive bacteria would explain the larger H incorporation compared to lime. The regression of that $\delta^2H_{n\ t0}$ values on that $\delta^2H_{n\ ti}$ values of leaves showed the largest change within the first four weeks (Fig. D-3) for beech. The incorporation rates into leaves, calculated as weekly rates, were higher for beech (2.3 %) compared to lime (0.8 %). This could be explained by a higher growth and higher biosynthetic activity and therefore higher glycolytic

activity of microorganisms compared to later stages of decomposition. In addition, the microorganisms are under more favourable (anabolic) conditions including the availability of easy degradable substrates at the beginning of the experiment connected with higher incorporation rates compared to less favourable conditions during later phases of decomposition when the easily available substrates were consumed and the water label is lost as a result of a catabolism-dominated metabolism.[12]

Lime leaves showed smaller C:N ratios compared to beech. In general, small C:N ratios are an indicator for bacteria dominated decomposition and microbial growth is favoured in litter with low C:N ratios.[69–71] Additionally, gram-negative bacteria prefer easy degradable substrates at early stages of decomposition. Gram-negative bacteria show faster growth rates[72] with a higher PLFAs MRT of 62-83 days,[49] which would imply, biosynthesis including glycolysis and the respirative cleavage of former ^{2}H-C bonds that would result in larger delabeling and thus, larger ambient water-H incorporation. However, soil microorganisms are C limited and mostly dormant, connected with a basic metabolism and slow biomass turnover rates[54] while the simultaneously fate of the proportion of leaf litter which is used as substrate by bacteria have to be considered. If the bacteria completely mineralize a proportion of the leaf litter, only the proportion of leaf litter untouched by bacteria with the initial $\delta^{2}H_{n\ leaves\ t0}$ values remains. The isotopic fractionation depends on the completeness and direction of the reactions. This is in line with our results, showing a more pronounced H fractionation for lime leaves (with higher C-mass losses) compared to beech. We suspect that lime leaves, with more favourable, labile and leachable compounds are decomposed in a non-selective way (>65 % C-mass loss in the first four weeks) - supported by no substantial changes in C:N ratios - as a consequence of the beneficial chemical composition of leaves with less transformation processes compared to beech leaves resulting in largely constant $\delta^{2}H_{n\ leaf}$ values over time (Fig. D-S2). In other words, the non-selective use of organic compounds in lime leaf litter is supported by constant C:N ratios over the experimental course. Although the incorporation of ambient water-H into the C-bonded H pool of leaves is smaller for lime than for beech, the incorporation was particularly evident after 20 weeks at the end of the exposure of leaf litter in the field. In general, later stages of decomposition are characterized by the colonization of fungi and gram-positive bacteria. Because this circumstance is not supported by C:N ratios - our rough indicator of decomposability, which did not change during the experiment for lime we cannot prove it. An alternative explanation is the increasing contribution of microorganisms to the litter and microorganism mixture. At the beginning, microbial biomass and C-turnover rates were high. Later, there are still microorganisms left, however it is no longer metabolized. As a consequence, this would imply that the microorganisms have a larger proportion of the remaining mass (leaves and microorganisms) during early stages of decomposition. In turn, this would mean that the determined incorporation becomes larger with time, because of the microbial proportion.

Contrary to our hypothesis, the decomposability of leaf litter and associated microbial activity were not decisive for the incorporation of ambient water-H incorporation. Instead, the persistence and

stabilization of biosynthesis products seems to be the driving force for the H incorporation. These findings might also explain the decomposability of lipids, which are less degradable organic compound and to successfully infer paleoclimate conditions by their H isotope signature. As not microbial activity, but substrate quality and ongoing transformation processes are rather responsible for ^{2}H depletion and the incorporation of ambient water-H into the C-bonded H fraction than the decomposability of the two studied leaf litter types, we have to reject Hypothesis 2.

6. Acknowledgement

We thank Franziska Heitmann and Diana Fiedler for sample preparation and Sabine Flaiz for advice and assistance in EA-IRMS analyses. The study was funded by the German Science Foundation (DFG, OE516/11-1).

7. References

(1) Coûteaux, M. M.; Bottner, P.; Berg, B. Litter decomposition, climate and liter quality. *Trends in ecology & evolution* **1995**, 10 (2), 63–66. DOI: 10.1016/S0169-5347(00)88978-8.

(2) Cornwell, W. K.; Cornelissen, J. H. C.; Amatangelo, K.; Dorrepaal, E.; Eviner, V. T.; Godoy, O.; Hobbie, S. E.; Hoorens, B.; Kurokawa, H.; Pérez-Harguindeguy, N.; Quested, H. M.; Santiago, L. S.; Wardle, D. A.; Wright, I. J.; Aerts, R.; Allison, S. D.; van Bodegom, P.; Brovkin, V.; Chatain, A.; Callaghan, T. V.; Díaz, S.; Garnier, E.; Gurvich, D. E.; Kazakou, E.; Klein, J. A.; Read, J.; Reich, P. B.; Soudzilovskaia, N. A.; Vaieretti, M. V.; Westoby, M. Plant species traits are the predominant control on litter decomposition rates within biomes worldwide. *Ecology letters* **2008**, 11 (10), 1065–1071. DOI: 10.1111/j.1461-0248.2008.01219.x.

(3) Schimel, J. P.; Schaeffer, S. M. Microbial control over carbon cycling in soil. *Frontiers in microbiology* **2012**, 3, 348. DOI: 10.3389/fmicb.2012.00348.

(4) Melillo, J. M.; Aber, J. D.; Linkins, A. E.; Ricca, A.; Fry, B.; Nadelhoffer, K. J. Carbon and nitrogen dynamics along the decay continuum: Plant litter to soil organic matter. *Plant and Soil* **1989**, 115 (2), 189–198. DOI: 10.1007/BF02202587.

(5) Mooshammer, M.; Wanek, W.; Hämmerle, I.; Fuchslueger, L.; Hofhansl, F.; Knoltsch, A.; Schnecker, J.; Takriti, M.; Watzka, M.; Wild, B.; Keiblinger, K. M.; Zechmeister-Boltenstern, S.; Richter, A. Adjustment of microbial nitrogen use efficiency to carbon:nitrogen imbalances regulates soil nitrogen cycling. *Nature communications* **2014**, 5, 3694. DOI: 10.1038/ncomms4694.

(6) Kessler, A.; Kreis, K.; Merseburger, S.; Wilcke, W.; Oelmann, Y. Incorporation of hydrogen from ambient water into the C-bonded H pool during litter decomposition. *Soil Biology and Biochemistry* **2021**, 162 (9). DOI: 10.1016/j.soilbio.2021.108407.

(7) Gerlt, J. A. Stabilization of Reactive Intermediates and Transition States in Enzyme Active Sites by Hydrogen Bonding. *Comprehensive Natural Products Chemistry*; Elsevier, **1999**; pp 5–29. DOI: 10.1016/B978-0-08-091283-7.00131-4.

(8) Knowles, J. R.; Albery, W. J. Perfection in enzyme catalysis: the energetics of triosephosphate isomerase. *Accounts of Chemical Research* **1977**, 10 (4), 105–111. DOI: 10.1021/ar50112a001.

(9) Rieder, S. V.; Rose, I. A. The mechanism of the triosephosphate isomerase reaction. *The Journal of biological chemistry* **1959**, 234 (5), 1007–1010.

(10) Whitman, C. P. Keto–Enol Tautomerism in Enzymatic Reactions. *Comprehensive Natural Products Chemistry*; Elsevier, **1999**; pp 31–50. DOI: 10.1016/B978-0-08-091283-7.00132-6.

(11) Yakir, D. Variations in the natural abundance of oxygen-18 and deuterium in plant carbohydrates. *Plant, Cell and Environment* **1992**, 15 (9), 1005–1020. DOI: 10.1111/j.1365-3040.1992.tb01652.x.

(12) Kessler, A.; Merseburger, S.; Kappler, A.; Wilcke, W.; Oelmann, Y. Incorporation of Ambient Water-H into the C-Bonded H Pool of Bacteria during Substrate-Specific Metabolism. *ACS Earth and Space Chemistry* **2022**, 6 (9), 2180–2189. DOI: 10.1021/acsearthspacechem.2c00085.

(13) Berg, J. M.; Tymoczko, J. L.; Stryer, L. *Biochemistry*; Freeman Palgrave Macmillan, 2012.

(14) Kreuzer-Martin, H. W.; Lott, M. J.; Dorigan, J.; Ehleringer, J. R. Microbe forensics: oxygen and hydrogen stable isotope ratios in Bacillus subtilis cells and spores. *Proceedings of the National Academy of Sciences of the United States of America* **2003**, 100 (3), 815–819. DOI: 10.1073/pnas.252747799.

(15) Kreuzer-Martin, H. W.; Chesson, L. A.; Lott, M. J.; Dorigan, J. V.; Ehleringer, J. R. Stable Isotope Ratios as a Tool in Microbial Forensics—Part 1. Microbial Isotopic Composition as a Function of Growth Medium. *Journal of Forensic Sciences* **2004**, 49 (5), 1–7. DOI: 10.1520/JFS2003226.

(16) Horita, J.; Vass, A. A. Stable-Isotope Fingerprints of Biological Agents as Forensic Tools. *Journal of Forensic Sciences* **2003**, 48 (1). DOI: 10.1520/JFS2002170.

(17) Paul, A.; Hatté, C.; Pastor, L.; Thiry, Y.; Siclet, F.; Balesdent, J. Hydrogen dynamics in soil organic matter as determined by ^{13}C and ^{2}H labeling experiments. *Biogeosciences* **2016**, 13 (24), 6587–6598. DOI: 10.5194/bg-13-6587-2016.

(18) Sachse, D.; Kahmen, A.; Gleixner, G. Significant seasonal variation in the hydrogen isotopic composition of leaf-wax lipids for two deciduous tree ecosystems (*Fagus sylvativa* and *Acer*

pseudoplatanus). *Organic Geochemistry* **2009**, 40 (6), 732–742. DOI: 10.1016/j.orggeochem.2009.02.008.

(19) Ladd, J. N.; Amato, M.; Oades, J. M. Decomposition of plant material in Australian soils. III. Residual organic and microbial biomass C and N from isotope-labelled legume material and soil organic matter, decomposing under field conditions. *Soil Research* **1985**, 23 (4). DOI: 10.1071/SR9850603.

(20) Nguyen Tu, T. T.; Egasse, C.; Zeller, B.; Bardoux, G.; Biron, P.; Ponge, J.-F.; David, B.; Derenne, S. Early degradation of plant alkanes in soils: A litterbag experiment using ^{13}C-labelled leaves. *Soil Biology and Biochemistry* **2011**, 43 (11), 2222–2228. DOI: 10.1016/j.soilbio.2011.07.009.

(21) Zeller, B.; Colin-Belgrand, M.; Dambrine, E.; Martin, F. Fate of nitrogen released from ^{15}N-labeled litter in European beech forests. *Tree physiology* **2001**, 21 (2-3), 153–162. DOI: 10.1093/treephys/21.2-3.153.

(22) Gamarra, B.; Kahmen, A. Low secondary leaf wax n-alkane synthesis on fully mature leaves of C3 grasses grown at controlled environmental conditions and variable humidity. *Rapid communications in mass spectrometry* **2017**, 31 (2), 218–226. DOI: 10.1002/rcm.7770.

(23) Liu, J. Seasonality of the altitude effect on leaf wax n-alkane distributions, hydrogen and carbon isotopes along an arid transect in the Qinling Mountains. *The Science of the total environment* **2021**, 778. DOI: 10.1016/j.scitotenv.2021.146272.

(24) Prescott, C. E.; Vesterdal, L. Decomposition and transformations along the continuum from litter to soil organic matter in forest soils. *Forest Ecology and Management* **2021**, 498 (1–4). DOI: 10.1016/j.foreco.2021.119522.

(25) Cotrufo, M. F.; Wallenstein, M. D.; Boot, C. M.; Denef, K.; Paul, E. The Microbial Efficiency-Matrix Stabilization (MEMS) framework integrates plant litter decomposition with soil organic matter stabilization: do labile plant inputs form stable soil organic matter? *Global Change Biology* **2013**, 19 (4), 988–995. DOI: 10.1111/gcb.12113.

(26) Bradford, M. A.; Tordoff, G. M.; Eggers, T.; Jones, T. H.; Newington, J. E. Microbiota, fauna, and mesh size interactions in litter decomposition. *Oikos* **2002**, 99 (2), 317–323. DOI: 10.1034/j.1600-0706.2002.990212.x.

(27) Chapman, S. K.; Newman, G. S. Biodiversity at the plant-soil interface: microbial abundance and community structure respond to litter mixing. *Oecologia* **2010**, 162 (3), 763–769. DOI: 10.1007/s00442-009-1498-3.

(28) Cleveland, C. C.; Neff, J. C.; Townsend, A. R.; Hood, E. Composition, Dynamics, and Fate of Leached Dissolved Organic Matter in Terrestrial Ecosystems: Results from a Decomposition Experiment. *Ecosystems* **2004**, 7 (3). DOI: 10.1007/s10021-003-0236-7.

(29) Kalbitz, K.; Schmerwitz, J.; Schwesig, D.; Matzner, E. Biodegradation of soil-derived dissolved organic matter as related to its properties. *Geoderma* **2003**, 113 (3-4), 273–291. DOI: 10.1016/S0016-7061(02)00365-8.

(30) Wijker, R. S.; Sessions, A. L.; Fuhrer, T.; Phan, M. 2H/1H variation in microbial lipids is controlled by NADPH metabolism. *Proceedings of the National Academy of Sciences of the United States of America* **2019**, 116 (25). DOI: 10.1073/pnas.1818372116.

(31) Sinsabaugh, R. L.; Antibus, R. K.; Linkins, A. E. An enzymic approach to the analysis of microbial activity during plant litter decomposition. *Agriculture, Ecosystems & Environment* **1991**, 34 (1-4), 43–54. DOI: 10.1016/0167-8809(91)90092-C.

(32) Jacob, M.; Viedenz, K.; Polle, A.; Thomas, F. M. Leaf litter decomposition in temperate deciduous forest stands with a decreasing fraction of beech (Fagus sylvatica). *Oecologia* **2010**, 164 (4), 1083–1094. DOI: 10.1007/s00442-010-1699-9.

(33) Finzi, A. C.; van Breemen, N.; Canham, C. D. Canopy Tree-Soil Interactions within Temperate Forests: Species Effects on Soil Carbon and Nitrogen. *Ecological Applications* **1998**, 8 (2), 440. DOI: 10.2307/2641083.

(34) Melillo, J. M.; Aber, J. D.; Muratore, J. F. Nitrogen and Lignin Control of Hardwood Leaf Litter Decomposition Dynamics. *Ecology* **1982**, 63 (3), 621–626. DOI: 10.2307/1936780.

(35) Faghihi, V.; Meijer, H. A. J.; Gröning, M. A thoroughly validated spreadsheet for calculating isotopic abundances (^{2}H, ^{17}O, ^{18}O) for mixtures of waters with different isotopic compositions. *Rapid communications in mass spectrometry* **2015**, 29 (15), 1351–1356. DOI: 10.1002/rcm.7232.

(36) Wetter Kontor GmbH. *https://www.wetterkontor.de/de/wetter/deutschland/monatswerte-station.asp?id=10738*.

(37) Schad, P. The International Soil Classification System WRB, Third Edition, **2014**. *Novel Methods for Monitoring*, 563–571. DOI: 10.1007/978-3-319-24409-9_25.

(38) Vance, E. D.; Nadkarni, N. M. Microbial biomass and activity in canopy organic matter and the forest floor of a tropical cloud forest. *Soil Biology and Biochemistry* **1990**, 22 (5), 677–684. DOI: 10.1016/0038-0717(90)90015-R.

(39) Colina-Tejada, A.; Amblès, A.; Jambu, P. Nature and origin of soluble lipids shed into the soil by rainwater leaching a forest cover of Pinus maritima sp. *European Journal of Soil Science* **1996**, 47 (4), 637–643. DOI: 10.1111/j.1365-2389.1996.tb01862.x.

(40) Wassenaar, L. I.; Hobson, K. A. Improved Method for Determining the Stable-Hydrogen Isotopic Composition (δD) of Complex Organic Materials of Environmental Interest. *Environmental Science & Technology* **2000**, 34 (11), 2354–2360. DOI: 10.1021/es990804i.

(41) Ruppenthal, M.; Oelmann, Y.; Wilcke, W. Optimized demineralization technique for the measurement of stable isotope ratios of nonexchangeable H in soil organic matter. *Environmental Science & Technology* **2013**, 47 (2), 949–957. DOI: 10.1021/es303448g.

(42) Coplen, T. B. Guidelines and recommended terms for expression of stable-isotope-ratio and gas-ratio measurement results. *Rapid communications in mass spectrometry* **2011**, 25 (17), 2538–2560. DOI: 10.1002/rcm.5129.

(43) Semaškienė, L. Small-leaved lime (Tilia cordata Mill.) in Lithuania: Phenotypical diversity and productivity of modal stands: *Summary of doctoral dissertation in biomedical sciences, forestry*, **2006**.

(44) Schieber, B.; Janík, R.; Snopková, Z. Phenology of four broad-leaved forest trees in a submountain beech forest. *Journal of Forest Science* **2009**, 55 (1), 15–22. DOI: 10.17221/51/2008-JFS.

(45) Soong, J. L.; Parton, W. J.; Calderon, F.; Campbell, E. E.; Cotrufo, M. F. A new conceptual model on the fate and controls of fresh and pyrolized plant litter decomposition. *Biogeochemistry* **2015**, 124 (1-3), 27–44. DOI: 10.1007/s10533-015-0079-2.

(46) Luo, Y.-H.; Steinberg, L.; Suda, S.; Kumazawa, S.; Mitsu, A. Extremely Low D/H Ratios of Photoproduced Hydrogen by Cyanobacteria. *Plant and Cell Physiology* **1991**, DOI: 10.1093/oxfordjournals.pcp.a078158.

(47) Yakir, D.; Deniro, M. J. Oxygen and Hydrogen Isotope Fractionation during Cellulose Metabolism in Lemna gibba L. *Plant physiology* **1990**, 93 (1), 325–332. DOI: 10.1104/pp.93.1.325.

(48) Luo, Y.-H.; Sternberg, L. D. S. L. Hydrogen and Oxygen Isotopic Fractionation During Heterotrophic Cellulose Synthesis. *Journal of Experimental Botany* **1992**, 43 (1), 47–50. DOI: 10.1093/jxb/43.1.47.

(49) Müller, K.; Marhan, S.; Kandeler, E.; Poll, C. Carbon flow from litter through soil microorganisms: From incorporation rates to mean residence times in bacteria and fungi. *Soil Biology and Biochemistry* **2017**, 115, 187–196. DOI: 10.1016/j.soilbio.2017.08.017.

(50) Romaní, A. M.; Fischer, H.; Mille-Lindblom, C.; Tranvik, L. J. Interactions of bacteria and fungi on decomposing litter: differential extracellular enzyme activities. *Ecology* **2006**, 87 (10), 2559–2569. DOI: 10.1890/0012-9658(2006)87[2559:IOBAFO]2.0.CO;2.

(51) Kramer, S.; Dibbern, D.; Moll, J.; Huenninghaus, M.; Koller, R.; Krueger, D.; Marhan, S.; Urich, T.; Wubet, T.; Bonkowski, M.; Buscot, F.; Lueders, T.; Kandeler, E. Resource Partitioning between Bacteria, Fungi, and Protists in the Detritusphere of an Agricultural Soil. *Frontiers in microbiology* **2016**, 7. DOI: 10.3389/fmicb.2016.01524.

(52) McMahon, S. K.; Williams, M. A.; Bottomley, P. J.; Myrold, D. D. Dynamics of Microbial Communities during Decomposition of Carbon-13 Labeled Ryegrass Fractions in Soil. *Soil Science Society of America Journal* **2005**, 69 (4), 1238–1247. DOI: 10.2136/sssaj2004.0289.

(53) Paul, E. A.; Clark, F. E., Eds. Soil Microbiology and Biochemistry; Academic Press, San Diego, 1996.

(54) Joergensen, R. G.; Wichern, F. Alive and kicking: Why dormant soil microorganisms matter. *Soil Biology and Biochemistry* **2018**, 116, 419–430. DOI: 10.1016/j.soilbio.2017.10.022.

(55) Tukey, H. B. The Leaching of Substances from Plants. *Annual Review of Plant Physiology* **1970**, 21 (1), 305–324. DOI: 10.1146/annurev.pp.21.060170.001513.

(56) Guggenberger, G.; Zech, W. Dissolved organic carbon in forest floor leachates: simple degradation products or humic substances? *Science of The Total Environment* **1994**, 152 (1), 37–47. DOI: 10.1016/0048-9697(94)90549-5.

(57) Kalbitz, K.; Solinger, S.; Park, J.-H.; Michalzik, B.; Matzner, E. Controls on the dynamics of dissolved organic matter in soils: A review. *Soil Science* **2000**, 165 (4), 277–304. DOI: 10.1097/00010694-200004000-00001.

(58) Parker, G. G. Throughfall and Stemflow in the Forest Nutrient Cycle. In Advances in Ecological Research Volume 13; *Advances in Ecological Research*; Elsevier, **1983**; pp 57–133. DOI: 10.1016/S0065-2504(08)60108-7.

(59) Mellec, A.; Meesenburg, H.; Michalzik, B. The importance of canopy-derived dissolved and particulate organic matter (DOM and POM) — comparing throughfall solution from broadleaved and coniferous forests. *Annals of Forest Science* **2010**, 67 (4), 411. DOI: 10.1051/forest/2009130.

(60) Augusti, A.; Betson, T. R.; Schleucher, J. Hydrogen exchange during cellulose synthesis distinguishes climatic and biochemical isotope fractionations in tree rings. *The New phytologist* **2006**, 172 (3), 490–499. DOI: 10.1111/j.1469-8137.2006.01843.x.

(61) Don, A.; Kalbitz, K. Amounts and degradability of dissolved organic carbon from foliar litter at different decomposition stages. *Soil Biology and Biochemistry* **2005**, 37 (12), 2171–2179. DOI: 10.1016/j.soilbio.2005.03.019.

(62) Berg, B.; Matzner, E. Effect of N deposition on decomposition of plant litter and soil organic matter in forest systems. *Environmental Reviews* **1997**, 5 (1), 1–25. DOI: 10.1139/a96-017.

(63) Kuzyakov, Y.; Friedel, J.K.; Stahr, K. Review of mechanisms and quantification of priming effects. *Soil Biology and Biochemistry* **2000**, 32 (11-12), 1485–1498. DOI: 10.1016/S0038-0717(00)00084-5.

(64) Bossuyt, H.; Denef, K.; Six, J.; Frey, S.D.; Merckx, R.; Paustian, K. Influence of microbial populations and residue quality on aggregate stability. *Applied Soil Ecology* **2001**, 16 (3), 195–208. DOI: 10.1016/S0929-1393(00)00116-5.

(65) Six, J.; Frey, S. D.; Thiet, R. K.; Batten, K. M. Bacterial and Fungal Contributions to Carbon Sequestration in Agroecosystems. *Soil Science Society of America Journal* **2006**, 70 (2), 555–569. DOI: 10.2136/sssaj2004.0347.

(66) Moore, T. R.; Trofymow, J. A.; Prescott, C. E.; Titus, B. D. Nature and nurture in the dynamics of C, N and P during litter decomposition in Canadian forests. *Plant and Soil* **2011**, 339 (1-2), 163–175. DOI: 10.1007/s11104-010-0563-3.

(67) Talbot, J. M.; Treseder, K. K. Interactions among lignin, cellulose, and nitrogen drive litter chemistry-decay relationships. *Ecology* **2012**, 93 (2), 345–354. DOI: 10.1890/11-0843.1.

(68) Kallenbach, C. M.; Frey, S. D.; Grandy, A. S. Direct evidence for microbial-derived soil organic matter formation and its ecophysiological controls. *Nature communications* **2016**, 7. DOI: 10.1038/ncomms13630.

(69) Sinsabaugh, R. L.; Carreiro, M. M.; Repert, D. A. Allocation of extracellular enzymatic activity in relation to litter composition, N deposition, and mass loss. *Biogeochemistry* **2002**, 60 (1), 1–24. DOI: 10.1023/A:1016541114786.

(70) Saiya-Cork, K.R.; Sinsabaugh, R.L.; Zak, D.R. The effects of long term nitrogen deposition on extracellular enzyme activity in an Acer saccharum forest soil. *Soil Biology and Biochemistry* **2002**, 34 (9), 1309–1315. DOI: 10.1016/S0038-0717(02)00074-3.

(71) Kirschbaum, M. The temperature dependence of organic-matter decomposition - still a topic of debate. *Soil Biology and Biochemistry* **2006**, 38 (9), 2510–2518. DOI: 10.1016/j.soilbio.2006.01.030.

(72) Rubino, M.; Dungait, J.A.J.; Evershed, R. P.; Bertolini, T.; Angelis, P. de; D'Onofrio, A.; Lagomarsino, A.; Lubritto, C.; Merola, A.; Terrasi, F. Carbon input belowground is the major C flux contributing to leaf litter mass loss: Evidences from a ^{13}C labelled-leaf litter experiment. *Soil Biology and Biochemistry* **2010**, 42 (7), 1009–1016. DOI: 10.1016/j.soilbio.2010.02.018

Section E

General Conclusion and Outlook

1. General Conclusion

Along a 2500 km climosequence in Argentina it was shown that the H isotopic composition of the C-bonded H pool (δ^2H_n values) in SOM strongly correlates with the H isotope composition of the local long-term precipitation (Ruppenthal et al., 2015). This circumstance can be explained by (i) microbial products and plant-derived compounds that underwent incorporation of ambient water-H into the C-bonded H fraction during heterotrophic decomposition and can be considered as the main constituent of SOM or (ii) roots that represent the major source of SOM, because δ^2H_n values of roots also depend on δ^2H values of the local long-term precipitation (Ruppenthal et al., 2015). We could show, that during leaf litter decomposition, there is an incorporation of ambient water-H into the C-bonded H pool of leaf litter of up to 9 % and <5 % into leached TOM over four weeks of incubation (**Section B**). Furthermore, we demonstrated that during substrate-specific metabolism, 61.1±18.5 % of C-bonded H of bulk bacterial biomass underwent exchange with ambient water-H (**Section C**). Finally, we determined an incorporation of 32±16.0 % into leaf litter during decomposition under field conditions (**Section D**). However, there is a lack of knowledge concerning the relevance of the individual compounds for SOM dynamics including their contribution to SOM.

Here, we used stable H isotope ratios of the C-bonded H fraction to study the incorporation of ambient water-H into the C-bonded H fraction of the bacterial biomass during metabolism and the incorporation into the C-bonded H pool of leaf litter and the decomposition products. Subsequently, our results provide new insights into the sources of SOM to explain the close correlation of δ^2H_n values of SOM on δ^2H values of the local long-term precipitation reported by Ruppenthal et al. (2015).

Our objective was to investigate

(i) the extent of incorporation of ambient water-H into the C-bonded H pool of individual compartments (bacteria, leaf litter and TOM) under different experimental conditions and

(ii) to assess the influence of bacteria, TOM and leaf litter as the source of SOM based on our results and the current knowledge of literature to explain the close correlation of δ^2H_n values of SOM on δ^2H values of the local long-term precipitation found by Ruppenthal et al. (2015).

Therefore, we (i) determined the bacterial performance (bacterial biomass production, growth and respiration) and the incorporation of ambient water-H into the C-bonded H pool of bulk bacterial biomass during substrate-specific metabolism by incubating two model organisms (gram-positive *B. atrophaeus* and gram-negative *E. Coli*) on a M9 minimal medium, supplemented with either D-glucose or D-lysine as the sole C-source over 12 and 24 h (**Section C**). Furthermore, we (ii) studied the incorporation of ambient water-H into the C-bonded H fraction into leaf litter and leached TOM of *Fagus sylvatica* L. (beech) and *Acer pseudoplatanus* L. (maple) during decomposition in a four-week incubation experiment using two ^2H enriched waters (**Section B**). Additionally, we (iii) planted three

to four-year-old trees of *Fagus sylvatica* L. - beech and *Tilia platyphyllos* SCOP. - lime in a greenhouse and watered them with waters differing in the isotopic signature to produce ^{2}H-enriched leaf litter. Afterwards, we performed a 20-week litterbag field experiment and determined the incorporation of ambient water-H into the C-bonded H pool of leaf litter and leached TOM during decomposition (**Section D**).

The data, materials and methods used are described in the individual sections (**Section B**, **C** and **D**). The only exception here is the calculation of the incorporation of ambient water-H into the C-bonded H fraction of leaf litter and leached TOM under laboratory conditions (**Section B**). Here, originally, the incorporation of ambient water-H into the C-bonded H pool of leaves and leached TOM samples was calculated via the slope of the regression of $\delta^{2}H_{n}$ values of OM on $\delta^{2}H$ values of the ^{2}H-enriched incubation waters (Fig. B-4). However, the slope of the regression cannot directly be equated with the incorporation (**Section C** and **D**) because mathematically, the slope is the product of the incorporation and the associated H isotope fractionation during incorporation. To disentangle these two processes, we recalculated the incorporation of ambient water-H into the C-bonded H fraction of leaf litter and leached TOM of **Section B** according to the approach used in **Section C** and **D**.

The incorporation of ambient water-H into the C-bonded H pool strongly depended on the considered compartment and the conditions under which the experiments were carried out (Fig. E-1).

Bacteria and leaf litter during the field study showed comparable incorporation rates (bacteria: 61.1 ± standard deviation of 18.5 % and leaf litter incubation: 32.0±16.0 %). The incorporation of ambient water-H into the C-bonded H pool of leaf litter during the laboratory incubation (5.4±1.3 %) differed significantly from bacteria and leaf litter during the field study ($p < 0.022$; Fig. E-1). Under optimal conditions, which includes the basic supply of nutrients and a favorable C-source, namely glucose, our results highlight the anabolic glycolysis pathway as the mechanism underlying the incorporation of ambient water-H into the C-bonded H pool of bacteria (**Section C**). Contrary to this, stressful conditions force bacteria into a catabolism-dominated metabolism that disables the incorporation of ambient water-H. During incubation, glucose concentrations decreased significantly with time (Fig. C-1a). Along with the positive effect of glucose on bacterial performance, showing an increased total biomass production, regarding growth and respiration (Fig. C-1b and Fig. C-2a, b; Table C-S1) there was a substantial H exchange of up to 80 % of bacterial C-bonded H with ambient water-H within 24 hours of incubation under optimal conditions in the laboratory (Table C-1; **Section C**). The microbial C turnover is a highly dynamic process which depends on microbial community and the availability of substrates with changing quality and quantity (Müller et al., 2017). During the decomposition of OM under natural conditions, sugars are the most abundant released monomers which serve as C and energy source for microorganisms (Gunina and Kuzyakov, 2015; Robbins and Taylor, 1989). Additionally, root exudates contain 40-50 % glucose (Hütsch et al., 2002). Furthermore, growth conditions and likely the related metabolic fluxes influence the H isotope fractionation associated with the incorporation of ambient water-H into bacterial

fractionation associated with the incorporation of ambient water-H into bacterial biomass (**Section C**). While we observed species-specific effects concerning the incorporation of ambient water-H into the C-bonded H pool of bulk bacterial biomass during anabolism under optimum conditions (**Section C**), for natural conditions, the reported incorporation rates into bacteria are assumed to be overestimated.

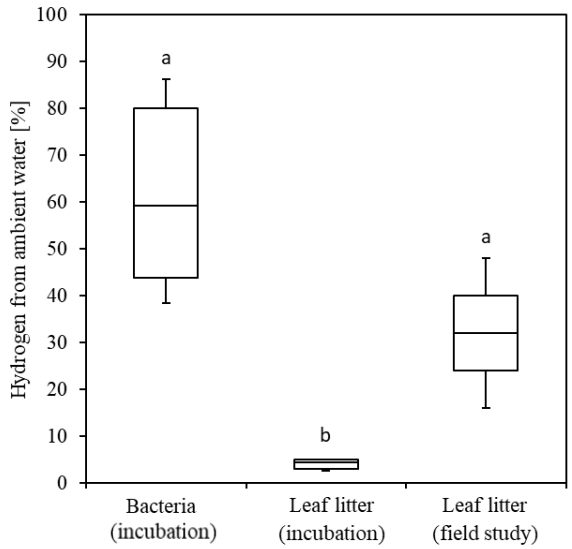

Fig. E-1: H exchange from ambient water-H into the C-bonded H pool of (i) bacteria (*B. atrophaeus* and *E. coli*) incubated over 24 h under optimal conditions in a M9 minimal medium supplemented with glucose as the sole carbon and energy source and constant temperature, (ii) leaf litter (*F. sylvatica* and *A. pseudoplatanus*) incubated over four weeks of decomposition under optimal water supply and temperature in the laboratory and (iii) leaf litter (*F. sylvatica* and *T. platyphyllos*) during 20 weeks of decomposition under non-optimal conditions of water supply and temperature. Lower-case letters indicate significant differences between each compound under differing experimental conditions. Error bars show the standard deviation of H exchange with ambient water-H for each compound under differing experimental conditions.

Anabolic activity can influence SOC storage with special attention to the fact that the most persistent C in soil is not derived from plant litter and their residues, but has been metabolized by microorganisms (Cotrufo et al., 2013; Liang and Balser, 2011; Lützow et al., 2006; Miltner et al., 2012). Growth rates of microorganisms depend on local environmental conditions (Vries and Shade, 2013) and bacterial metabolism is triggered by external signals e.g. when nutrients become limiting, high mineral composition, pH, temperature, moisture and high cell densities. However, knowledge on reaction pathways of metabolic activity under sub-optimal growth conditions is scarce (Bergkessel et al., 2016; Lempp et al., 2020).

Due to the high incorporation rates of ambient water-H into the C-bonded H pool of bulk bacterial biomass during anabolic metabolism, our results provide indications that bacterial products and

necromass could be used to explain the close correlation of δ^2H_n values of SOM on δ^2H values of local precipitation and therefore bacterial products can significantly contribute to SOM. While $\delta^{13}C$ values of PLFAs showed a pronounced incorporation into the soil microbial biomass of litter-derived C (Rubino et al., 2010), microbial products can contribute to SOM with up to 80 % (Whalen et al., 2022). Furthermore, there are indications that the quantification of stabilized microbial compounds in SOM are based on an incomplete extraction of microbial compounds (Angst et al., 2021). Therefore, microbial inputs to SOM are underestimated. Contrary to this, Buckeridge et al. (2022) showed that a high proportion of SOM consists of microbial necromass and transformation products. In more detail, Prescott and Vesterdal (2021) showed that labile components during early stages of decomposition stimulate the production of microbial biomass, necromass and microbial products. Moreover, later stages are characterized by the transformation into microbial products. C isotope tracing studies show evidence for the accumulation of labile compounds which are important SOM forms and microbial products in stable SOM forms (Martin et al., 1974; Prescott and Vesterdal, 2021; Voroney et al., 1989). Likewise, Kallenbach et al. (2016) illustrated that SOM largely consists of microbial products with the proportion of novel compounds between 73 and 100 %. In line, there is a growing number of assertions that stabilized SOM dominantly consists of microbial biomolecules (Castellano et al., 2015; Cotrufo et al., 2013; Liang et al., 2017; Miltner et al., 2012). Kögel-Knabner (2002) illustrated that microbial biomass significantly contributes to SOM formation representing an important source for SOM. Here, bacterial cell walls account for up to 90 % of the bacterial dry weight (Malanovic and Lohner, 2016) and represent stable components which in biomacromolecular structure are similar to that postulated for SOM (Kleber et al., 2007). This is in line with the results of Kindler et al. (2006, 2009) and Simpson et al. (2007), showing that a large portion of SOM consists of microbially derived compounds by using NMR analyses.

According to Simpson et al. (2007) and Liang and Balser (2011), non-living microbial necromass can account for up to 80 % to the formation of SOC. Here, microbial biomass and residues are preferentially entrapped in small pores and aggregates increasing the stability of microbial residues and their contribution to SOM (Angst et al., 2021; Miltner et al., 2012). Furthermore, it has to be considered that the H incorporation into the C-bonded H pool of bacterial biomass depends on the growth phase (**Section C**). In summary, the pronounced H incorporation into bulk bacterial biomass of up to 80 % provides indications that the microbial H pool can be used as an indicator of OM transformation processes and bacterial products play a central role for SOM dynamics and can therefore be used to explain the close correlation of δ^2H_n values in SOM with δ^2H values of the local long-term precipitation found by Ruppenthal et al. (2015).

Contrary to the direct input of microbial biomass, degradation products and microbial metabolites are leached during the decomposition process. To our knowledge, δ^2H_n values of leached compounds during decomposition have never been investigated. For the leached TOM in a leaf litter incubation experiment under favorable conditions for microorganisms (sufficient water supply and optimum

temperature), we found that up to 9 % of C-bonded H underwent exchange with ambient water-H attributed to microbial processes (**Section C**). However, the small incorporation rates during microbial processing that were less compared to incorporation rates into bacterial biomass, would not be sufficient to overprint the aridity signal present in plant organic matter and shift δ^2H_n values of SOM towards those of long-term rainfall. In the field, under suboptimal conditions for microorganisms (unfavorable water supply and large temperature changes), we were not able to calculate incorporation rates (**Section D**). Under natural conditions, δ^2H_n values of leached TOM can be explained by the influence of the steady replenishment of external microorganisms carrying the site-specific characteristics of δ^2H_n values of precipitation in combination with a constant H fractionation between leaf litter and leached TOM highlighting the influence of microbial compounds to TOM. Here, for both studies, leached decomposition products and microbial metabolites are characterized by an incorporation of ambient water-H via the intracellular glycolysis-gluconeogenesis metabolic pathway (Horita and Vass, 2003; Kreuzer-Martin et al., 2003; Ruppenthal et al., 2015).

The relatively low incorporation rates under laboratory conditions can be explained by the comparatively short experimental duration and the interrupted replenishment of leached TOM (**Section B**). While this replenishment is constant in the field under natural conditions, the pool of microorganisms, including microorganisms which were already present on the leaf surfaces at the beginning of incubation, gets exhausted with ongoing time. Furthermore, I have to add that the leachate was discharged in both experiments preventing the recycling of decomposed and microbial products within the system. In this regard, Prescott and Vesterdal (2021) emphasized that litter decomposition is not a one-way process. Instead, plant material is broken down and transformed into *de novo* materials. Hence, the recycling and feedbacks represent an effective "soil microbial loop" by multiple cycles of decomposition, assimilation and consumption by soil microbes that leads to an incorporation of litter C into the long-term microbial pool (Prescott and Vesterdal, 2021; Malik et al., 2016). This internal recycling, considering that bacterial biomass turns over 2-3 times during a growing season (Moore et al., 2005), could have resulted in less variable δ^2H_n values especially under field conditions (**Section D**). With respect to the microbial influence on the production of the leached TOM, the biotic production of volatile organic compounds during decomposition is reported to be 5-10 times higher compared to the abiotic production (McBride et al., 2020), highlighting the microbial importance for the production of leached TOM. For this reason, Müller et al. (2017) argue that resource availability modifies the microbial contribution to SOM turnover and formation and microbial metabolites can directly contribute to the formation of SOM (Kallenbach et al., 2016). Likewise, microbial biomass shows faster turnover times compared to plant residues (Kästner, 2000).

Once easily available compounds were transformed and leached, the decomposition of recalcitrant litter components starts and late stages of decomposition are again characterized by high efficiency of SOM formation with physical transfer of brittle little residues and little microbial activity which can be underlined by the common asymptotic mass remaining in litter bags experiments, but no

preferential loss of any chemical compounds (Cotrufo et al., 2015). Because we could not prove a substantial incorporation into leached TOM during laboratory incubation (**Section B**), it can be assumed that plant-derived soluble compounds and brittle little residues in the leached OM, which were metabolized and underwent transformation through the glycolysis-gluconeogenesis pathway inside the cells during decomposition, play a subordinate role as the source of SOM and rather directly stimulate microbial growth. As a result, the proportion of the microbial input is decisive for the extent of the observed incorporation which supports the significance of the microbial input to SOM.

Leaves represent the starting material for decomposition. Here, the litter C loss as direct input to the soil is reported to be twice as much as the fraction released as CO_2 (Rubino et al., 2010). During leaf litter decomposition, the incorporation of ambient water-H into the C-bonded H pool of leaf litter under optimal water supply and temperature during the laboratory incubation was <5 % and up to 48 % under field conditions with changing water regimes and varying temperatures. In the laboratory, leaf litter decomposition was only studied over four weeks of incubation associated with much lower C-mass losses of 32 % to initial C-stock compared to 70 % during natural conditions (Fig. D-1a). Additionally, the comparatively small incorporation rates in **Section B** and **D** can be attributed to the facts that leaf litter is less decomposable than substrates used in microbial culture studies (Fogel et al., 2016; Kreuzer-Martin et al., 2004, 2006) which is also supported by an incomplete consumption of leaf litter.

Contrary to the fundamental assumption that the incorporation depends on the decomposability of leaf litter including that faster decomposition is associated with a higher leaf litter C-mass loss and higher microbial activity and therefore should result in a more pronounced microbial H incorporation into the C-bonded H pool of leaf litter, this was not verified neither during leaf litter incubation (beech vs. maple, **Section B)** nor under natural conditions (beech vs. lime; **Section D)**. However, the observed differences between incorporation rates into leaf litter under laboratory and field conditions in contrast to optimized nutrient availability and pH during microbial incubation (**Section C**) challenges the view on the microbial influence on leaf litter decomposition. With regard to the observed incorporation rates in leaf litter material, I suspect that ongoing microbial transformation processes including the persistence and stabilization of biosynthesis products are the driving force for the observed H-exchange in leaf litter (**Section C**). This is supported by Prescott and Vesterdal (2021) illustrating that during decomposition litter mass loss becomes negligible and microbial transformation products build up a new C pool that increases in mass.

C-mass loss strongly depended on litter quality (**Section B** and **D**), which is supported by Coûteaux et al. (1995), showing that litter quality is the driving factor for litter decomposition. The observed mass loss of leaf litter strongly depended on tree species, both under laboratory conditions (beech < maple; Fig. B-2; Table B-1) and under field conditions (beech < lime; Fig. D-1). Transformation processes of plant compounds and the breaking down of complex materials is not necessarily associated with mineralization (Liang et al., 2017), which could explain our findings that the incorporation does not

directly depend on mass loss (**Section B** and **D**). However, there are direct effects of the substrate quality on decomposition (**Section B** and **D**). Generally, high substrate quality stimulates the accumulation of microbial residues resulting in a higher substrate-use efficiency and a higher microbial biomass which can potentially form SOM (Cotrufo et al., 2013). As a result of significant differences between incorporation rates in pure cultures of gram-positive and gram-negative bacteria (**Section C**), there is profound knowledge that there are also differences regarding the decomposition of different substrates between gram-positive and gram-negative bacteria (Kuzyakov et al., 2000). This results in the observed H isotope fractionation and incorporation rates (Table C-1; **Section C**). Additionally, undecomposed fragments of leaf litter enter the soil which can initiate SOM aggregation and play a crucial role for long-term C stabilization mechanisms (Del Galdo et al., 2003; Jastrow and Six, 2002). SOM is a continuum of different stages of decomposition (Rubino et al., 2010). The observed incorporation rates into the different studied compartments (bacteria, leached TOM and leaf litter) challenges the view on the continuous nature of SOM and its sources. There are many studies focusing on microbial or plant-derived SOM, but there is still a lack of knowledge with respect to stabilized SOM (Angst et al., 2021). Contrary to the reported incorporation during bacterial metabolism (**Section C**), which are most likely overestimated for SOM dynamics, the proportion of microorganisms to SOM and the contribution of microbial necromass to soils does not mirror its contribution to the effective stabilized SOM. Furthermore, the contribution of microbial inputs depends on ecosystem properties. Notably, C which does not derive from microbial biomass does not have to be entirely composed of plant derived C (Angst et al., 2021). Commonly, it is assumed that leaf litter is gradually transformed to more stable forms, including a variety of physical, chemical, faunal and microbial processes (Sollins et al., 1996). However, the significance of the microbial influence on the stabilization and destabilization of SOM is still in its infancy. In summary, the products of microbial transformation processes of plant litter do contribute more to stabilized SOM than plant-litter compounds (Mambelli et al., 2011).

As aridity affects δ^2H_n values of aboveground plant organic matter, Ruppenthal et al. (2015) indicated that there is a constant offset between δ^2H values of precipitation and δ^2H_n values of SOM along a climosequence in Argentina with identical apparent fractionation, irrespective of potentially differing chemical composition of SOM. However, our results showed that the incorporation is not directly driven by microbial activity and mineralization. Moreover, incorporation rates depended on the substrate quality of leaf litter. Therefore, unfavorable leaf litter quality is linked to successive decomposition and the gradually building up of microbial metabolites. Hence, incorporation instantly takes place with regards to the favorability of leaf litter quality. The importance of the plant species becomes increasingly important when it comes to different decomposition processes due to leaf specific properties (Angst et al., 2021; Zech et al., 2011). Consequently, differences of leaf litter quality should be reflected in a larger deviation of δ^2H_n values of SOM in dependence of δ^2H values of precipitation, which could be achieved by H-exchange with the H isotopic composition of

precipitation. However, Ruppenthal et al. (2015) showed that δ^2H_n values of SOM were not influenced by plant species composition or other environmental variables, such as soil type or soil properties with a nearly constant H fractionation between SOM and precipitation along the climosequence.

Additionally, the contribution of microbial necromass to SOC differs depending on environmental factors (Liang et al., 2019). These findings suggest that the microbial modification and microbial input is not the driving factor of the close correlation of δ^2H_n values of SOM on δ^2H values of precipitation, because the observed incorporation into OM under natural conditions strongly depended on leaf litter quality as presented in **Section D**. Furthermore, the influence of the microclimate for microorganisms must be taken into account. Here, the accumulation and contribution of bacterial necromass to SOC dynamics is shown to be ecosystem-specific and depend on climate (Wang et al., 2021).

On a global scale, the correlation of δ^2H_n values in SOM on δ^2H values in precipitation could also be caused by two counterbalancing, opposing processes. On the one hand, during warmer and moist climatic conditions, as a result of higher microbial activity, microorganisms incorporate more H into their biomass ending up in SOM. On the other hand, under colder and drier climatic conditions, because of reduced microbial activity, less ambient water-H is incorporated into the bacterial C pool, but the signal is maintained and accumulated over a longer period of time. As a net effect and despite different turnover and humus formation rates, the correlation of δ^2H_n values of SOM and δ^2H values of precipitation remains.

An alternative explanation is that δ^2H_n values of roots is H-isotopically close to soil water and there is a close correlation between δ^2H_n values of roots and δ^2H_n values of SOM (Ruppenthal et al., 2015). Those findings relate to the belowground root biomass that makes a major contribution to SOM. After Rasse et al. (2005), plant roots are an important source of SOM, while root-derived C represents >60 % of microbial biomass (Kramer et al., 2010) and 45 % of stabilized SOM is root-derived (Jackson et al., 2017). Interestingly, fine roots are decomposed slower than thicker roots (Fan and Guo, 2010; Goebel et al., 2011; Sun et al., 2013). Although fine roots produce higher amounts of OM in soil, thick roots potentially generate more stable SOM (Prescott and Vesterdal, 2021). With regard to the sources of SOM, there are strong interactions between litter, roots and microbes (Berg and McClaugherty, 2008; Bending, 2003; Miltner et al., 2012).

The aridity effect was not observable in the roots, likely because assimilates transported to the roots served as educts of biosynthesis reactions associated with the incorporation of root-water H, which is isotopically close to soil water, so that no incorporation has to take place before the roots die off, are decomposed and humus is subsequently formed. Although there is a strong correlation of δ^2H_n values in SOM and δ^2H values of local precipitation. On the one hand, I argue that the hypothesis for the roots as a source of SOM is still persistent. On the other hand, the incorporation of ambient water-H during leaf litter decomposition could also be an explanation for the observed correlation of δ^2H_n values in SOM on δ^2H values of local precipitation because (i) bacteria showed very high incorporation rates during metabolism (**Section C**) with a contribution of microbial products to SOM

of up to 80 % (Whalen et al., 2022) and (ii) δ^2H_n values of leached OM show almost an overprinting by δ^2H values of ambient water-H (**Section D**). Furthermore it has to be taken into account, that (iii) under field conditions there are multiple cycles of decomposition, assimilation and consumption (Prescott and Vesterdal, 2021; Salamanca et al., 2003), resulting in an overprinting of δ^2H_n values of the decomposition products via microbial activity, which is methodologically difficult to implement and has to be taken into account for future studies.

2. Outlook

The results of the present work provide fundamental knowledge about the incorporation of ambient water-H into the C-bonded H pool of bacteria, leaf litter and leached TOM during decomposition under varying conditions. Our results can be used to study growth conditions of bacteria under different environmental conditions together with different bacterial activities and metabolism. Furthermore, δ^2H_n values of bacteria improve the understanding of the microbial modification of δ^2H_n values in SOM and can be used to assess the microbial input to SOM. Furthermore, our results show that the incorporation of ambient water-H into the C-bonded H pool of leaf litter and leached TOM stress the microbial influence on the solid phase and the leached TOM and provide information on the decomposition and microbial activity under different environmental conditions. Finally, I used the determined incorporation rates to evaluate the influence of the individual compartments as the source for the SOM. With regard to the current state of research I suspect that the belowground root input is a crucial source for SOM. Additionally, our results highlight the relevance of microbial products as source of SOM. With respect to this, the relevance of soil microbial processes, rather than plant biomass production, should be focused when studying soil C dynamics. Therefore, future studies should concentrate on the mechanistic understanding of the production of leached TOM and the contribution of microbially derived compounds to leached TOM and investigate plant-derived and microbially derived compounds in SOM in consideration of climatic conditions, plant and microorganism communities and soil properties in order to provide deeper insights into the formation and the persistence of SOM under changing environmental conditions.

3. References

Angst, G., Pokorný, J., Mueller, C.W., Prater, I., Preusser, S., Kandeler, E., Meador, T., Straková, P., Hájek, T., van Buiten, G., Angst, Š., 2021. Soil texture affects the coupling of litter decomposition and soil organic matter formation. Soil Biology and Biochemistry 159, 108302.

Bending, G.D., 2003. Litter decomposition, ectomycorrhizal roots and the 'Gadgil' effect. New Phytologist 158, 228–229.

Berg, B., McClaugherty, C., 2008. Plant Litter. Decomposition, Humus Formation, Carbon Sequestration. Springer Berlin, Heidelberg.

Bergkessel, M., Basta, D.W., Newman, D.K., 2016. The physiology of growth arrest: uniting molecular and environmental microbiology. Nature Reviews. Microbiology 14, 549–562.

Buckeridge, K.M., Creamer, C., Whitaker, J., 2022. Deconstructing the microbial necromass continuum to inform soil carbon sequestration. Functional Ecology 36, 1396–1410.

Castellano, M.J., Mueller, K.E., Olk, D.C., Sawyer, J.E., Six, J., 2015. Integrating plant litter quality, soil organic matter stabilization, and the carbon saturation concept. Global Change Biology 21, 3200–3209.

Cotrufo, M.F., Soong, J.L., Horton, A.J., Campbell, E.E., Haddix, M.L., Wall, D.H., Parton, W.J., 2015. Formation of soil organic matter via biochemical and physical pathways of litter mass loss. Nature Geoscience 8, 776–779.

Cotrufo, M.F., Wallenstein, M.D., Boot, C.M., Denef, K., Paul, E., 2013. The microbial efficiency-matrix stabilization (MEMS) framework integrates plant litter decomposition with soil organic matter stabilization: do labile plant inputs form stable soil organic matter? Global Change Biology 19, 988–995.

Coûteaux, M.M., Bottner, P., Berg, B., 1995. Litter decomposition, climate and liter quality. Trends in Ecology & Evolution 10, 63–66.

Del Galdo, I., Six, J., Peressotti, A., Cotrufo, F.M., 2003. Assessing the impact of land-use change on soil C sequestration in agricultural soils by means of organic matter fractionation and stable C isotopes. Global Change Biology 9, 1204–1213.

Fan, P., Guo, D., 2010. Slow decomposition of lower order roots: a key mechanism of root carbon and nutrient retention in the soil. Oecologia 163, 509–515.

Fogel, M.L., Griffin, P.L., Newsome, S.D., 2016. Hydrogen isotopes in individual amino acids reflect differentiated pools of hydrogen from food and water in *Escherichia coli*. Proceedings of the National Academy of Sciences of the United States of America 113, 4648-4653.

Goebel, M., Hobbie, S.E., Bulaj, B., Zadworny, M., Archibald, D.D., Oleksyn, J., Reich, P.B., Eissenstat, D.M., 2011. Decomposition of the finest root branching orders: linking belowground dynamics to fine-root function and structure. Ecological Monographs 81, 89–102.

Gunina, A., Kuzyakov, Y., 2015. Sugars in soil and sweets for microorganisms: Review of origin, content, composition and fate. Soil Biology and Biochemistry 90, 87–100.

Horita, J., Vass, A.A., 2003. Stable-isotope fingerprints of biological agents as forensic tools. Journal of Forensic Sciences 48, 122-6.

Hütsch, B.W., Augustin, J., Merbach, W., 2002. Plant rhizodeposition — an important source for carbon turnover in soils. Journal of Plant Nutrition and Soil Science 165, 397-407.

Jackson, R.B., Lajtha, K., Crow, S.E., Hugelius, G., Kramer, M.G., Piñeiro, G., 2017. The ecology of soil carbon: Pools, vulnerabilities, and biotic and abiotic controls. Annual Review of Ecology, Evolution, and Systematics 48, 419–445.

Jastrow, J., Six, J., 2002. Organic Matter Turnover, Dekker, M., New York, Encyclopedia of Soil Science, 936-942.Kallenbach, C.M., Frey, S.D., Grandy, A.S., 2016. Direct evidence for microbial-derived soil organic matter formation and its ecophysiological controls. Nature Communications 7.

Kästner, M., 2000. "Humification" Process or Formation of Refractory Soil Organic Matter, in: Rehm, H.J., Reed, G., Pühler, A., Stadler, P., Environmental Processes II. Soil Decontamination, Wiley-VCH, Weinheim, New York, Biotechnology Set, 89–125.

Kindler, R., Miltner, A., Thullner, M., Richnow, H.-H., Kästner, M., 2009. Fate of bacterial biomass derived fatty acids in soil and their contribution to soil organic matter. Organic Geochemistry 40, 29–37.

Kleber, M., Sollins, P., Sutton, R., 2007. A conceptual model of organo-mineral interactions in soils: self-assembly of organic molecular fragments into zonal structures on mineral surfaces. Biogeochemistry 85, 9–24.

Kramer, C., Trumbore, S., Fröberg, M., Cisneros Dozal, L.M., Zhang, D., Xu, X., Santos, G.M., Hanson, P.J., 2010. Recent (<4 year old) leaf litter is not a major source of microbial carbon in a temperate forest mineral soil. Soil Biology and Biochemistry 42, 1028–1037.

Kreuzer-Martin, H.W., Chesson, L.A., Lott, M.J., Dorigan, J.V., Ehleringer, J.R., 2004. Stable isotope ratios as a tool in microbial forensics - Part 1. Microbial isotopic composition as a function of growth medium. Journal of Forensic Sciences 49, 1–7.

Kreuzer-Martin, H.W., Lott, M.J., Dorigan, J., Ehleringer, J.R., 2003. Microbe forensics: oxygen and hydrogen stable isotope ratios in *Bacillus subtilis* cells and spores. Proceedings of the National Academy of Sciences of the United States of America 100, 815–819.

Kreuzer-Martin, H.W., Lott, M.J., Ehleringer, J.R., Hegg, E.L., 2006. Metabolic processes account for the majority of the intracellular water in log-phase *Escherichia coli* cells as revealed by hydrogen isotopes. Biochemistry 45, 13622-30.

Kuzyakov, Y., Friedel, J.K., Stahr, K., 2000. Review of mechanisms and quantification of priming effects. Soil Biology and Biochemistry 32, 1485–1498.

Lempp, M., Lubrano, P., Bange, G., Link, H., 2020. Metabolism of non-growing bacteria. Biological Chemistry 401, 1479–1485.

Liang, C., Amelung, W., Lehmann, J., Kästner, M., 2019. Quantitative assessment of microbial necromass contribution to soil organic matter. Global Change Biology 25, 3578–3590.

Liang, C., Balser, T.C., 2011. Microbial production of recalcitrant organic matter in global soils: implications for productivity and climate policy. Nature Reviews. Microbiology 9, 75.

Liang, C., Schimel, J.P., Jastrow, J.D., 2017. The importance of anabolism in microbial control over soil carbon storage. Nature Microbiology 2, 17105.

Lützow, M.v., Kögel-Knabner, I., Ekschmitt, K., Matzner, E., Guggenberger, G., Marschner, B., Flessa, H., 2006. Stabilization of organic matter in temperate soils: mechanisms and their relevance under different soil conditions - a review. European Journal of Soil Science 57, 426–445.

Malanovic, N., Lohner, K., 2016. Antimicrobial peptides targeting gram-positive bacteria. Pharmaceuticals 9, 59.

Malik, A.A., Chowdhury, S., Schlager, V., Oliver, A., Puissant, J., Vazquez, P.G.M., Jehmlich, N., Bergen, M. von, Griffiths, R.I., Gleixner, G., 2016. Soil fungal: Bacterial ratios are linked to altered carbon cycling. Frontiers in Microbiology 7, 1247.

Mambelli, S., Bird, J.A., Gleixner, G., Dawson, T.E., Torn, M.S., 2011. Relative contribution of foliar and fine root pine litter to the molecular composition of soil organic matter after in situ degradation. Organic Geochemistry 42, 1099-1108.

Martin, J.P., Haidfr, K., Farmkr, W.J., Fustec-Mathon, E., 1974. Decomposition and distribution of residual activity of some ^{13}C-microbial polysaccharides and cells, glucose, cellulose and wheat straw in soil. Soil Biology and Biochemistry 6, 221–230.

McBride, S.G., Choudoir, M., Fierer, N., Strickland, M.S., 2020. Volatile organic compounds from leaf litter decomposition alter soil microbial communities and carbon dynamics. Ecology 101, e03130.

Miltner, A., Bombach, P., Schmidt-Brücken, B., Kästner, M., 2012. SOM genesis: Microbial biomass as a significant source. Biogeochemistry 111, 41–55.

Moir, A., 2006. How do spores germinate? Journal of Applied Microbiology 101, 526–530.

Moore, J.C., McCann, K., Ruiter, P.C. de, 2005. Modeling trophic pathways, nutrient cycling, and dynamic stability in soils. Pedobiologia 49, 499–510.

Müller, K., Marhan, S., Kandeler, E., Poll, C., 2017. Carbon flow from litter through soil microorganisms: From incorporation rates to mean residence times in bacteria and fungi. Soil Biology and Biochemistry 115, 187–196.

Prescott, C.E., Vesterdal, L., 2021. Decomposition and transformations along the continuum from litter to soil organic matter in forest soils. Forest Ecology and Management 498, 119522.

Rasse, D.P., Rumpel, C., Dignac, M.-F., 2005. Is soil carbon mostly root carbon? Mechanisms for a specific stabilisation. Plant and Soil 269, 341–356.

Robbins, J.W., Taylor, K.B., 1989. Optimization of *Escherichia coli* growth by controlled addition of glucose. Biotechnology and Bioengineering 34, 1289–1294.

Rubino, M., Dungait, J.A.J., Evershed, R.P., Bertolini, T., Angelis, P. de, D'Onofrio, A., Lagomarsino, A., Lubritto, C., Merola, A., Terrasi, F., 2010. Carbon input belowground is the

major C flux contributing to leaf litter mass loss: Evidences from a ^{13}C labelled-leaf litter experiment. Soil Biology and Biochemistry 42, 1009–1016.

Ruppenthal, M., Oelmann, Y., del Valle, H.F., Wilcke, W., 2015. Stable isotope ratios of nonexchangeable hydrogen in organic matter of soils and plants along a 2100-km climosequence in Argentina: New insights into soil organic matter sources and transformations? Geochimica et Cosmochimica Acta 152, 54–71.

Salamanca, E.F., Kaneko, N., Katagiri, S., 2003. Rainfall manipulation effects on litter decomposition and the microbial biomass of the forest floor. Applied Soil Ecology 22, 271–281.

Simpson, A.J., Song, G., Smith, E., Lam, B., Novotny, E.H., Hayes, M.H.B., 2007. Unraveling the structural components of soil humin by use of solution-state nuclear magnetic resonance spectroscopy. Environmental Science & Technology 41, 876–883.

Sollins, P., Homann, P., Caldwell, B.A., 1996. Stabilization and destabilization of soil organic matter: mechanisms and controls. Geoderma 74, 65–105.

Sun, T., Mao, Z., Han, Y., 2013. Slow decomposition of very fine roots and some factors controlling the process: a 4-year experiment in four temperate tree species. Plant and Soil 372, 445–458.

Voroney, R.P., Paul, E.A., Anderson, D.W., 1989. Decomposition of wheat straw and stabilization of microbial products. Canadian Journal of Soil Science, 63–77.

Vries, F.T. de, Shade, A., 2013. Controls on soil microbial community stability under climate change. Frontiers in Microbiology 4, 265.

Wang, B., An, S., Liang, C., Liu, Y., Kuzyakov, Y., 2021. Microbial necromass as the source of soil organic carbon in global ecosystems. Soil Biology and Biochemistry 162, 108422.

Whalen, E.D., Grandy, A.S., Sokol, N.W., Keiluweit, M., Ernakovich, J., Smith, R.G., Frey, S.D., 2022. Clarifying the evidence for microbial- and plant-derived soil organic matter, and the path toward a more quantitative understanding. Global Change Biology 28, 7167-7185.

Zech, M., Pedentchouk, N., Buggle, B., Leiber, K., Kalbitz, K., Marković, S.B., Glaser, B., 2011. Effect of leaf litter degradation and seasonality on D/H isotope ratios of n-alkane biomarkers. Geochimica et Cosmochimica Acta 75, 4917–4928.

Appendix

Supporting Information of Section B

Table B-S1: $\delta^2H_{n\ leaf\ litter}$ and $\delta^2H_{n\ TOM}$ of replicates with means and standard deviation for beech and maple differentiated according to the type of isotopically labeled water (+50 ‰, +250 ‰) for the incubation period of four weeks (n = 3).

	$\delta^2H_{n\ leaf\ litter}$ [‰VSMOW] Incubation time [weeks]					$\delta^2H_{n\ TOM}$ [‰VSMOW] Incubation time [weeks]			
	0	1	2	3	4	1	2	3	4
Beech 50:	-80.5	-92.4	-81.6	-83.5	-81.4	-69.3	-56.5	-75.6	-118.8
	-80.5	-90.3	-84.2	-81.9	-79.8	-74.8	-76.3	-74.6	-115.5
	-80.5	-91.3	-85.5	-81.6	-82.1	-108.3	-68.0	-79.9	-116.8
mean	-80.5±0	-91.4±0.9	-83.8±1.6	-82.3±0.9	-81.1±0.9	-84.1±17.2	-66.9±8.1	-76.7±2.3	-117.0±1.4
Beech 250	-80.53	-76.3	-76.2	-75.5	-68.5	-64.7	-58.3	-59.0	-92.2
	-80.53	-81.3	-76.4	-79.8	-72.3	-56.5	-64.2	-58.6	-63.1
	-80.53	-86.8	-80.2	-75.7	-72.6	-114.7	-46.9	-64.9	-92.5
mean	-80.5±0	-81.5±4.3	-77.6±1.8	-77.0±1.9	-71.2±1.9	-78.6±25.8	-56.5±7.1	-60.9±2.9	-82.6±13.8
Maple 50	-98.9	-89.0	-97.30	-103.1	-102.6	-75.2	-67.7	-78.9	-84.6
	-98.9	-97.0	-97.8	-90.8	-96.2	-62.4	-79.9	-81.2	-84.7
	.98.9	-100.8	-102.5	-104.3	-94.6	-75.2	-79.8	-84.9	-82.9
mean	-98.9±0	-95.62±4.9	-99.21±2.4	-99.4±6.1	-97.82±3.5	-70.9±6.1	-75.8±5.7	-81.7±2.5	-84.1±0.8
Maple 250	-98.9	-96.9	-83.7	-103.3	-92.3	-43.1	-107.6	-117.4	-67.9
	-98.9	-91.4	-86.6	-94.6	-86.9	-78.3	-111.7	-120.4	-68.8
	-98.9	-100.4	-95.9	-93.5	-87.7	-91.8	-72.2	-67.8	-62.1
mean	-98.9±0	-96.2±3.7	-88.8±5.2	-97.1±4.4	-88.9±2.4	-71.0±20.5	-97.1±17.4	-101.9±24.2	-66.3±2.9

Table B-S2: Repeated measure ANOVA results for effects of time, water label (water) and tree species on $\delta^2H_{n\ TOM}$ values with significant interactions. Significant effects are displayed in bold.

Factors	nDF	F	P
$\delta^2H_{n\ TOM}$			
Time	3	1.68	0.199
Water	1	1.31	0.285
Tree species	1	0.48	0.510
Time × Tree species	**3**	**7.26**	**0.001**
Tree species × Water	**1**	**5.94**	**0.041**

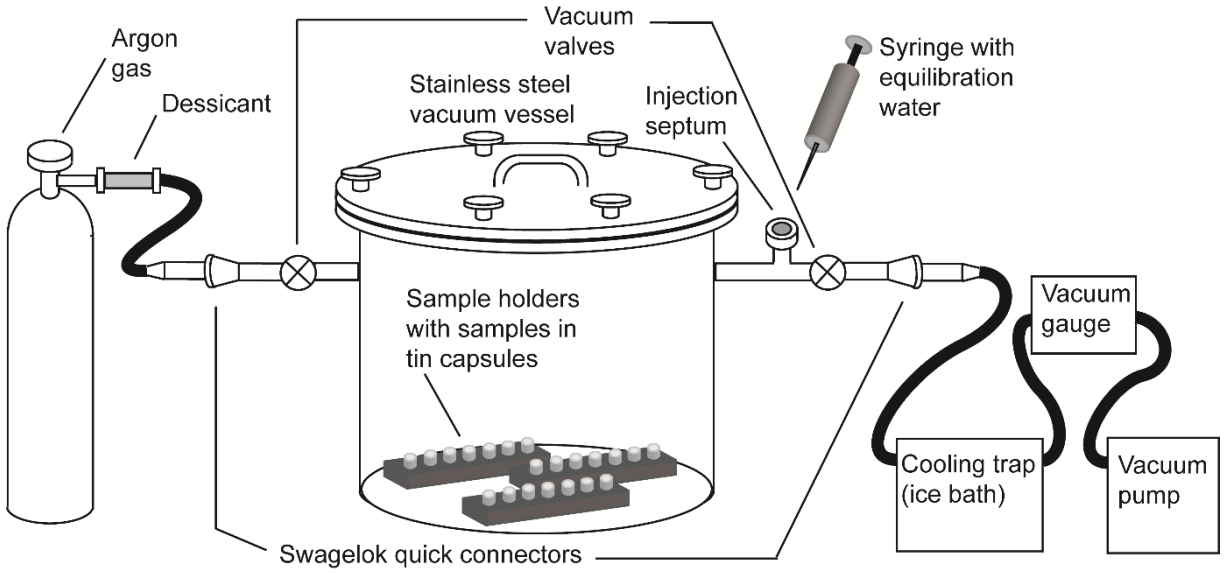

Fig. B-S1: Schematic graph of the water steam equilibration device.

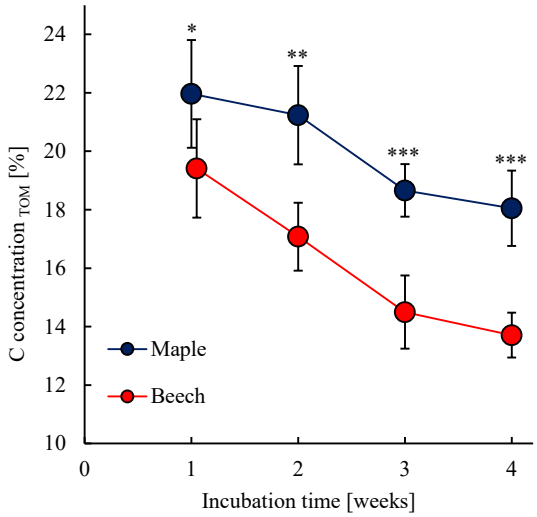

Fig. B-S2: Carbon concentrations in leached total organic matter (TOM) according to tree species (beech and maple) during the course of the four-week incubation. Error bars show the standard deviation for each time step (n = 6). To ease readability, the sampling times have been shifted slightly. Asterisks indicate significant differences between tree species at a given incubation interval (* p <0.05; ** p <0.01; *** p <0.001).

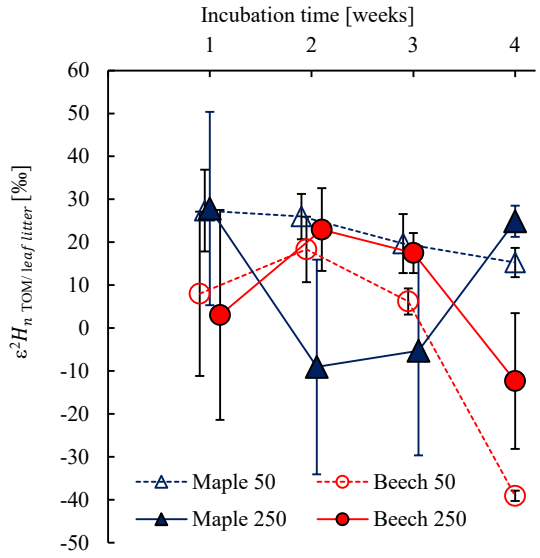

Fig. B-S3: Net apparent H isotope fractionation ε^2H_n (‰) between leached TOM and leaf litter of beech and maple, differentiated according to the type of isotopically labelled water (+50 ‰, +250 ‰) over the incubation period of four weeks. Error bars show the standard deviation of $\varepsilon^2H_{n\ TOM/\ leaf\ litter}$ for each time step (n = 3). To ease readability, the sampling times have been shifted slightly.

Supporting Information of Section C

Medium preparation

The medium contained 200 mL salt stock solution (64 g Na_2HPO_4 x $7H_2O$, 15 g KH_2PO_4, 2.5 g NaCl and 5 g NH_4Cl per liter), 2 mL of 1M $MgSO_4$, 0.1 mL of 1M $CaCl_2$, 1 mL of 1M MOPS buffer, 8 mL vitamin mix solution (stock solution: 10 mg Biotin, 12.7 mg Thiamin-HCl per 100 mL) and 1 mL trace element solution (stock solution: 625 mg $FeCl_3$ x 6 H_2O, 22.5 mg $ZnSO_4$ x 7 H_2O, 22.5 mg $CuSO_4$ x 5 H_2O, 22.5 mg $CoCl_2$ x 6 H_2O and 15 mg $MnSO_4$ x H_2O per 50 mL). The total volume of each replicate inoculum supplemented with either glucose or lysine was 100 mL.

Sample processing

Cells at each time step were harvested by centrifuging the cultures at 3400 *g* for 10 min (Rotanata 400RS, Hettich, Germany). The supernatants were collected and frozen. Cell culture pellets were washed in 10 mL of 0.9 % NaCl and centrifuged again at 3400 *g* for 10 min (Rotanata 400RS, Hettich, Germany). This washing procedure was repeated once to get rid of medium residues. Finally, the resulting cell pellets were washed with 20 mL 0.9 % NaCl, transferred into smaller tubes (Eppendorf, Germany) and centrifuged for 10 min at 8000 *g* (Biofuge pico, Heraeus Instruments, Germany). Afterwards the resulting pellets were frozen at -80 °C and lyophilized for analysis (LyoCube 4-8 LSCplus, Martinchrist, Germany).

Calculation of respiration

Based on the reaction equation, 1 mL of 1 M NaOH can react with a maximum of 22 mg CO_2 (Eq. S1).

$$2NaOH + CO_2 \rightarrow Na_2CO_3 + H_2O \qquad \text{(Eq. S1)}$$

The extent of respiration (CO_2 formation) was derived from the measurements of the electrical conductivity (EC). This requires the calibration of the EC with the mass of released CO_2 determined by titration of the remaining NaOH with HCl. Therefore, the mass of CO_2 (MCO_2) is proportional to the difference between the EC of NaOH at the beginning ($EC(t_0)$) and the electrical conductivity of NaOH at time i ($EC(t_i)$). Here, the EC of freshly prepared NaOH was measured at the beginning and several times during CO_2 exposition. At the end of the incubation, the excess NaOH was determined via titration with HCl. Based on the regression of the difference of EC (t_0) and EC (t_i) on MCO_2 the respiration was inferred for all samples. For the calculation of MCO_2, the difference between EC (t_0) and EC (t_i) was divided by the slope of the previously described calibration of 0.236 (Eq. S2; Wollum and Gomez[1]) followed by the subtraction of the mass of CO_2 of the control treatments ($MCO_{2\,Con}$; identical setup but without bacteria at time i).

$$MCO_2[mg] = \frac{EC_{(t0)}\left[\frac{1}{\Omega}\right] - EC_{(ti)}\left[\frac{1}{\Omega}\right]}{0.236\left[\frac{1}{\Omega}\right]} - MCO_{2\ Con}[mg] \quad \text{(Eq. S2)}$$

Steam equilibration setup, stable H analysis and quality specifications

The equilibration setup consisted of a stainless-steel vacuum vessel, which was connected to a vacuum pump at the one end and to an Ar flask at the other end. Samples were weighed in tin (Sn) capsules and were placed in the steel vessel. Afterwards, the vessel was evacuated for one hour and subsequently disconnected from the vacuum line, before 3.5 mL of the equilibration water was injected with a syringe through a silicone rubber septum. Then, the vessel was placed in a fan-assisted heating oven at 120 °C overnight. This time is necessary to reach the isotopic equilibrium between the exchangeable H fraction of samples and the injected equilibrium water H.[1] At the next day, the vessel was reconnected to the vacuum line and evacuated for 1.5 h. Subsequently, we used Ar (purity grade 5.0) to depressurize the vessel to ambient air pressure. This procedure minimizes re-equilibration of the samples with ambient air. Samples were sealed airtight with end-cutting pliers while the Ar continuously flushed the vessel. This procedure always took less than 30 seconds. We used three waters of known δ^2H_W values (AWI = -268±1 ‰, ^{2}H enriched= +113±1 ‰ and Millipore water = -75 ‰). This approach guaranteed effective replacement of all isotopically exchangeable sample H with the hydrogen of the equilibrium water.[1] Unfortunately, we are not aware of studies dealing with the hydrolysis during steam equilibration at 120 °C. Khuwijitjaru et al.[2] reported that the hydrolysis of fatty acid esters and the conversion to free fatty acids was reached at temperatures of 340 °C. Archuleta[3] found little decomposition at operating temperatures of 280 °C and 300 °C for oils and fats, whereas decomposition occurred at 325 °C. For glycerol, decomposition was strongly evident at 325 °C but not at lower temperatures. Holiday et al.[4] reported hydrolysis of soybean, linseed, and coconut oils to free fatty acids with water at a density of 0.7 g/mL and temperatures of 260-280 °C while some geometric isomerization was observed at temperatures as low as 250 °C. Decomposition of polyethylene terephthalate (PET) polybutylene terephthalate (PBT) and polyethylene 2,6-naphthalate (PEN) was observed at temperatures over 300 °C.[5] However, the mentioned temperatures are far above our used temperature of 120 °C so we consider hydrolysis of ester bonds as highly unlikely during our steam equilibration. The stable hydrogen isotope ratios of steam-equilibrated bulk samples of bacterial biomass were measured with a TC/EA-IRMS device (vario PYRO Cube and Isoprime visION, Elementar Analysesysteme GmbH, Germany). The samples in tin capsules were pyrolyzed in the EA filled with glassy carbon granulate reactor at 1450 °C. Several studies mentioned both materials, Sn and Zn capsules as suitable.[6–8] Many δ^2H studies note the use of Sn capsules without further explanations.[9–12] We used Sn capsules, because Sn is the softer material, which can be more easily crimp-sealed. For Ag capsules we realized, that a gas-tight crimp-sealing only lasts

sufficiently long when much more force is applied as compared with Sn. We see the so-called cold-welding by hand tools[13] as a questionable practice for Ag, since a pressure of 4950 kg/cm² for 30 s at room-temperature is only sufficient when the thin Ag sheets were pre-heated but if not, even 7000 kg/cm² are insufficient.[14] For this study, we used the crimp-sealing technique of Sn capsules with the same tools as described in Ruppenthal et al.[15]. We tested the exchange with ambient air by filling a Sn capsule with the volatile acetone and found that the weight of acetone in the capsules remained constant for weeks.[16] Similarly, Ruppenthal et al.[15] sealed water in tin capsules, without a weight loss over a period of a month. Furthermore, we tested the tightness of crimp-sealed Sn capsules by measuring steam-equilibrated samples immediately after equilibration and days later and found that δ^2H values did not change. Finally, we measured GISP and IAEA-CH7 both in Ag and Sn capsules and the values were undistinguishable from the certified or recommended values (GISP: -188.8±1.9 ‰ (n = 72) in Ag capsules vs. -189.3±1.1 ‰ (n = 46) in Sn capsules; IAEA-CH7: -100.3±1.5 ‰ (n = 88) vs. -100.6±1.7 ‰ (n = 90). In addition, we measured USGS57 biotite and USGS58 muscovite in Sn capsules yielding δ^2H values of 93.8±1.7 ‰ and 31.3±0.9 ‰, respectively, which is indistinguishable from the reference values of 91.5±2.4 ‰ and 28.4±1.6 ‰, respectively, given by the USGS, which were measured in Ag capsules.[17] Moreover, we never detected a H_2 blank in Sn capsules. Thus, the use of Sn capsules instead of Ag reduces outliers, increases repeatability, prevents re-equilibration and is reliable for the steam equilibration device. The H^{3+}-correction factor for the produced H^{3+} ions in the ion source was ascertained before each measurement cycle using the IRMS software (ionOS, Elementar, Germany) and varied between 7.1 and 7.4 ppm nA^{-1}. To calibrate the measured δ^2H values, the two certified international laboratory standards USGS46 (certified as -235.8±0.7 ‰) and GFLES-1 (certified as 80.1±0.5 ‰) delivered by USGS in sealed silver tubes were used. The certified H isotope standard material VSMOW2 (certified as 0±0.4 ‰) delivered by USGS in sealed silver tubes was included as duplicate measurements to determine the trueness and the precision of our measurements and yielded δ^2H values of -2.1±2.5 ‰ (n = 77). δ^2H values are expressed relative to VSMOW-SLAP scale in per mill.

Statistical analyses

All statistical analyses were conducted with SPSS 11.5 (SPSS Inc., USA) and/or Microsoft Excel 2010 (Microsoft Corp., USA) software. Prior to statistical analyses, the test prerequisites were checked (normal distribution: Shapiro-Wilk test; homogeneity of variances: Levene's test). If normal distribution of residues or variance homogeneity of the analyzed data was violated, data were transformed. To approach normal data distribution, data was $\log_{10}$-transformed. In case of heteroscedasticity, we used the Huynh-Feldt- or Greenhose-Geisser-correction according to Girden.[18] Significant differences between bacterial species, the used substrates or labeled waters during the temporal course of the incubation were analyzed using repeated measures analysis of variance

(rmANOVA) with main effects for the mentioned factors and the corresponding interactions. *T tests* were *used to* compare the means of the labeled water, bacterial species, and to assess a significant deviation from zero.

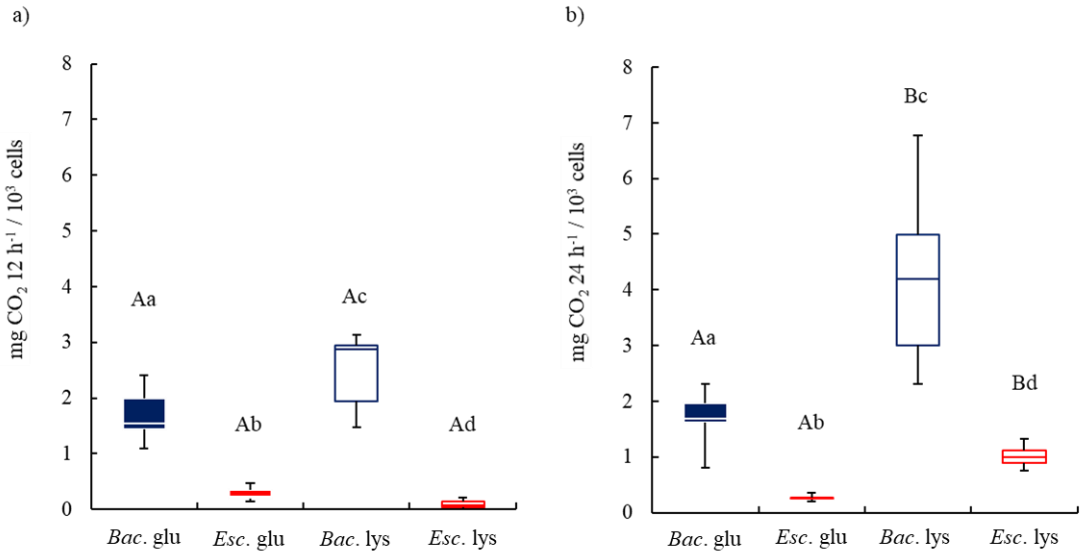

Fig. C-S1: CO_2 production per 10^3 cells of *B. atrophaeus* (*Bac.*) and *E. coli* (*Esc.*) grown on glucose (glu) or lysine (lys) after 12 h (a) and 24 h (b) of incubation. Uppercase letters indicate significant substrate-specific differences ($p < 0.05$) and lowercase letters significant differences between bacterial species ($p < 0.05$). Error bars show the standard deviation of the Optical Density values and CO_2 production for each treatment ($n = 9$).

Table C-S1: Repeated measures ANOVA results for effects of time, bacterial species, substrate and water treatment (water) on the substrate consumption, bacterial growth, bacterial respiration, exchangeable H fraction (x_e), the hydrogen isotope signature of bacterial species ($\delta^2H_{n\ bac}$), H incorporation, and the associated isotope fractionation ($\varepsilon_{BacBiom/w}$) for *B. atrophaeus* and *E. coli*. DF is degrees of freedom, F is F value, and P is error probability. Non-significant interactions between factors are not displayed.

Fixed terms	DF	F	P
Substrate consumption			
Time	1	45.04	<0.001
Bacterial species	1	5.57	0.026
Substrate	1	454.51	<0.001
Water	2	0.67	0.420
Time × Bacterial species	1	17.08	<0.001
Time × Substrate	1	38.88	<0.001
Bacterial species × Substrate	1	16.45	<0.001
Bacterial growth			
Time	1	25.37	<0.001
Bacterial species	1	34.94	<0.001
Substrate	1	345.13	<0.001
Water	2	0.51	0.605
Time × Bacterial species	1	24.68	<0.001
Time × Substrate	1	42.45	<0.001
Bacterial respiration			
Time	1	95.53	<0.001
Bacterial species	1	215.01	<0.001
Substrate	1	182.51	<0.001
Water		0.251	0.780
Time × Bacterial species	1	46.59	<0.001
x_e			
Time	1	2.878	0.102
Bacterial species	1	8.770	0.006
Substrate	1	0.211	0.650
Water	2	3.546	0.043

Table continued on the next page.

$\delta^2H_{n\ bac}$			
Time	1	10.52	0.003
Bacterial species	1	265.69	<0.001
Substrate	1	1478.31	<0.001
Water	2	122.74	<0.001
Time × Bacterial species	1	144.09	<0.001
Time × Substrate	1	6.473	0.018
Bacterial species × Substrate	1	4.89	0.037
Bacterial species × Water	2	4.63	0.019
Substrate × Water	2	105.75	<0.001
H incorporation (glucose only)			
Time	1	0.15	0.719
Bacterial species	1	348.51	<0.001
$\varepsilon_{BacBiom/w}$			
Time	1	295.36	<0.001
Bacterial species	1	13924.05	<0.001
Time × Bacterial species	1	1320.02	<0.001

Table C-S2: Repeated measures ANOVA results for effects of time, bacterial species, substrate and water treatment (water) on bacterial biomass and respiration per 10^3 cells with significant interactions for *B. atrophaeus* and *E. coli.* DF is degrees of freedom, F is F value, and P is error probability. Non-significant interactions between factors are not displayed.

Fixed terms	nDF	F	P
Bacterial biomass			
Time	1	25.37	<0.001
Bacterial species	1	34.94	<0.001
Substrate	1	345.13	<0.001
Water		0.513	0.605
Time × Bacterial species	1	24.68	<0.001
Time × Substrate	1	42.45	<0.001
Respiration/ 10^3 cells			
Time	1	21.386	<0.001
Bacterial species	1	249.35	<0.001
Substrate	1	53.46	<0.001
Time × Substrate	1	22.41	<0.001
Bacterial species × Substrate	1	2641	<0.001

Table C-S3: Exchangeable H fraction for *B. atrophaeus* und *E. coli* before incubation (in the LB-medium) and for the two time steps (12 and 24 hours) after incubation (in the M9 minimal medium) with either glucose or lysine as sole carbon source.

Bacterial species	**Exchangeable H-fraction [%]**				
	Before incubation	After incubation			
		Glucose		Lysine	
		12 h	24 h	12 h	24 h
B. atrophaeus	19.1	22.7±3.2	25.7±1.0	20.9±2.7	24.2±3.4
E. coli	25.3	18.6±2.3	19.5±2.6	20.1±4.1	19.3±3.9

References cited in the Supporting Information

(1) Ruppenthal, M.; Oelmann, Y.; Wilcke, W. Isotope ratios of nonexchangeable hydrogen in soils from different climate zones. *Geoderma* **2010**; 155: 231–241.

(2) Khuwijitjaru, P. Kinetics on the hydrolysis of fatty acid esters in subcritical water. *Chemical Engineering Journal* **2004**; 99: 1–4.

(3) Archuleta, R. C. Non-catalytic steam hydrolysis of fats and oils 1991.

(4) Holliday, R. L.; King, J. W.; List, G. R. Hydrolysis of Vegetable Oils in Sub- and Supercritical Water. *Industrial and Engineering Chemistry Research* **1997**; 36: 932–935.

(5) Kumagai, S.; Morohoshi, Y.; Grause, G.; Kameda, T.; Yoshioka, T. Pyrolysis versus hydrolysis behavior during steam decomposition of polyesters using ^{18}O-labeled steam. *RSC Advances* **2015**; 5: 61828–61837.

(6) Gehre, M.; Renpenning, J.; Gilevska, T.; Qi, H.; Coplen, T. B.; Meijer, H. A. J.; Brand, W. A.; Schimmelmann, A. On-line hydrogen-isotope measurements of organic samples using elemental chromium: an extension for high temperature elemental-analyzer techniques. *Analytical Chemistry* **2015**; 87: 5198–5205.

(7) Oerter, E.; Singleton, M.; Davisson, L. Hydrogen and oxygen stable isotope signatures of goethite hydration waters by thermogravimetry-enabled laser spectroscopy. *Chemical Geology* **2017**; 475: 14–23.

(8) Schimmelmann, A.; Qi, H.; Dunn, P. J. H.; Camin, F.; Bontempo, L.; Potočnik, D.; Ogrinc, N.; Kelly, S.; Carter, J. F.; Abrahim, A.; Reid, L. T.; Coplen, T. B. Food Matrix Reference Materials for Hydrogen, Carbon, Nitrogen, Oxygen, and Sulfur Stable Isotope-Ratio Measurements: Collagens, Flours, Honeys, and Vegetable Oils. *Journal of agricultural and food chemistry* **2020**; 68: 10852–10864.

(9) Filot, M. S.; Leuenberger, M.; Pazdur, A.; Boettger, T. Rapid online equilibration method to determine the D/H ratios of non-exchangeable hydrogen in cellulose. *Rapid communications in mass spectrometry: RCM* **2006**; 20: 3337–3344.

(10) Koehler, G.; Wassenaar, L. I. Determination of the hydrogen isotopic compositions of organic materials and hydrous minerals using thermal combustion laser spectroscopy. *Analytical Chemistry* **2012**; 84: 3640–3645.

(11) Paul, A.; Hatté, C.; Pastor, L.; Thiry, Y.; Siclet, F.; Balesdent, J. Hydrogen dynamics in soil organic matter as determined by ^{13}C and ^{2}H labeling experiments. *Biogeosciences* **2016**; 13: 6587–6598.

(12) Ruppenthal, M.; Oelmann, Y.; del Valle, H. F.; Wilcke, W. Stable isotope ratios of nonexchangeable hydrogen in organic matter of soils and plants along a 2100-km climosequence in Argentina: New insights into soil organic matter sources and transformations? *Geochimica et Cosmochimica Acta* **2015**; 152: 54–71.

(13) Qi, H.; Gröning, M.; Coplen, T. B.; Buck, B.; Mroczkowski, S. J.; Brand, W. A.; Geilmann, H.; Gehre, M. Novel silver-tubing method for quantitative introduction of water into high-temperature conversion systems for stable hydrogen and oxygen isotopic measurements. *Rapid communications in mass spectrometry: RCM* **2010**; 24: 1821–1827.

(14) van Duzee, G. R.; Thomas, J. M. Cold Welding of Silver. *Journal of the Electrochemical Society*. **1940**; 77: 341.

(15) Ruppenthal, M.; Oelmann, Y.; Wilcke, W. Optimized demineralization technique for the measurement of stable isotope ratios of nonexchangeable H in soil organic matter. *Environmental Science and Technology* **2013**; 47: 949–957.

(16) Kessler, A.; Kreis, K.; Merseburger, S.; Wilcke, W.; Oelmann, Y. Incorporation of hydrogen from ambient water into the C-bonded H pool during litter decomposition. *Soil Biology and Biochemistry* **2021**; 162: 108407.

(17) Qi, H.; Coplen, T. B.; Gehre, M.; Vennemann, T. W.; Brand, W. A.; Geilmann, H.; Olack, G.; Bindeman, I. N.; Palandri, J.; Huang, L.; Longstaffe, F. J. New biotite and muscovite isotopic reference materials, USGS57 and USGS58, for $\delta^{2}H$ measurements–A replacement for NBS 30. *Chemical Geology* **2017**; 467: 89–99.

(18) Girden, E. ANOVA. SAGE Publications, Inc, 2455 Teller Road, Thousand Oaks California 91320 United States of America **1992**.

Supporting Information of Section D

Litterbag experiment and sample processing

The experiment was conducted with filled litterbags put in top cut HDPE free draining lysimeters (Roth, Germany) which were closed at the bottom and placed on the soil surface (Fig. D-S1). Each litterbag-lysimeter combination was connected to a glass bottle (Schott AG, Germany) via a PVC tube. Discharge out of the lysimeters was aligned with a small slope in the field, to guarantee the complete outlet of the percolates and exclude anaerobic conditions within the lysimeters and litterbags during decomposition. To prevent external leaf input, a PE net was stretched over the containers. At each time step (4, 12 and 20 weeks) one set of litterbag replicates (n = 36) was collected. Percolate samples of each litterbag container were taken in bi-weekly intervals, with exception for the first time point after four weeks because of dry conditions with no precipitation. After sampling, percolate and precipitation samples were immediately frozen at -20 °C. In the laboratory, litterbags were opened and residual leaves were cleaned manually from macrofauna and dirt, dried in a drying oven at 40 °C for 48 hours and subsequently weighed. Additionally, the amount of percolates ($M_{percolate}$) for each replicate was determined by weighing. Individual percolate samples taken in biweekly intervals were merged to one composite sample that matched with the collection of the corresponding litterbag samples (e.g., six biweekly samples merged to one composite sample for each of the litterbag replicates collected after 12 weeks). However, for the litterbags that were exposed to field conditions for 20 weeks, we kept the biweekly percolate samples in favour of a higher temporal resolution. Percolate samples were not filtered. Therefore, the term TOM for OM originated from percolates was used. TOM of percolates was gained by lyophilization at NaProFood GmbH, Germany. For all subsequent chemical analyses, leaf and TOM samples were ground (Pulverisette 5, Fritsch, Germany).

Steam equilibration and stable H analysis

The steam equilibration setup is composed of a stainless-steel vacuum vessel which is connected to the vacuum pump at the one end and to an Argon-flask at the other end. Ground leaf and TOM samples were weighed in tin capsules (IVA Analysetechnik GmbH + Co KG) placed in brass sample holder. Steam equilibration was conducted by using two equilibration waters with measured δ^2H values (δ^2H_{ew}) (AWI= -268 ‰ and deionized water= -75 ‰) resulting in two aliquots of one and the same sample equilibrated with a different water. After Ruppenthal et al.[1] this approach guarantees the full exchange of isotopically exchangeable H with the corresponding equilibrium water H. Through a silicone rubber septum, 3.5 mL of equilibration water (corresponding to a ratio of exchangeable sample H to equilibration water H of at least 1:100) was injected into the evacuated vessel using a syringe. While disconnecting the vessel from the vacuum line with quick connectors (Swaglock Company, USA) and putting the vessel into a fan-assisted heating oven at 120 °C overnight, equilibration took place. The vessel was reconnected to the vacuum line at the next morning and the equilibration water vapour was evacuated while the residual heat of the vessel caused drying the

samples for approx. 2 h. After the vessel cooled down, it was repressurized to ambient pressure with dried Ar gas (purity grade 5.0) while the flushing avoids isotopic reequilibration of equilibrated samples with ambient air moisture. Equilibrated samples were sealed airtight with end cutting pliers in the vessel during continuous flow of Ar into the vessel. After Equilibration, samples were taken transferred to the autosampler of the Thermal Conversion/Elemental Analyzer-Isotope Mass Spectrometer (TC/EA-IRMS) for δ^2H analysis. The sample removal from the argon-filled vessel and the subsequently sealing never exceeded 30 s which minimized the risk of reequilibration of sample H with ambient moisture H. The samples in tin (Sn) capsules were pyrolyzed in the EA filled with glassy carbon granulate reactor at 1450 °C. Several studies mentioned both materials, Sn and Zn capsules as suitable.[2–4] Many δ^2H studies note the use of Sn capsules without further explanations.[5–8] We used Sn capsules, because Sn is the softer material, which can be more easily crimp-sealed. For Ag capsules we realized, that a gas-tight crimp-sealing only lasts sufficiently long when much more force is applied as compared with Sn. We see the so-called cold-welding by hand tools[9] as a questionable practice for Ag, since a pressure of 4950 kg/cm² for 30 s at room-temperature is only sufficient when the thin Ag sheets were pre-heated but if not, even 7000 kg/cm² are insufficient.[10] For this study, we used the crimp-sealing technique of Sn capsules with the same tools as described in Ruppenthal et al.[11]. We tested the exchange with ambient air by filling a Sn capsule with the volatile acetone and found that the weight of acetone in the capsules remained constant for weeks.[12] Similarly, Ruppenthal et al.[11] sealed water in tin capsules, without a weight loss over a period of a month. Furthermore, we tested the tightness of crimp-sealed Sn capsules by measuring steam-equilibrated samples immediately after equilibration and days later and found that δ^2H values did not change. Finally, we measured GISP and IAEA-CH7 both in Ag and Sn capsules and the values were undistinguishable from the certified or recommended values (GISP: -188.8±1.9 ‰ (n = 72) in Ag capsules vs. -189.3±1.1 ‰ (n = 46) in Sn capsules; IAEA-CH7: -100.3±1.5 ‰ (n = 88) vs. -100.6±1.7 ‰ (n = 90). In addition, we measured USGS57 biotite and USGS58 muscovite in Sn capsules yielding δ^2H values of +93.8±1.7 ‰ and +31.3±0.9 ‰, respectively, which is indistinguishable from the reference values of +91.5±2.4 ‰ and +28.4±1.6 ‰, respectively, given by the USGS, which were measured in Ag capsules.[13] Moreover, we never detected a H_2 blank in Sn capsules. Thus, the use of Sn capsules instead of Ag reduces outliers and increases repeatability, prevents re-equilibration and is reliable for the steam equilibration device. Precipitation samples were pipetted in tin capsules as well and sealed with end cutting pliers.

Stable hydrogen isotope ratios of equilibrated leaf (δ^2H_{leaf}) and TOM (δ^2H_{TOM}) samples as well as precipitation samples (δ^2H_{prec}) were measured via a TC/EA-IRMS device (vario, Pyro Cube and Isoprime 100, Elementar Analysesysteme GmbH, Germany). In the EA reactor, samples were pyrolzed at 1450 °C. The glassy carbon tube of the EA was packed with glassy carbon granules while we used a glassy carbon cup on the top of the granules to collect molten tin capsules and ash residues. δ^2H analysis of blank tin capsules did not show a measurable H_2 blank. The correction factor for

H_3^+ ions produced in the ion source was determined before measurements of each batch of 120 samples using the automated procedure of the IRMS software (Ion vantage, Elementar GmbH, Germany). Over six weeks of δ^2H analysis, the H_3^+ correction factor varied between 7.2 and 7.6 ppm nA^{-1}. We used three certified international laboratory standards USGS46 (certified as -235.8±0.7 ‰), VSMOW2 (certified as 0±0.4 ‰) and GFLES-2 (+159.9±0.5 ‰) delivered by USGS and sealed in silver tubes. Reproducibility of a certified H isotope standard material IAEA-CH7 (certified as -100.3±2.0 ‰) which was included as duplicate measurements to determine the trueness and the precision of our measurements was -101.5±3.6 ‰ (n = 54). All δ^2H values are expressed relative to VSMOW-SLAP scale in per mill. Furthermore, C and N concentrations of initial leaves (before the litterbag experiment) and the remaining leaves (after exposure in the field) as well as lyophilized TOM were measured with the vario EL III Element Analyzer (Elementar Analysesysteme GmbH, Germany).

Calculations and statistical evaluation

The proportion of C-bonded H with the respective δ^2H_n value of leaf and TOM samples via a mass balance approach[14] adopted by Ruppenthal et al.[1] Therefore, the total H pool of a sample (H_t) is composed of an exchangeable O-, N- and S-bonded H fraction (H_{ex}) that isotopically exchanges with water-H and a C-bonded H fraction (H_n) with respective δ^2H_{ex} and δ^2H_n values. δ^2H values of the total pool (δ^2H_t) could be measured directly and this pool can be described by Eq. S1.[5,14–17]

$$\delta^2 H_t = (1 - x_e)\delta^2 H_n + x_e \delta^2 H_{ex} \quad \text{(Eq. S1)}$$

xe represents the H fraction that isotopically exchanged during equilibration. For different organic compounds, this fraction varies from 0.0 for simple hydrocarbons up to 0.4 (i.e. 40 wt.% of H_t) for complex compounds like cellulose, kerogen or humic acid.[5,14,16,18] In SOM, the fraction of isotopically exchangeable H varies substantially and depends on the degree of humification and the leaf quality input. The δ^2H_{ex} value is equal to the δ^2H value of the equilibration water (δ^2H_{ew}) with the equilibrium fractionation factor ($\alpha_{ex\text{-}w}$), if the exchangeable H fraction of a sample is in isotopic equilibrium with the equilibration water (Eq. S2).[1]

$$\alpha_{ex-w} = \frac{\delta^2 H_{ex} + 1000}{\delta^2 H_{ew} + 1000} \quad \text{(Eq. S2)}$$

The equilibrium fractionation factor $\alpha_{ex\text{-}w}$ depends on the chemical composition and the equilibration temperature of the analyzed samples. However, the direct experimental determination of $\alpha_{ex\text{-}w}$ for chemically complex organic substances is hard to determine, because it is necessary to asses $\alpha_{ex\text{-}w}$

values through δ^2H values of isotopically equilibrated samples with those of samples with chemically removed H.[14] Several studies[14,18,19] used an approximation of $\alpha_{ex\text{-}w}$ for substances like humic acid, kerogen, keratin or collagen. Here, a provisional value for $\alpha_{ex\text{-}w}$ of 1.08 was assigned, which is based on the cellulose equilibrium isotopic fractionation factor between isotopically exchangeable H and water-H at 114 °C, which has been experimentally determined by Schimmelmann.[15] Over a range of 1.06 to 1.10 for $\alpha_{ex\text{-}w}$, the use of provisional $\alpha_{ex\text{-}w}$ value is admissible and the isotopic shift, which is caused by the equilibration procedure is a function of isotopically exchangeable H and xe, which has been shown via a sensitivity analysis by Schimmelmann et al.[20] and Wassenaar and Hobson.[14] Because of this circumstance, in our study, we used a $\alpha_{ex\text{-}w}$ value of 1.08.

If xe is constant among aliquots, a plot of δ^2H_t versus δ^2H_{ew} should result in a straight line defined by Eq. S3, which is derived by solving Eq. S2 for δ^2H_{ex} and substituting into Eq. S1.[1]

$$\delta^2 H_t = x_e \alpha_{ex-w} \delta^2 H_{ew} + (1 - x_e)\delta^2 H_n + 1000 x_e (\alpha_{ex-w} - 1) \quad \text{(Eq. S3)}$$

When the isotopically exchangeable H fraction is in equilibrium with the water-H, δ^2H_n from Eq. S3 is equivalent to δ^2H of the C-bonded H fraction in the sample. Therein, δ^2H_n can be calculated by rearranging Eq. S3 to Eq. S4.[1]

$$\delta^2 H_n = \frac{\delta^2 H_t - 1000 x_e (\alpha_{ex-w} - 1) - x_e \alpha_{ex-w} \delta^2 H_{ew}}{(1 - x_e)} \quad \text{(Eq. S4)}$$

Different physical conditions during equilibration e.g. temperature fluctuations can cause uncertainties in the isotopic sample equilibration and errors concerning the determination of δ^2H_n values. Here, in a previous study[12] we used three waters for equilibration of leaf litter samples resulting in more reliable regression analysis of δ^2H_t values on δ^2H_{ew} values of equilibrated samples and an increase of the accuracy of δ^2H_n determinations.[1] However, in this study we used two waters, which is sufficient to determine reliable δ^2H_n values. For further information about the steam equilibration and the calculation of δ^2H_n values see Ruppenthal et al.[1]

Statistical analyses

All statistical analyses were conducted with SPSS 11.5 (SPSS Inc., USA) and/or Microsoft Excel 2010 (Microsoft Corp., USA) software. Prerequisites for statistical analyses were checked (normal distribution: Shapiro-Wilk test; homogeneity of variances: Levene's test). If normal distribution of residues or variance homogeneity was violated, data were $\log_{10}$-transformed. In case of heteroscedasticity we used the Huynh-Feldt- or Greenhose-Geisser-correction according to Girden.[21] Significant differences between tree species or among leaf labels during the temporal course of the

decomposition experiment were analyzed using repeated measure analysis of variance (rmANOVA) while *t-tests* were *used to* determine differences between the means of tree species and leaf label for a given sampling interval.

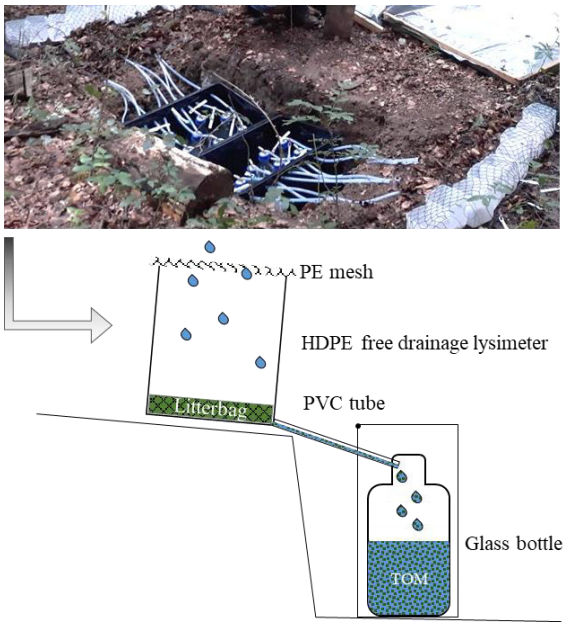

Fig. D-S1: Experimental setup consisting of free drainage lysimeters filled with litterbags connected to a glass bottle via a PVC tube to collect TOM samples. A PE mesh at the top of the lysimeters was installed to prevent external leaf litter input and undisturbed permeability of precipitation was ensured.

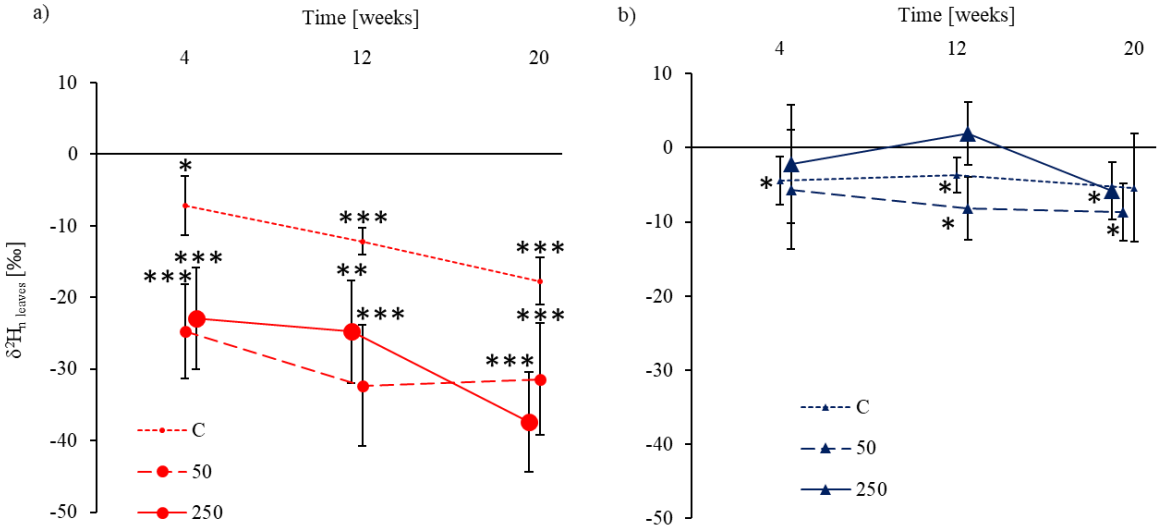

Fig. D-S2: $\delta^2H_{n\ leaves\ (ti\text{-}t0)}$ for beech (a) and lime (b) differentiated according to the type of leaf label treatment (C: δ^2H= -70 ‰, 50: δ^2H= +50 ‰, and 250: δ^2H= +250 ‰) during the 20 weeks of decomposition. Error bars show the standard deviation of $\delta^2H_{n\ leaves}$ for each time step (n = 6). To ease readability, the sampling times have been shifted slightly along the x axis. Asterisks indicate significant differences from zero at a given time step (* p <0.05; ** p <0.01, *** p <0.001).

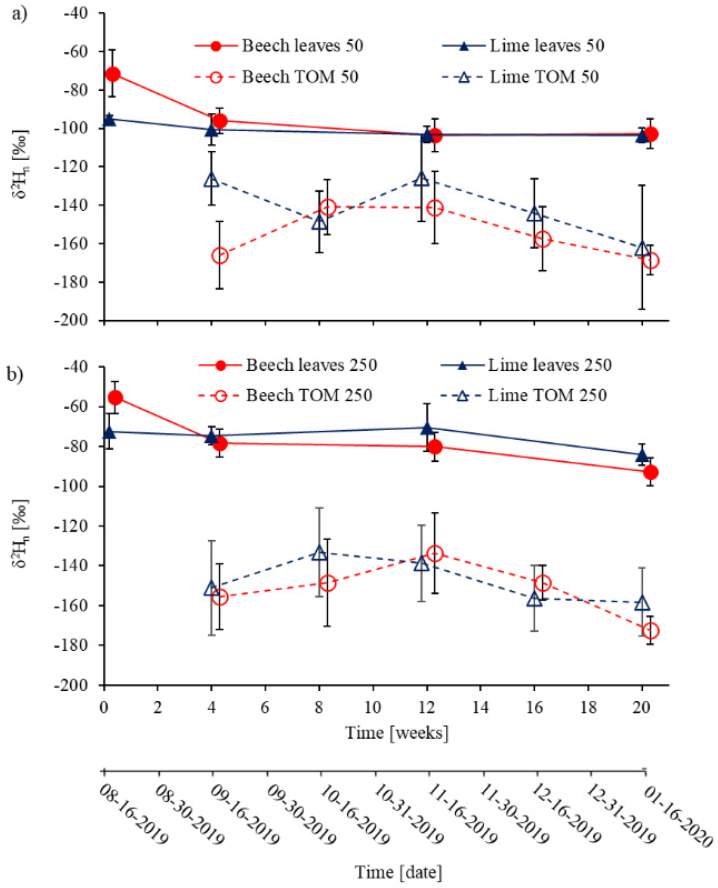

Fig. D-S3: δ^2H_n values of leaves and biweekly bulked TOM (with exception for the first time step after four weeks) for beech and lime according to the type of leaf label treatment 50: δ^2H= +50 ‰ (a) and 250: δ^2H= +250 ‰ (b) during the 20 weeks of decomposition. Error bars show the standard deviation for each time step (n = 6). To ease readability, the sampling times have been shifted slightly along the x axis. Asterisks indicate significant differences from zero at a given time step (* $p < 0.05$; ** $p < 0.01$; *** $p < 0.001$).

Table D-S1: Repeated measure ANOVA results for effects of time, site, tree species and leaf label and the corresponding interactions of factors on the mass losses of solid-state leaves (relative mass loss), C:N, the exchangeable H fraction of leaves (xe_{leaves}) and TOM (xe_{TOM}), the hydrogen isotope signature of leaves ($\delta^2H_{n\ leaves}$), the hydrogen isotope signature of TOM according to leaf sampling time steps ($\delta^2H_{n\ TOM\ l}$) and biweekly intervals ($\delta^2H_{n\ TOM\ b}$) and the associated isotope fractionation ($\varepsilon_{TOM/leaves}$) for beech and lime. DF is degrees of freedom, F is F value, and P is error probability.

Fixed terms	nDF	F	P
Relative mass loss			
Time	3	84.82	<0.001
Site	1	0.12	0.734
Tree species	1	414.47	<0.001
Leaf label	2	0.55	0.582
Time × Site	2	0.42	0.663
Time × Tree species	2	2.12	0.130
Time × Leaf label	2	1.11	0.361
Site × Tree species	1	0.30	0.590
Site × Leaf Label	2	1.57	0.227
Tree species × Leaf label	2	2.24	0.126
C:N			
Time	2	1.10	0.343
Site	1	0.232	0.635
Tree species	1	48.42	<0.001
Leaf label	2	1.50	0.244
Time × Site	2	2.59	0.087
Time × Tree species	2	0.22	0.806
Time × Leaf label	4	0.78	0.546
Site × Tree species	1	0.52	0.480
Site × Leaf Label	2	0.48	0.626
Tree species × Leaf label	2	0.67	0.521
$\boldsymbol{xe}_{\textbf{leaves}}$			
Time	3	110.01	<0.001
Site	1	0.66	0.426
Tree species	1	20.94	<0.001
Leaf label	2	0.78	0.468
Time × Site	3	0.39	0.760
Time × Tree species	3	40.43	<0.001
Time × Leaf label	6	1.64	0.148
Site × Tree species	1	0.003	0.960
Site × Leaf Label	2	0.009	0.991
Tree species × Leaf label	2	4.36	0.023

Table continued on the next page.

xe_{TOM}

Time	2	2.07	0.14
Site	1	0.17	0.684
Tree species	1	0.07	0.794
Leaf label	2	2.16	0.143
Time × Site	2	0.43	0.656
Time × Tree species	2	2.23	0.121
Time × Leaf label	4	1.20	0.325
Site × Tree species	1	0.02	0.896
Site × Leaf Label	2	0.76	0.483
Tree species × Leaf label	2	5.47	0.013

$\delta^2H_{n\ leaves}$

Time	2	18.87	<0.001
Site	1	0.12	0.733
Tree species	1	0.33	0.572
Leaf label	2	112.07	<0.001
Time × Site	2	0.52	0.599
Time × Tree species	2	3.53	0.037
Time × Leaf label	4	4.99	0.002
Site × Tree species	1	0.283	0.599
Site × Leaf Label	2	1.06	0.361
Tree species × Leaf label	2	6.88	0.004

$\delta^2H_{n\ TOM\ l}$

Time	2	0.65	0.528
Site	1	0.96	0.340
Tree species	1	3.98	0.061
Leaf label	2	0.03	0.975
Time × Site	2	0.07	0.932
Time × Tree species	2	0.08	0.922
Time × Leaf label	4	0.54	0.709
Site × Tree species	1	0.71	0.793
Site × Leaf Label	2	0.26	0.774
Tree species × Leaf label	2	0.24	0.792

$\delta^2H_{n\ TOM\ b}$

Time	4	3.86	0.006
Site	1	1.53	0.228
Tree species	1	1.69	0.206
Leaf label	2	0.28	0.755
Time × Site	4	0.61	0.655
Time × Tree species	4	0.49	0.744
Time × Leaf label	8	1.07	0.391
Site × Tree species	1	0.66	0.425
Site × Leaf Label	2	2.00	0.158
Tree species × Leaf label	2	0.47	0.634

Table continued on the next page.

$\varepsilon^2H_{TOM/\ leaves}$			
Time	2	0.61	0.560
Site	1	0.55	0.487
Tree species	1	3.652	0.105
Time × Site	2	0.51	0.615
Time × Tree species	2	1.00	0.394
Site × Tree species	1	0.08	0.788

Table D-S2: Repeated measure ANOVA results for effects of time, tree species and leaf label on the mass losses of solid-state leaves (relative mass loss), C:N, the exchangeable H fraction of leaves ($xe_{\ leaves}$) and TOM ($xe_{\ TOM}$), the hydrogen isotope signature of leaves ($\delta^2H_{n\ leaves}$), the hydrogen isotope signature of TOM according to leaf sampling time steps ($\delta^2H_{n\ TOM\ l}$) and biweekly intervals ($\delta^2H_{n\ TOM\ b}$) and the associated isotope fractionation ($\boldsymbol{\varepsilon}_{TOM/leaves}$) for beech and lime. Non-significant interactions between factors are not displayed.

Fixed terms	nDF	F	P
Relative mass loss			
Time	3	3742.39	<0.001
Tree species	1	420.62	<0.001
Leaf label	2	0.56	0.577
C:N			
Time	2	1.32	0.277
Tree species	1	55.59	<0.001
Leaf label	2	1.53	0.236
$xe_{\ leaves}$			
Time	3	81.35	<0.001
Tree species	1	35.78	<0.001
Leaf label	2	0.36	0.703
Time × Tree species	3	42.11	<0.001
$xe_{\ TOM}$			
Time	3	3.23	0.049
Tree species	1	1.26	0.273
Leaf label	2	2.04	0.153

Table continued on the next page.

$\delta^2H_{n\ leaves}$			
Time	2	17.42	<0.001
Tree species	1	0.345	0.561
Leaf label	1	117.87	<0.001
Time × Tree species	2	3.26	0.045
Time × Leaf label	4	4.61	0.003
Tree species × Leaf label	2	7.23	0.003
$\delta^2H_{n\ TOM\ l}$			
Time	2	8.41	0.001
Tree species	1	2.25	0.144
Leaf label	2	1.06	0.378
$\delta^2H_{n\ TOM\ b}$			
Time	4	4.30	0.003
Tree species	1	1.73	0.199
Leaf label	2	0.22	0.805
$\varepsilon^2H_{\ TOM/\ leaves}$			
Time	2	0.183	0.835
Tree species	1	5.741	0.043

Table D-S3: Results for the coefficient of determination and the slope of the linear regressions of $\delta^2H_{n\ t0}$ on $\delta^2H_{n\ ti}$ values of leaves of beech and lime with the corresponding statistical parameters.

Time	4 weeks			12 weeks			20 weeks		
Leaf label	C	+50 ‰	+250 ‰	C	+50 ‰	+250 ‰	C	+50 ‰	+250 ‰
$\varepsilon^2H_{n\ (ti-t0)}$									
Beech	-8.0	-26.6	-24.3	-13.5	-34.8	-26.2	**-19.6**	**-33.8**	**-39.6**
Lime	-5.0	-6.2	-2.4	-4.1	-9.1	2.1	**-6.1**	**-9.6**	**-12.6**

Table D-S4: Overall ratios of the amount of biweekly bulked leached TOM (M_{TOM}) to leaf C-mass loss (C-mass loss) summarized for both tree species (non-significance of tree species). Despite the non-significant time effect data is presented for all time steps.

Time	4 weeks	12 weeks	20 weeks
M_{TOM}/ C-mass loss	2.02±1.43	2.41±2.06	2.33±1.48

References cited in the Supporting Information

(1) Ruppenthal, M.; Oelmann, Y.; Wilcke, W. Isotope ratios of nonexchangeable hydrogen in soils from different climate zones. *Geoderma* **2010**; 155: 231–241.

(2) Khuwijitjaru, P. Kinetics on the hydrolysis of fatty acid esters in subcritical water. *Chemical Engineering Journal* **2004**; 99: 1–4.

(3) Archuleta, R. C. Non-catalytic steam hydrolysis of fats and oils 1991.

(4) Holliday, R. L.; King, J. W.; List, G. R. Hydrolysis of Vegetable Oils in Sub- and Supercritical Water *Industrial and Engineering Chemistry Research* **1997**; 36: 932–935.

(5) Filot, M. S.; Leuenberger, M.; Pazdur, A.; Boettger, T. Rapid online equilibration method to determine the D/H ratios of non-exchangeable hydrogen in cellulose. *Rapid communications in mass spectrometry: RCM* **2006**; 20: 3337–3344.

(6) Koehler, G.; Wassenaar, L. I. Determination of the hydrogen isotopic compositions of organic materials and hydrous minerals using thermal combustion laser spectroscopy. *Analytical Chemistry* **2012**; 84: 3640–3645.

(7) Paul, A.; Hatté, C.; Pastor, L.; Thiry, Y.; Siclet, F.; Balesdent, J. Hydrogen dynamics in soil organic matter as determined by 13 C and 2 H labeling experiments. *Biogeosciences* **2016**; 13: 6587–6598.

(8) Ruppenthal, M.; Oelmann, Y.; del Valle, H. F.; Wilcke, W. Stable isotope ratios of nonexchangeable hydrogen in organic matter of soils and plants along a 2100-km climosequence in Argentina: New insights into soil organic matter sources and transformations? *Geochimica et Cosmochimica Acta* **2015**; 152: 54–71.

(9) Qi, H.; Gröning, M.; Coplen, T. B.; Buck, B.; Mroczkowski, S. J.; Brand, W. A.; Geilmann, H.; Gehre, M. Novel silver-tubing method for quantitative introduction of water into high-temperature conversion systems for stable hydrogen and oxygen isotopic measurements. *Rapid communications in mass spectrometry: RCM* **2010**; 24: 1821–1827.

(10) van Duzee, G. R.; Thomas, J. M. Cold Welding of Silver. II. *Journal of the Electrochemical Society*. **1940**; 77: 341.

(11) Ruppenthal, M.; Oelmann, Y.; Wilcke, W. Optimized demineralization technique for the measurement of stable isotope ratios of nonexchangeable H in soil organic matter. *Environmental Science and Technology* **2013**; 47: 949–957.

(12) Kessler, A.; Kreis, K.; Merseburger, S.; Wilcke, W.; Oelmann, Y. Incorporation of hydrogen from ambient water into the C-bonded H pool during litter decomposition. *Soil Biology and Biochemistry* **2021**; 162: 108407.

(13) Qi, H.; Coplen, T. B.; Gehre, M.; Vennemann, T. W.; Brand, W. A.; Geilmann, H.; Olack, G.; Bindeman, I. N.; Palandri, J.; Huang, L.; Longstaffe, F. J. New biotite and muscovite isotopic

reference materials, USGS57 and USGS58, for δ^2H measurements–A replacement for NBS 30. *Chemical Geology* **2017**; 467: 89–99.

(14) Wassenaar, L. I.; Hobson, K. A. Improved Method for Determining the Stable-Hydrogen Isotopic Composition (δD) of Complex Organic Materials of Environmental Interest. *Environmental Science and Technology* **2000**; 34: 2354–2360.

(15) Schimmelmann, A. Determination of the concentration and stable isotopic composition of nonexchangeable hydrogen in organic matter. *Analytical Chemistry* **1991**; 63: 2456–2459.

(16) Feng, X.; Krishnamurthy, R.V.; Epstein, S. Determination of ratios of nonexchangeable hydrogen in cellulose: A method based on the cellulose-water exchange reaction. *Geochimica et Cosmochimica Acta* **1993**; 57: 4249–4256.

(17) Sessions, A. L.; Hayes, J. M. Calculation of hydrogen isotopic fractionations in biogeochemical systems. *Geochimica et Cosmochimica Acta* **2005**; 69: 593–597.

(18) Schimmelmann, A. Determination of the concentration and stable isotopic composition of nonexchangeable hydrogen in organic matter. *Analytical Chemistry* **1991**; 63: 2456–2459.

(19) Sauer, P. E.; Schimmelmann, A.; Sessions, A. L.; Topalov, K. Simplified batch equilibration for D/H determination of non-exchangeable hydrogen in solid organic material. *Rapid communications in mass spectrometry: RCM* **2009**; 23: 949–956.

(20) Schimmelmann, A.; Lewan, M. D.; Wintsch, R. P. D/H isotope ratios of kerogen, bitumen, oil, and water in hydrous pyrolysis of source rocks containing kerogen types I, II, IIS, and III. *Geochimica et Cosmochimica Acta* **1999**; 63: 3751–3766.

(21) Girden, E. ANOVA. SAGE Publications, Inc, 2455 Teller Road, Thousand Oaks California 91320 United States of America **1992**.

Danksagung

Ganz besonders möchte ich mich bei meiner Erstbetreuerin Prof. Dr. Yvonne Oelmann für die hervorragende Betreuung und Unterstützung bei der Durchführung meiner Dissertation bedanken. Ihre stetige Bereitschaft zu Diskussionen, Anmerkungen sowie Gespräche auf intellektueller und persönlicher Ebene haben mich stets motiviert und maßgeblich zum Gelingen dieser Arbeit beigetragen.

Ebenso möchte ich mich bei meinem Zweitbetreuer Prof. Dr. Wolfgang Wilcke für seinen umfassenden Rat, seine Anmerkungen und die gemeinsamen Diskussionen während meiner gesamten Arbeit bedanken.

Des Weiteren gebührt mein Dank Frau Prof. Dr. Eva Lehndorff für die Zweitkorrektur meiner Dissertation.

Bei meinem Projektpartner Stefan Merseburger bedanke ich mich für den angenehmen Austausch mit vielen Diskussionen und Ideen. Die gegenseitige Unterstützung habe ich immer sehr wertgeschätzt.

PD Dr. Harald Neidhardt möchte ich für die vielen fachlichen als auch privaten Gespräche danken. Durch seine positive Art hat er jederzeit einen großen Beitrag zu einer schönen Arbeitsatmosphäre und einem herzlichen Miteinander beigetragen.

Meinen Freund:innen und Arbeitskolleg:innen Simon Hauenstein, Eva Koller-France, Christiane Nagel, Wen Shao sowie Yao Li möchte ich für die vielen schönen und lustigen Momente innerhalb der Arbeitsgruppe danken. An die gemeinsame Zeit denke ich immer wieder gerne zurück.

Ein großes Dankeschön geht auch an Rita Mögenburg, Genoveva Tscholl und Sabine Flaiz, die mich sowohl bei den Analysen im Labor als auch mit ihrem technischen Know-how jederzeit unterstützten.

Gleichermaßen möchte ich mich bei meinen Eltern, die mir mein Studium ermöglicht haben und mich in all meinen Entscheidungen liebevoll unterstützt haben, bedanken.

Herzlichst bedanken möchte ich mich bei meiner Freundin Jasmin Niederhofer. Sie unterstützte mich während meiner gesamten Doktorarbeit und hat mich auch nach Rückschlägen immer wieder neu motiviert.

Abschließend möchte ich all meinen Freund:innen in- und außerhalb meiner WG danken. Sie gaben mir den perfekten Rückhalt und schafften mir stets ein einzigartiges Umfeld.